The Thesis Committee for Jay Ravi Mehta
Certifies that this is the approved version of the following thesis:

Redesign of the Total Wrist Prosthesis to Address Wrist Rotation

APPROVED BY
SUPERVISING COMMITTEE:

Supervisor:

Richard Crawford

Ashish Deshpande

Redesign of the Total Wrist Prosthesis

to Address Wrist Rotation

by

Jay Ravi Mehta, B.S.M.E.

Thesis

Presented to the Faculty of the Graduate School of

The University of Texas at Austin

in Partial Fulfillment

of the Requirements

for the Degree of

Master of Science in Engineering

The University of Texas at Austin

May 2013

Dedication

This thesis is dedicated to Jesus, my parents, my professors, and my fiancée who loved and built me up despite all my shortcomings.

Acknowledgements

Dr. Richard Crawford has been the perfect thesis supervisor. He inspired me when my motivation waned, pushed me when I was satisfied with less than I was capable of, gave me room to grow, and guided me to the best of his ability. I would also like to thank Dr. Ashish Deshpande and Dr. Rick Neptune for their guidance and for answering my questions throughout the progress of my research.

Abstract

Redesign of the Total Wrist Prosthesis

to Address Wrist Rotation

Jay Ravi Mehta, M.S.E.

The University of Texas at Austin, 2013

Supervisor: Richard Crawford

The human wrist is a vital joint in daily life, and it is subject to injuries and disease. Currently, severe wrist disease is normally treated with wrist arthrodesis, which is normally reliable but results in a fixed wrist incapable of allowing wrist motion. Another method of treating a nonfunctional or severely painful wrist is wrist arthroplasty where the wrist joint is replaced with an implant that allows wrist movement. As of yet, a suitable wrist implant has not been developed, especially for the case of the post-traumatic, young male wrist, and most current wrist implants fail from failure of the bone-implant interface. Through simulation and literature review, it is concluded that implants that restrict axial rotation are bound to fail overtime. With this conclusion, a new wrist implant prototype is designed that incorporates state of the art materials, fluid film lubrication, proper kinematics, a suitable range of motion, and more. This implant contributes several improvements to the field of wrist arthroplasty.

Table of Contents

List of Tables

List of Figures

CHAPTER 1

INTRODUCTION AND PROBLEM BACKGROUND

Prosthetics and medical implants are artificial devices that replace a missing or damaged body part in the human body. They have existed for millennia and have steadily improved over the years. Common prosthetics and implants include prosthetic legs, feet, arms, knee implants, hip implants and more. These amazing devices enable people with disabled joints to carry out many daily activities that they would not be able to otherwise.

The prosthetics field has seen great advances in the past century with new materials, new testing and experiment techniques, better understanding of joint anatomy, and more. The hip and knee implants have become very viable joint replacements over time. However, of all major joints, the wrist has lagged far behind the knee and hip.

1.1 THE WRIST

The wrist is the joint which allows movement between the hand and forearm on the arm. The wrist is a complex joints. It is made up of 8 carpal bones which interact with the five metacarpals, the radius and the ulna. Figure 1 displays the bony makeup of the wrist. These carpal and metacarpal bones are connected with a system of many ligaments, shown in Figure 2, which vary in stiffness and mechanical properties. Over the supporting structure, the joint is covered with tendons which produce wrist and finger motion; Figure 3 gives a view of the dorsal muscles and tendons. [1-9].

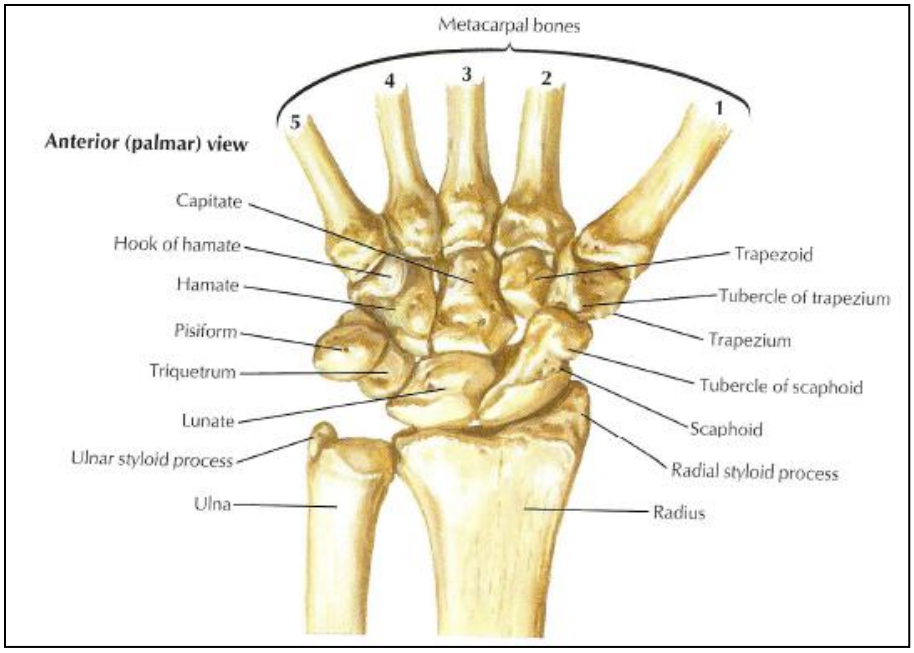

Figure 1: Bony structures of the wrist [7]

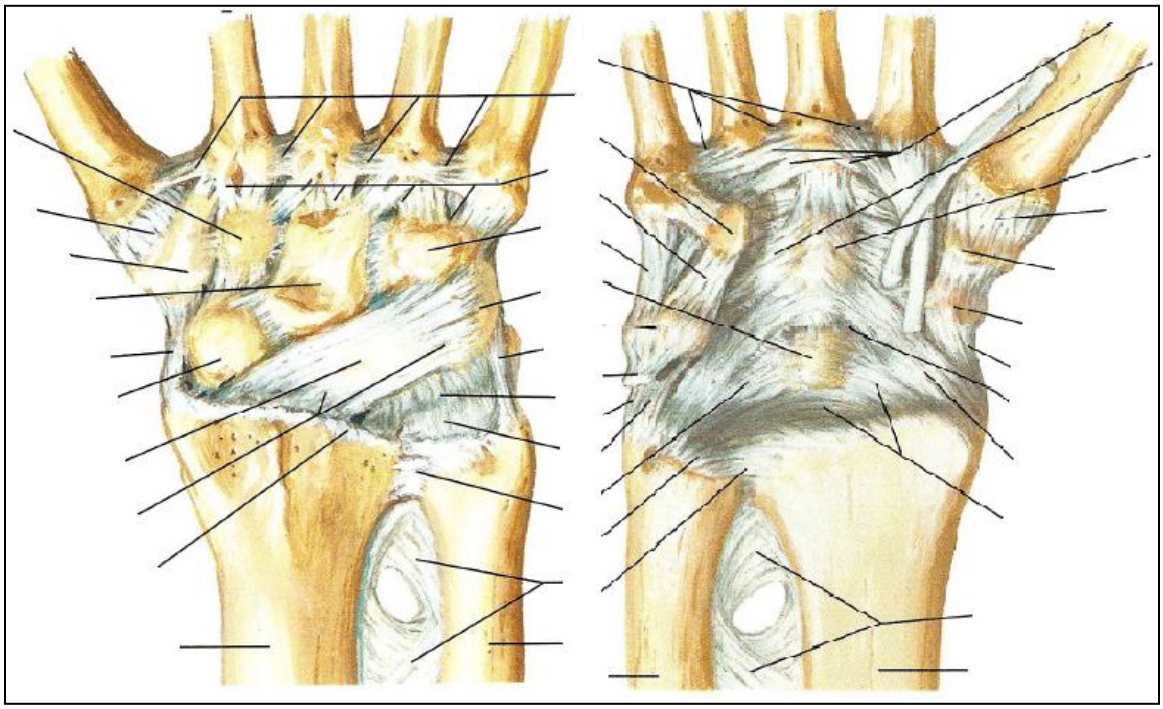

Figure 2: Ligaments of the wrist [7]

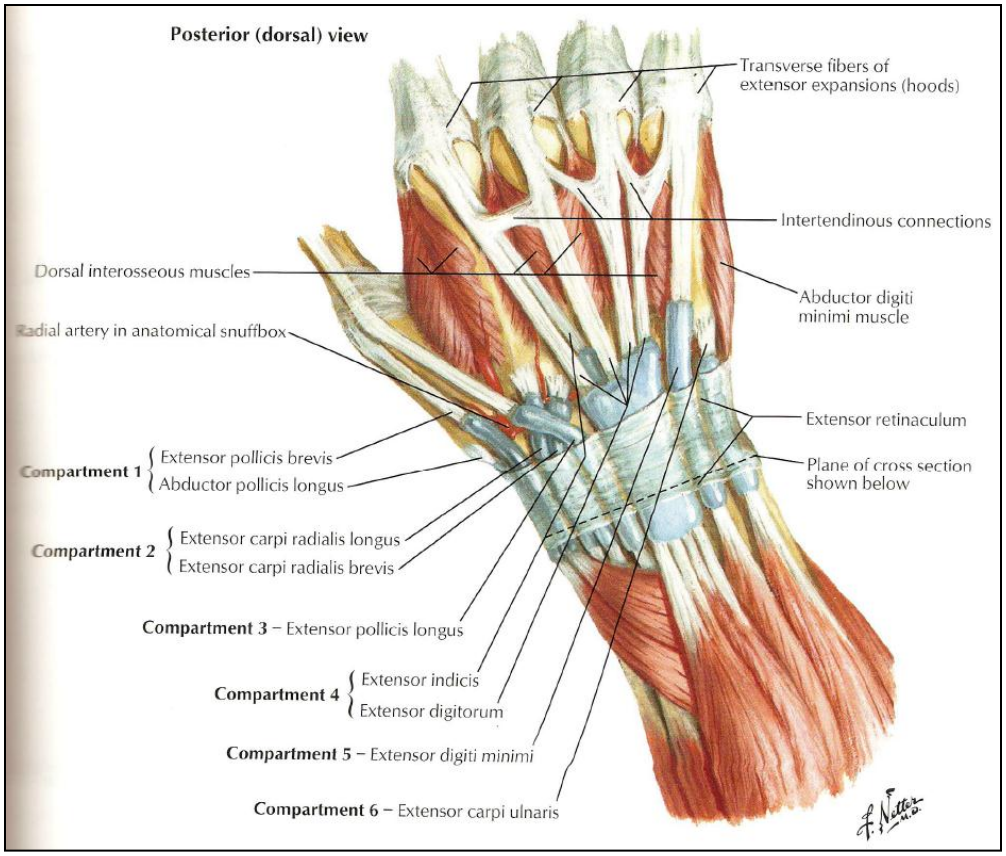

Figure 3: Musculotendon structures across wrist [7]

The wrist has a large range of motion and is subjected to various loadings over a lifetime. The basic movements of the wrist are shown below in Figure 4. Flexion and extension motion, abbreviated FEM, are rotations about one main axis and exhibit the greatest range of motion (close to 180° total). Radial deviation and ulnar deviation, abbreviated RUD, are rotations about the other main axis and exhibit a sizable range of motion as well. The wrist handles fairly large loads, addressed later, for a joint with such small bones, and it is no wonder that the wrist often develops several types of problems.

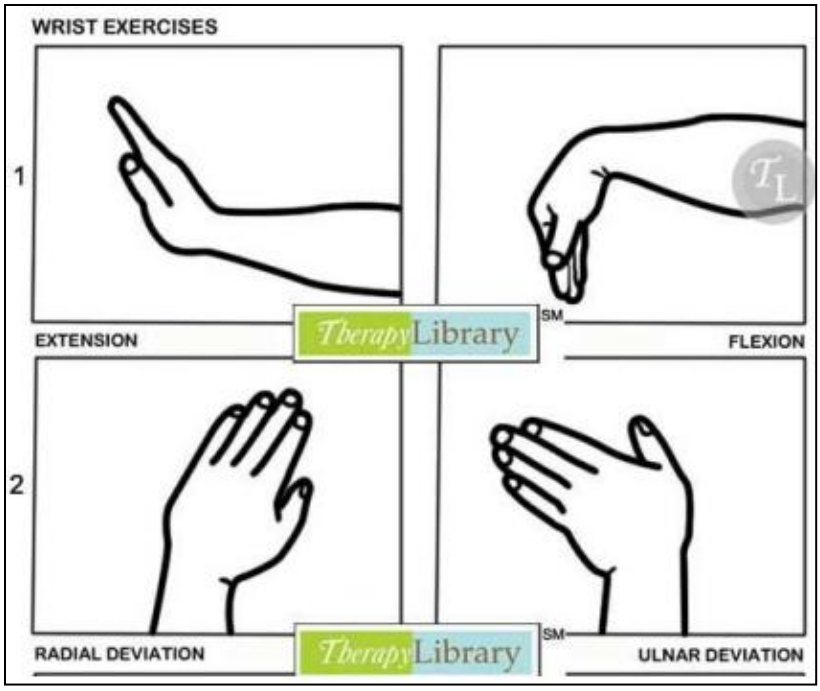

Figure 4: Wrist movements [10]

1.2 WRIST PROBLEMS

The wrist can be disabled in several ways. The first is tendon and nerve problems such as carpal tunnel syndrome and tendonitis usually caused by overuse. These issues can usually be addressed through therapy and rest if caught early enough but many times require surgical intervention.

Second, there are fractures and sprains which are known as traumatic injuries. These injuries often lead to post-traumatic arthritis and disability if the injury is severe enough. In cases that require surgery, the treatment is almost always wrist fusion, also known as arthrodesis [11].

Lastly, arthritis commonly affects the wrist. There are two types of arthritis: osteoarthritis and rheumatoid arthritis. Osteoarthritis is the breakdown of cartilage

through years of wear and tear and is a normal result of aging. Osteoarthritis is the most common joint disorder and is usually much less chronic of a wrist disease compared to rheumatoid arthritis; thus it is treated nonsurgically generally. [12]

Rheumatoid arthritis is the more serious of the two types of arthritis, affecting nearly 1% of the US population, and it commonly affects the wrist: within two years of diagnosis, 50+% have wrist pain, and, within 10 years, 90% develop wrist disease [13-14]. Rheumatoid arthritis is an autoimmune disease where the body's immune system attacks healthy joint tissue causing joint inflammation and deformity [15]. This type of arthritis literally destroys the wrist over time [16]. Thus, almost every case requires some form of surgery to deal with chronic pain and disability.

All these problems lead to a loss of wrist functionality which can drastically reduce quality of life.

1.3 IMPORTANCE OF A FUNCTIONAL WRIST

The wrist is one of the most essential joints since so many tasks depend on fine motor control across this joint [17]. A study of quality of life concluded that 12 years with a normal wrist is equivalent to 30 years with a painful nonfunctional wrist; this kind of quality of life loss is similar to that of paraplegia and blindness! [18] Another study determined that life with destroyed rheumatoid wrists is about half as valuable as life with a normal wrist and much of the morbidity from rheumatoid arthritis can be attributed to hand and wrist dysfunction [14].

From the Disability of the Arm, Shoulder, and Hand (DASH) questionnaire, some key daily tasks that require a functional wrist are opening a tight jar, writing, turning a key, placing an object on an overhead shelf, doing heavy household chores, carrying a shopping bag or briefcase, changing a light bulb, washing and drying hair, washing the

back, putting on a sweater, and transportation. [19]. Some other tasks from various other sources include, answering a telephone, drinking, eating soup with a spoon, getting up from a chair, buttoning a shirt, perineal care, and turning a door knob [20-21]. As can be seen, a non-functional, painful wrist can significantly impair daily function in many ways and markedly reduce independence and personal hygiene. Thus, a functional wrist is almost essential for good quality of life.

1.4 CASE AGAINST WRIST FUSION

The traditional and most accepted treatment for severe wrist problems is total wrist arthrodesis or intercarpal fusion where the wrist is fixed permanently in one position. [8, 11, 13, 18, 21-30]. The goal of wrist arthrodesis is to relieve pain, improve joint alignment, and restore skeletal stability in people with advanced arthritis and otherwise diseased wrists with the main drawback of no wrist motion [22]. Compared to total wrist arthroplasty (TWA), where a total wrist prosthesis is implanted to replace the damaged joint, arthrodesis is widely considered a safe, durable, easy, less costly, and extremely reliable treatment which solves the problem of wrist pain. However, in reality, arthrodesis is not as superior as it seems.

With current TWA and the advanced tools available, the surgery difficulty for arthrodesis and TWA is very comparable. Also, arthrodesis is not complication-free at all, with close to a 17% total complication rate compared to 30% for TWA. In many cases arthrodesis does not eliminate pain [11, 21, 23, 25, 32]. There are several cases of arthrodesis failures where the fusion plate fractures or loosens over time. Tendon adhesions and friction between the fusion implant and natural wrist structures are also fairly common. Most importantly, the possibility of pain not being completely eliminated or returning is a large risk to be considered.

Just recently, new research has shown that total wrist arthroplasty is comparable in cost-utility to arthrodesis. Cost-utility is measured in Quality-Adjusted Life-Years (QALY) gained with treatment, and the standard for accepting a procedure currently is $50,000 to $100,000 per QALY. Both TWA and arthrodesis cost no more than $2500/QALY compared to nonsurgical treatment; both treatments add much quality of life at an economical cost and thus should not be considered cost prohibitive. So even though total wrist arthroplasty is marginally more expensive than arthrodesis, the increased quality of life from arthroplasty easily justifies the additional cost. [11, 13-14, 18]

The main reason arthrodesis is not a desirable treatment is the loss of motion. From a recent study, only 40% of patients were satisfied one year after wrist fusion, and 100% of patients desire wrist motion again [13, 23-25, 32-33]. Arthrodesis becomes very debilitating as many of the key daily activities mentioned above become impossible for the patient and result in definite loss of independence [11, 28, 32, 34]. It is for this reason that almost every patient with one fused wrist will prefer even an imperfect TWA over the fused wrist; the motion allowed by the prosthetic wrist permits the patient to carry on with daily life and this generally balances the probable failure of the implant. [8, 11, 13, 21, 24, 28, 32, 35].

Additionally, almost every current wrist implant can be salvaged easily with arthrodesis. In other words, if the total wrist arthroplasty fails, it can almost always be remedied with wrist fusion. Based on these considerations, arthrodesis should be a last resort with TWA being the initial treatment if possible [13, 28-29, 31, 33, 36-37]. In some cases, the failed prosthesis can be salvaged with a soft-tissue arthroplasty such as the Silastic or Swanson implant (described below), which preserves some wrist motion for several years [31].

1.5 REVIEW OF PREVIOUS WRIST PROSTHESES

With the focus shifted to wrist prostheses, a review of previous popular wrist implants is helpful to see the strengths and weaknesses of various designs. Though wrist prostheses' success has lagged far behind hip and knee prostheses, considerable progress has been made over the years following advances in materials, fixation techniques, and kinematics knowledge. The main goals of each implant are to relieve pain and provide a functional range of motion.

Each of the various implants can be grouped into one of four categories: elastomer, constrained, ball and socket, and universal type. Elastomer implants replace the wrist by fixing a flexible elastomer between the hand and forearm; the implant relies on its elastic properties to allow some motion at the wrist. Constrained implants actively constrain the motion between the hand and forearm, usually through some sort of pinned mechanism such as a universal joint. The ball and socket implants are semi-constrained in that they define the center of rotation but rely on the natural soft tissue structure to determine range of motion and to hold the joint together; they allow rotation in all 3 axes and do not permit translation. The universal types are very similar to ball and socket implants except they only allow FEM and RUD and no axial rotation.

1.5.1 Elastomer Prostheses

Swanson

The Swanson is the first popular wrist prosthesis developed and was designed in 1967. It is a double-stemmed, flexible hinge silicone prosthesis, which acts essentially like a spacer between the hand and forearm and allows some motion [27]. There have been several updates to the initial design to address breakage and wear, including titanium grommets (to protect the elastomer from rubbing against sharp bone) and new

materials that are more biocompatible and resistant to wear and fatigue [8, 38-39]. The latest design with grommets and new polymer is shown in Figure 5. The device gives average ranges of motion of 24° flexion, 21° extension, 10° radial deviation, and 15° ulnar deviation as shown graphically in Figure 6.

Figure 5: Latest Swanson Implant [40]

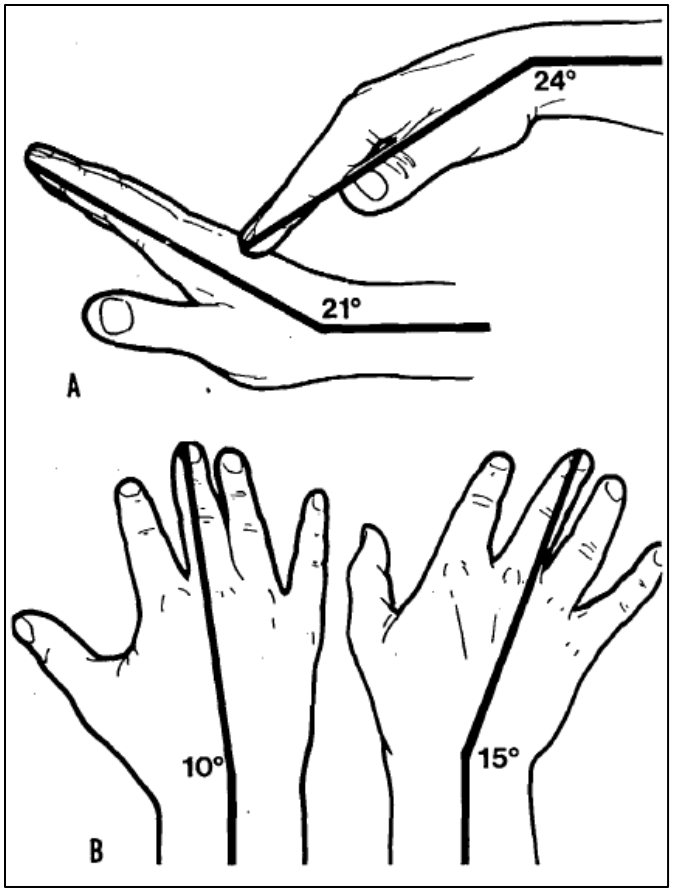

Figure 6: Average postoperative range of motion after Swanson implant [36]

The success of the implant was fairly short lived with many complications. From a study of a six year follow-up of 19 patients, 65% experienced little pain after operation, but fracture occurred in 65% as well by the time of the six year follow-up. The implant subsided (drifted deeper into the bone) and improvements deteriorated quickly over time in all cases [36]. A similar study with a 2.5 year follow-up confirmed good initial pain relief in most patients and some range of motion, but not quite enough for all daily activities. After 2.5 years, 61% had good results and there was a 25% revision rate. Implant fracture, tendon imbalance, and silicone synovitis, an inflammatory reaction to silicone particles, were quite common. For all cases of revision, arthrodesis of the wrist

was commonly performed along with soft tissue procedures [8]. Currently, this implant is generally not used because of its high complication rate and short life.

Though it used to be the gold standard in arthroplasty there are not many reasons to consider this implant over others besides its relative ease in implementation and revision. Disadvantages of this design include likely fracture, abrasion related silicone synovitis, and imbalance due to the simple one piece elastomer design [41].

1.5.2 Constrained

Trispherical

The Trispherical wrist prosthesis uses a ball and socket articulation constrained by a fixed axle mechanism fixed in the radius and metacarpals; it can be seen in Figure 7 and Figure 8. As shown, the carpal component has a long stem inserted into the third metacarpal with a shorter stem inserted into the base of the second metacarpal to resist rotation. Both the radial and carpal components are made of titanium alloy and inserted using bone cement. The bearing surfaces are on the carpal component and composed of ultra-high-molecular-weight polyethylene, UHMWPE. It is a constrained implant, similar to a hinge mechanism, so it actively limits the range of motion and prevents dislocation through its bearing and axle mechanism. The device was designed to provide 15° of RUD motion, 90° flexion, 80° of extension and 10° of axial rotation. [40-42]

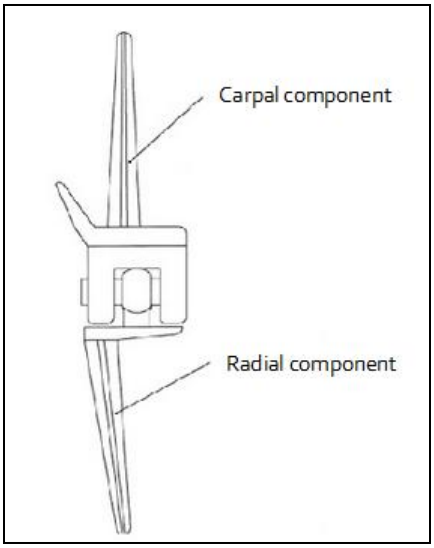

Figure 7: Trispherical schematic [41]

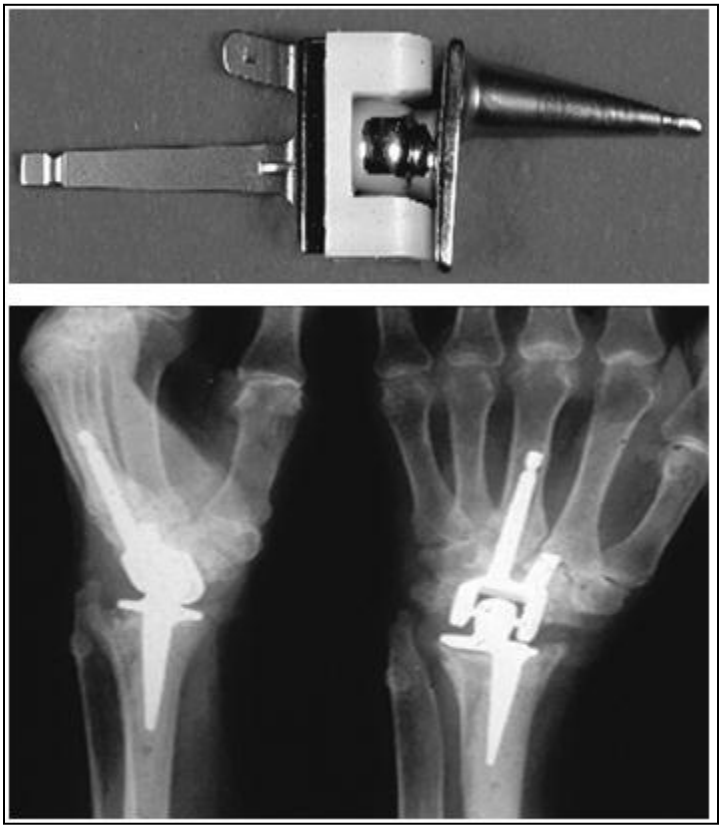

Figure 8: Trispherical wrist prosthesis and implanted position [40]

A five year follow-up study showed encouraging results; 35 out of 38 wrists had satisfactory pain relief, all 38 were stable and balanced, 30 out of 38 achieved a FEM arc greater than 20°. There was one revision for loosening, another required arthrodesis because of misalignment and persistent pain, and three implants subsided into the third metacarpal and led to limited range of motion but were not revised because of improvement over preoperative status [42]. A nine year follow-up study with 34 patients also reported good results with few complications (loosening, pain, and tendon attritiion) [8]. However, there is a report of a catastrophic failure of the axle and severe synovitis from titanium and polyethylene wear [44]. There are several cases of metacarpal perforation and loosening of the carpal component in clinical records [41].

The main advantage to this design is that it actively prevents dislocation with its axle design. The key disadvantages include restricted free articulation resulting in reduced range of motion, additional stresses due to the pin joint, especially at the cement interfaces between the stems and bone, and carpal component loosening and metacarpal perforation [41].

1.5.3 Ball and Socket

Mueli

The Meuli prosthesis was developed in the 1970s and is one of the earliest and most internationally used wrist prostheses. It is a ball and socket design and is normally implanted using cement or is press fitted. The carpal component has two large stems that are inserted into the metacarpals. Figure 9 shows the three iterations of the design over the years ending with MWP III prosthesis. Initially there was no axial offset of the stems and a polyester ball. Imbalance and reactions to the polyester resulted in the offset stems and change to polyethylene bearing material. The current MWP III has a body made of

Protasul 100, a titanium alloy, with porous finish. The ball coated with titanium nitride is attached to the radial component. The ball articulates against a deep UHMWPE socket in the carpal component. A schematic of the design and implantation location are shown in Figure 10. On average, the device provided a range of motion of 30° of flexion, 40° of extension, 10° of radial deviation, and 10° of ulnar deviation [23, 27, 40-41].

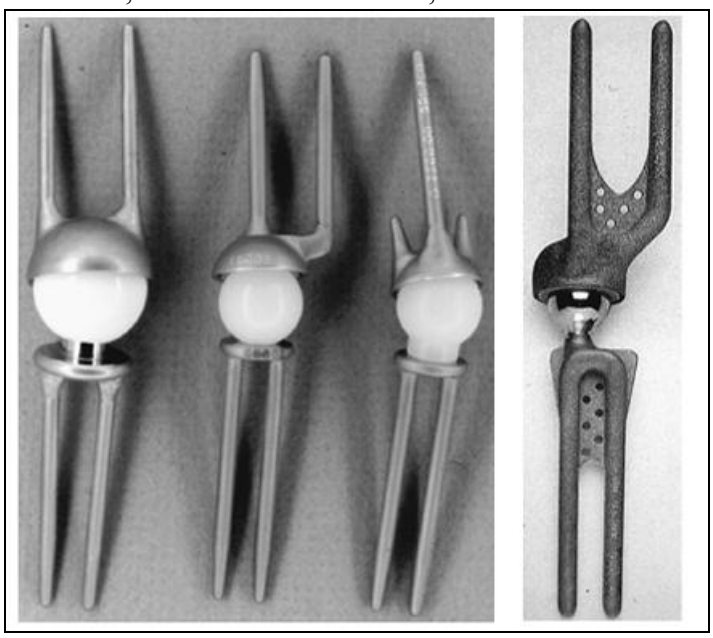

Figure 9: Iterations of the Meuli Implant [40]

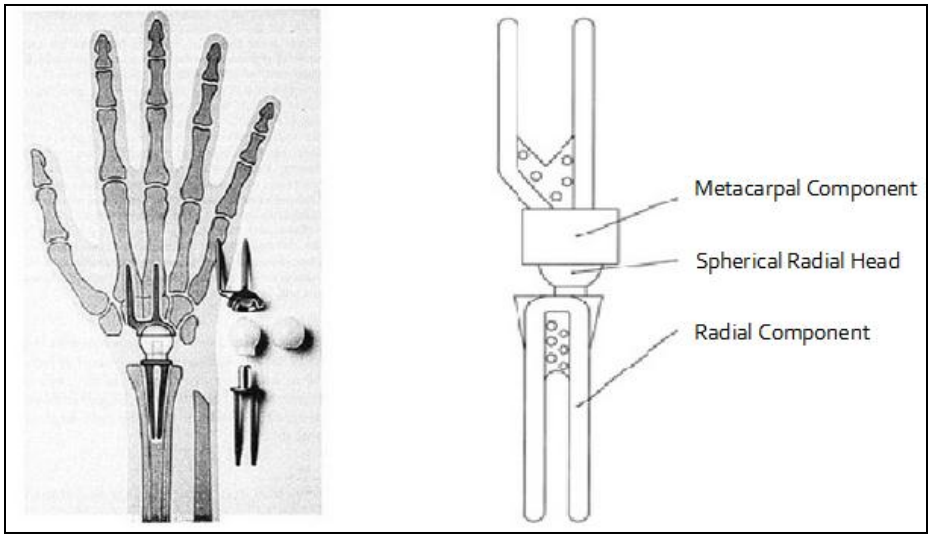

Figure 10: MWP III wrist implant [41]

The design rationale was based on Youm's work on determining that the center of rotation was fixed and lay in the head of the capitate. The goal is to recreate the lunocapitate motion and approximate this motion with a ball and socket. Also, the ball and socket design allows three degrees of freedom, reducing the stresses on the bone-implant interfaces through the stems. Initial concerns of this design being unable to handle forearm torques were unfounded based on successful implementation [40].

The initial designs were very prone to soft tissue balance issues and deformity from tendon imbalance. In a study of 140 implants, 8.6% experienced dislocation, 12.1% had imbalance, and 2.9% had loosening problems. Later papers reported much higher failure rates with dislocation often resulting from malpositioning of the implant [40]. The key advantage of this prosthesis was basing the design on a ball joint, such that there is little possibility for failure at the central area, and reducing stress at the bone-implant interface. The many disadvantages include the high failure rate from metacarpal perforation and loosening of the stem, dislocation, and large dissection of the radius [41].

Elos and Gibbon

The three versions of the Elos prosthesis were preliminary versions of the final Gibbon or Motec prosthesis. It is a relatively new screw fixated ball and socket design seen in Figure 11. The ball is fixed in the carpals with a single screw which has undergone several revisions. The socket is fixed in the radius with a wider and shorter screw. Both screws are made of titanium alloy and coated with Bonit, a resorbable calcium phosphate coating to aid in osseointegration (improves fixation greatly). The articulating components are made of cobalt chrome-molybdenum alloy treated with chromium nitride for greater wear resistance. The range of motion in FEM is generally improved to between 136° and 160°. [37, 45]

Figure 11: Gibbon Prosthesis [37]

In a study of 189 wrist implants, including 23 Elos and 76 Gibbon implants, the Gibbon implants had low survival rates with 77% of the Gibbon implants surviving after four years and only 57% of Elos implants surviving after five years. The main drawback of this design was loosening of the distal/carpal component. The strengths of this design are the stable articulation, potential reduction in stress on the bone-implant interface due to the ball and socket articulation very little bone resection, no pain-related revision, and fewer wear particles than the conventional metal on polyethylene articulation. [37, 45]

1.5.4 Universal Type

Volz

The Volz prosthesis was created in 1973. It was the first attempt to create a biaxial motion of the wrist. This prosthesis creates a toroidal articulation with two different radii of curvature for FEM and RUD, restricting translation and axial rotation. The initial design can be seen in Figure 12; the metal carpal component articulates against the polyethylene cup on the radial component. A large section of the radius was resected to insert the radial component which was fixed using bone cement. The carpal component was installed similarly. The two pronged carpal component was extremely unsuccessful; it was later revised to a single prong design and is now discontinued. The range of motion was designed for 90° FEM and 50° RUD, but in reality it was closer to 49° FEM and 25° RUD. [8, 23, 27, 40-41]

Figure 12: Initial Volz Prosthesis [40]

Good results were noted initially but progressively worsened. One study showed that 79% had signs of bone resorption along the radial component, where another documented a 24% rate of loosening of the carpal component as seen in Figure 13. Almost 25% of the implants were judged to be imbalanced on top of these other problems. The many drawbacks of this design were the large amount of bone resection needed, loosening, bone resorption, wrist imbalance, some cases of tendon inflammation and carpal tunnel syndrome, difficult surgery and dislocation. There were no notable strengths. [8, 23, 27, 40]

Figure 13: Loosened Volz carpal component [27]

Biaxial

The Biaxial prosthesis was created in 1982 and was the first ellipsoidal articulation design [27]. The popular design can be seen in Figure 14 and Figure 15. The distal metal component articulates against the metal backed polyethylene cup on the radial component. The distal component is fixed into the third metacarpal with a long stem and a shorter prong in the trapezoid to resist rotation; longer stems and a multiple stem design are being considered to address loosening. The radial component has ulnar and palmar offsets to attempt to create a more natural motion. Both stems are coated with porous material to enhance fixation and most are installed without cement [23, 40]. The average range of motion is 29° in flexion, 36° in extension, 10° in radial deviation, and 20° in ulnar deviation [41].

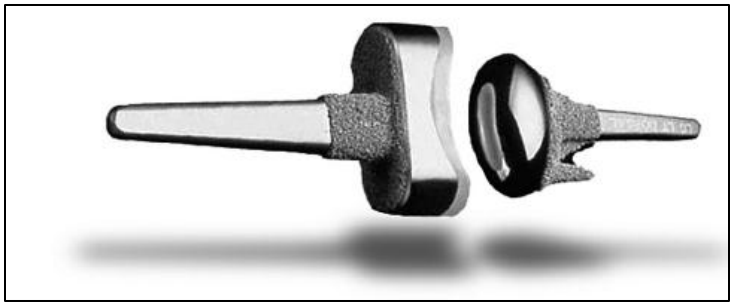

Figure 14: Biaxial prosthesis [37]

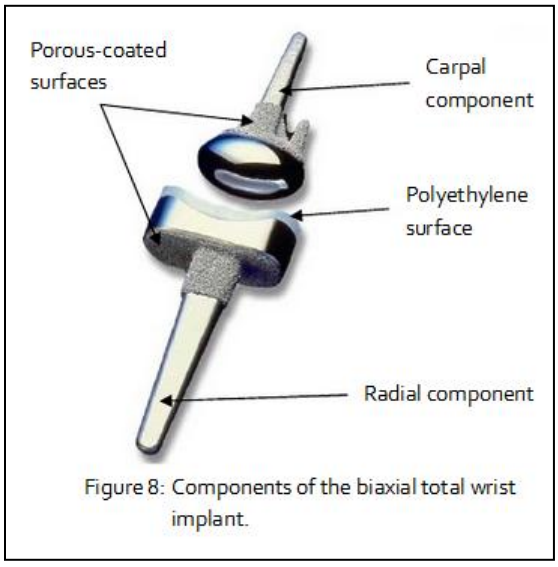

Figure 15: Biaxial prosthesis overview [41]

The implant has about an overall 80% survival rate at five years [8, 37, 40]. The main problems were distal component loosening, severe pain, metacarpal fractures, imbalance, and implant subsidence. The strengths of this design were relatively natural, stable motion and easier revision when implanted without cement [23, 27, 37, 40].

Universal and Universal 2 Total Wrist Arthroplasty

The Universal Total Wrist Arthroplasty (TWA) prosthesis was developed in 1990 and is the current gold standard for TWA (wrist prosthesis). The prosthesis is shown in

Figure 16. The carpal plate is made of titanium alloy with a HDPE ovoid insert attached to the end. It is fixed with a central stem and two locking variable angle screws; the stem and ulnar screw remain in the carpals mostly and the radial screw often extends into the 2nd metacarpal, as shown in Figure 17. The radial component is also made of titanium alloy and is fixed without cement into the radius. Both the carpal plate and radial component have a porous coating to improve fixation [27, 40]. Originally the articulation was toroidal, but after cases of dislocation and loosening it was revised to an ellipsoidal articulation after finding that the ellipsoidal shape was more stable through a range of movement. The radial cup was also widened to prevent dislocations. After this update, the implant was renamed to Universal 2 [23, 26, 27]. The average range of motion is about 41° flexion, 36° extension, 7° radial deviation, and 13° ulnar deviation [41].

Figure 16: Universal TWA [40]

Figure 17: Implanted Universal TWA [27]

The prosthesis has improved functionality in most cases though there are still cases of loosening and dislocation. One study with the original implant reported 75% survival rate at five years and 60% at seven years [32]. The original design study showed pain reduction in 88% of cases with over 30% complications [8]. The Universal 2 has greater survivability than the original design, but is still not problem-free. The main drawbacks are carpal component loosening, dislocation, and rare impingement on other bones. Strengths include reduced bone resection, stability, well improved mobility, and cement-free fixation [23, 26, 27, 29, 46].

Destot

The Destot prosthesis was designed in 1991 in France and Belgium and it was designed specifically for posttraumatic arthritis. All the components are displayed in Figure 18. The radial and carpal stems are made of 316-L stainless steel, sand blasted for better osseointegration and fixation, and are installed without cement for fixation. The carpal component is fixed with a stem and 4.5 mm screw. It has a polyethylene cylinder

between the plate and the condylar/ellipsoidal component to allow rotation between the ellipsoidal contact surface and plate. The radial component has an ellipsoid cup made of UHMWPE backed by the radial stem. The average range of motion of is 41° extension, 48° flexion, 12° radial deviation, and 22° ulnar deviation [8, 17].

Figure 18: Parts of the Destot implant [17]

In an early study, 85% of patients experienced good range of motion, grip strength improved in all, and 85% still survived after four years. The main weakness was metacarpal stem loosening because of the long screw and damage in implants with

younger patients. The strengths included great balance because the soft tissue structure was preserved in the posttraumatic wrists and the extra degree of motion through the cylindrical connector may reduce stresses in the bone-implant interface [8, 17].

Remotion

The Remotion implant is fairly similar to the Universal TWA, but it has a few differences. The full implant and a close up of the parts of the carpal component are shown in Figure 19 and Figure 20. The carpal plate is made of cobalt chromium alloy with a titanium coating for bone ingrowth. It is fixed with the central peg pressfit into the third metacarpal and two 4.5 mm cancellous variable angle screws on either side of the central peg inserted into the 2nd and 5th carpo-metacarpal joints. The carpal plate has a slight bend to mimic the natural arch of the distal carpal row. The UHMWPE ellipsoid is snap fit onto the ball at the end of the plate. The innovative feature is that the design allows 10° of rotation between the ellipsoid articulation piece and the plate it is attached to (see Figure 20); this extra degree of freedom actually acts as a damper and helps mimic the dart thrower's motion of the wrist. The radial component has a deep ellipsoid cup and is also made of cobalt chromium alloy with a titanium coating. It is press-fit into the radius and preserves the rim of the radius, which prevents stability issues with tendons. The palmar surface is also undercut to avoid any damage to nerves or tendons. The average range of movement is 31° flexion, 31° extension, 7° radial deviation, and 17° ulnar deviation [23, 34]

Figure 19: Remotion prosthesis [23]

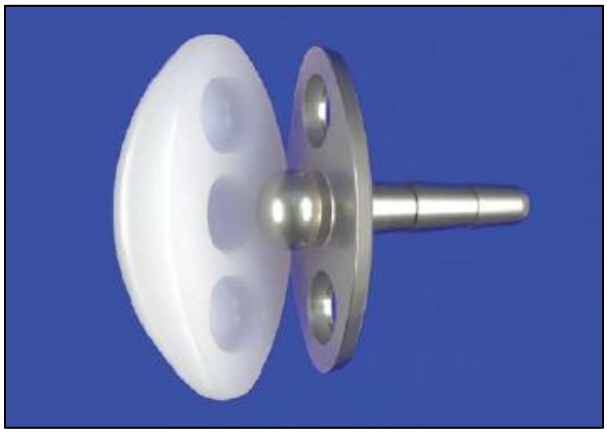

Figure 20: Remotion carpal component [23]

This prosthesis is relatively new with few results so far. Early results show promise with improvements in pain and function and few complications (mainly loosening) [34]. Preliminary results for 60 patients showed no complications at all at one year, with all but one patient reporting improvement in pain and function and no signs of radiologic loosening [23]. Figure 21 shows a successful implant. The weaknesses are not evident right now, possibly loosening overtime. The many strengths of this design

include cementless fixation, stability, minimal bone resection preserving the rim of the radius, some axial rotation to reduce stresses on bone, and osseointegrative fixation.

Figure 21: Succesful Remotion implant [23]

1.6 OTHER TWA DESIGNS

There are many other TWA designs that are similar to the ones mentioned above. The Gschwind-Scheirer-Bahler Wrist, Hamas Implant, Loda implant, and Pech Implant are all ball and socket designs [23]. The Weber-Mayo TWA, Guépar Prosthesis, Clayton-Ferlic-Volz Prosthesis, Cardan-Type Implant, Taleisnik Implant, RWS Prosthesis, Anatomic Physiologic Wrist Prosthesis, Osseointegration Swedish Design, House Wrist Prosthesis, Avanta Prosthesis, Giachino Device, Total Modular Wrist Implant Arthroplasty are all universal joint designs, most with ellipsoidal or toroidal contact surfaces [23]. Most are international designs and are not available in the United

States for various reasons, and some are still being designed. They share much in common with the designs mentioned; more information is available from the sources provided.

1.7 THE NEED

The wrist prostheses described above have various strengths and weaknesses, but the fact is that they still have not met the full needs of patients with wrist disabilities and do not survive nearly as long as hip and knee implants. Most of the implants are designed for the rheumatoid wrist since it generally undergoes less stress due to atrophied muscles and limited activity of elderly patients. Expected gains are often lower because of the level of disability that often comes with severe rheumatoid arthritis. But the greatest need is seen in the post-traumatic, young male for which almost every current implant is not designed [11, 17, 34, 43]. In almost every case, the young male undergoes arthrodesis for a nonfunctional or severely painful wrist after trauma, and, as described earlier, wrist fusion is extremely debilitating [11, 17, 43]. The inadequacies of current implants are evident. The purpose of this research is to address these inadequacies. Thus, the following hypothesis is proposed:

1.8 HYPOTHESIS

Any implant that restricts axial wrist rotation, whether it be a constrained type or universal type implant (like the gold standard: Universal2), will loosen and fail overtime due to the stresses due to the prosthesis preventing wrist rotation and transferring stresses to the bone-prosthesis interfaces.

This hypothesis will be tested and proven in the next chapter. Following that, a solution to this problem is proposed through a new wrist implant design.

CHAPTER 2

HYPOTHESIS TEST

2.1 SIMULATION BACKGROUND

In the past, much progress in wrist kinematics, prosthesis design, stress analysis for various wrist problems, and musculoskeletal simulation has been made through simulation [4, 6, 26, 47-49, 50-52]. Other studies rely solely on experiments to reach important conclusions [26, 53-57]. Though many studies combine simulation with experimentation for full validation, significant conclusions can be made using simulation alone.

Simulation and experimentation have their respective strengths. Simulation could be very inexpensive and faster than experiments (depending on model complexity). Certain key variables often immeasurable through experiment can be estimated through simulation. However, simulations can be difficult to validate without experimental results, often require unrealistic assumptions to reduce model complexity, and could require a very complex model, various software licenses and extensive computing power. Experiments are usually more straightforward unlike a complicated model and represent the real world by reducing the number of assumptions. However, experiments are often very costly, they take much time to set up and conduct, and there is always a degree of measurement error.

Due to cost and time constraints and the availability of needed software and computing power, simulation was used for testing the hypothesis. Nonetheless, future experimental validation would be desirable. In the following sections, several models and simulations are developed to show that restricting axial rotation can lead to carpal component loosening in a TWA.

2.2 BUILDING THE MODELS

The simulation computes the reactions to axial torques for an ellipsoidal prosthesis based on the basic shape and characteristics of the Universal 2 Total Wrist System implant. To begin the simulation process, several models have to be created. To create the models several variable values are needed such as wrist torques and forces, bone properties, implant and bony mass size among others.

2.2.1 Wrist torques and forces

Compressive forces

The wrist mainly undergoes compressive forces with the muscles crossing the wrist acting to compress the wrist in many motions that involve gripping an object. Thus, compressive forces should be considered first when designing a wrist implant. The problem that arises is the literature does not agree on the level of force to design for.

Various studies have estimated that the wrist experiences between 118-200 N during ordinary activities, which is the approximate load passing through the wrist when grasping a 1 kg load [1, 3, 49]. A cadaveric study found that the total static tendon preload just to hold the wrist in a neutral position was 74.2 N and found maximum tendon forces to just accomplish standard wrist movements approaching 250 N [55]. Recent finite element models showed startling results; during maximal grip loading, one study showed joint contact forces ranging from 1.5 to 2 times body weight (1200-1800 N) [58] and another study finding a total load of 647.5 N with just half of the maximum gripping force [47]. Previous finite element studies had applied forces up to 1000 N through the tendons [58]. Lastly, a non-invasive experimental study fitting a simpler 3 dimensional mathematical model to the wrist and elbow joints found wrist forces up to

2800 N for moderate activity, though the many avenues for experimental error to propagate lead one to caution concerning this study.

These differences need to be resolved before moving forward. As the implant is being designed for the healthy, young, adult male, forces much greater than those seen for simple wrist movement and low gripping force will be easily seen. The young male can be expected to regularly go through strenuous activity, such as weight lifting, pushups, basketball, football, etc. With this in mind, the implants should be designed to regularly accommodate forces of 1200 N (the lower bound of joint loading at maximal gripping force) [58] with extreme loads of 3600 N (3 times the standard loading). This will be used in the design section.

Axial Rotation torques

There was surprisingly little information on the axial rotation torques that the wrist alone goes through, so forearm torques were researched as almost all forearm torques must pass through the wrist in some form to reach the hand. The first study tested 51 men and women ranging from 22 to 45 years of age. The study found average peak torques (occurred in supination) for men to be 11.9 Nm +/- 3.7 Nm on the right side and 10.4 Nm +/- 3.3 Nm on the left side and for women 6.0 Nm +/- 1.4 Nm on the right side and 5.0 Nm +/- 1.2 Nm on the left side [59]. The other study obtained data on 24 male subjects with an average age of 24.6 years. They found that the mean maximum torques to be 16.2 Nm (in supination) which was in agreement with 3 similar studies [60]. Thus, a wrist implant should be designed to withstand wrist or forearm torques of 16.2 Nm: the simulation is based on the assumption that the young male wrist would routinely experience torques half of this value: 8.1 Nm. These are the external loads that will be applied for the simulations.

2.2.2 Bone Properties

Next, various properties of bone were needed to define a material for the implant to be inserted into. The properties of bone vary widely depending on gender, age, genetics, and physical history. In general, there are two types of bone: cortical and trabecular/cancellous. As seen in Figure 22, cortical bone is a dense, hard structure that forms the outer layer of bones, and trabecular bone is a more porous, soft structure that is found past the cortical layer [61, 64]. Table 1 summarizes some of the ranges of macroscale properties found for the two types of bones from one source [61]. What complicates this is that most of these properties depend greatly on the microscale, so the strength of bone is extremely localized and this could help explain the great variance in properties.

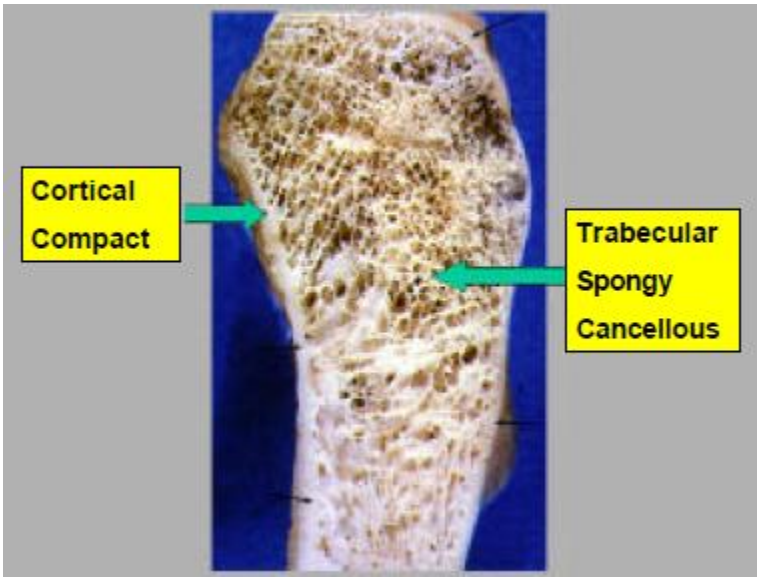

Figure 22: Cortical and trabecular bone structure [61]

Table 1: Bone properties summary [61, 63]

	Young's Modulus (GPa)	Shear Modulus (GPa)	Compressive strength (MPa)	Tensile Strength (MPa)	Shear Strength (MPa)	Density (g/cm^3)
Cortical Bone	4-27	2-9	30-160	45-175	50-70	1.8-2.2
Trabecular Bone	1-11		7-180			1.5-1.9

The main variable that affects bone properties is age as bone loses density over time as a result of various biological processes. The scale of bone loss can be seen in Table 2, with the T-score being the number of standard deviations from peak bone density of a young adult [62]. From the table, it can be seen that women experience much greater bone density loss over time. This most likely contributes to the fact that women have much greater rates of implant failure. Bone density loss results in reduced strength as there is less material to endure load.

Table 2: Effect of aging on bone density [62]

Age	Average Woman		Average Man	
	mg/cm2	T-score	mg/cm2	T-score
25	955	0	1055	0.81
35	943	-0.08	1038	0.67
45	920	-0.33	1002	0.38
55	876	-0.64	990	0.28
65	809	-1.19	969	0.11
75	740	-1.75	928	-0.1
85	679	-2.24	899	-0.78

Previous finite element simulations of the wrist have used values of 18 GPa and 100 MPa for modulus of elasticity (E) of cortical and cancellous bone, respectively, and Poison's ratio of 0.2 and 0.25 respectively [5, 47]. These studies were probably modeling an elderly or combination of male and female wrist as the value for Young's modulus of cancellous bone is much lower than any of the experimental studies. Instead, the lower end of the scale for Young's modulus for cancellous bone of 1 MPa from Table 1 will be

used as a conservative, yet more realistic, estimate for young male cancellous bone which is normally not osteoporotic and better able to self-heal [61, 63].

It has been shown previously that trabecular bone is both linearly elastic and fails at low strains, so it behaves like a linear elastic solid despite the complex microstructure. Also, for trabecular bone studies have strongly correlated density with Young's modulus, which reinforces the ability to compare cortical and cancellous bone (the main difference is porosity/density) [64].

The fatigue properties of bone are the unknown currently for good reason as it is very difficult to assign a set value for fatigue strength with all the variability in bone properties. A study on the fatigue strength of human cortical bone concluded that at infinite life the fatigue strength for bone is under 60 MPa for all modes of loading, and the fatigue strength in shear is actually about 20 MPa; cortical bone is three to four times weaker in shear [65]. Cancellous bone has undergone many fewer fatigue studies, with several studies focusing on FEA of individual trabeculae instead of the full bone structure [66]. Experiments have found both types of bone to experience creep (increasing strain with time at constant load) [63, 67] with the time to failure for trabecular bone fitting to Equation {1} where $\mathbf{T_B}$ is the time in seconds to fail, σ is the stress, and $\mathbf{E}_0$ is the modulus of elasticity [64].

$$\mathbf{T_B} = 9.66 \cdot 10^{-33} \left(\frac{\Delta\sigma}{\mathbf{E}_0} \right)^{-16.18} \tag{1}$$

However, further studies have shown that the residual strain accumulation is much more due to fatigue than creep for cyclic fatigue [64, 68]. The commonly used fatigue measurement is number of cycles to failure fitted by a power law equation similar to Equation (2) [64].

$$\mathbf{N_f} = \mathbf{X}\left(\frac{\Delta\sigma}{\mathbf{E}_0}\right)^{\mathbf{y}} \tag{2}$$

A comprehensive review and experiment concluded this relationship for cancellous bone to be fitted with Equation (3) (also depicted in Figure 23) [64].

$$\mathbf{N_f} = 4.70 \cdot 10^{-19}\left(\frac{\Delta\sigma}{\mathbf{E}_0}\right)^{-9.31} \tag{3}$$

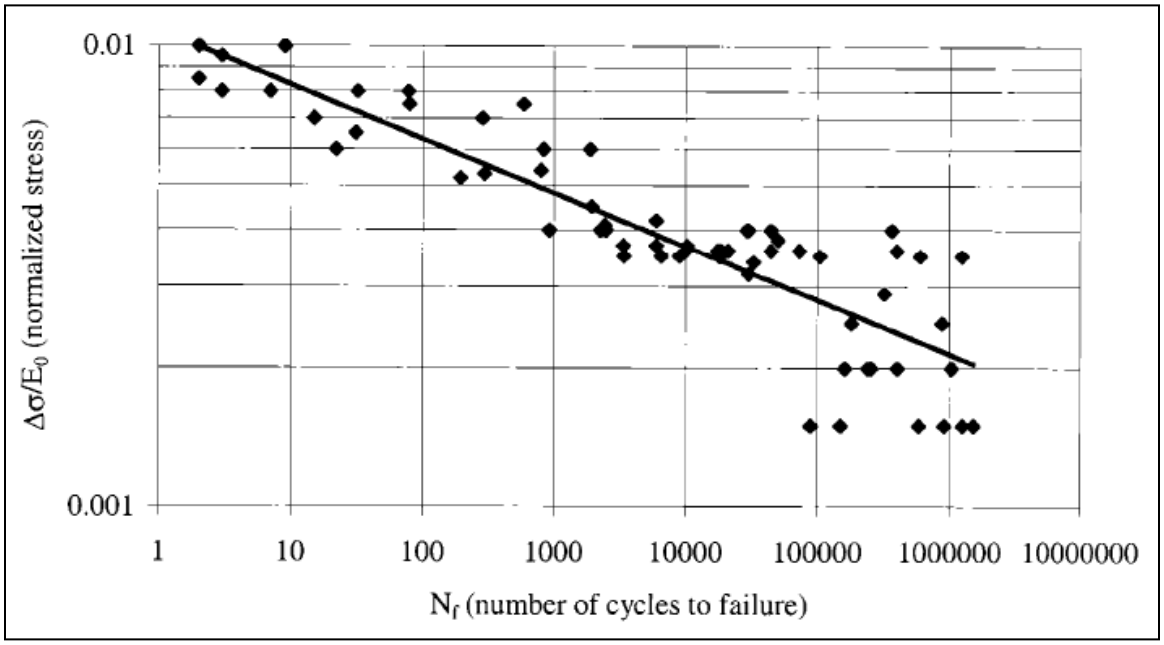

Figure 23: S-N curve for cancellous bone [64]

Though the study shows no such thing as infinite life for bone, an effective endurance limit for 1,000,000 cycles can be conservatively estimated at $\Delta\sigma / \mathbf{E}_0 \approx 0.0013$ (the lower limit of Figure 23). The normalized stress level, ratio of stress to modulus of elasticity ($\Delta\sigma / \mathbf{E}_0$), is the main focus. Essentially, the stress the bone can endure is directly proportional to the modulus of elasticity of the bone. Equation (4) is the final relationship for the endurance stress limit for cancellous bone [64].

$$\Delta\sigma \approx 0.0013 \cdot \mathbf{E}_0 \tag{4}$$

To model the bone, a solid block of cancellous bone is designed. There are several reasons for this; for current TWA, the most promising results are found when the carpal bones are fused by packing them with cancellous bone, which creates a solid bony mass for the implant to be screwed into. Also, the carpal bones are classified as small cuboidal bones, or short bones, with a thin cortical layer and mostly made up of cancellous bone. Thus, for computational efficiency, simplicity, and a conservative estimate, the bone into which the implant with be fixed is a solid cancellous mass. The key properties are summarized in Table 3**.**

Table 3: Summary of key bone properties [5, 47, 61, 63, 64]

Young's Modulus (GPa)	1
Poisson's ratio	0.25
Compressive strength (MPa)	7
Density (g/cm^3)	1.5
Endurance limit (MPa)	1.3

2.2.3 Building the bone mass

As mentioned earlier, a solid mass (rectangular prism) was used for the bone mass with holes for screws and carpal stem used to fixate the carpal component. The dimensions were determined using images from the visual human project [131] which is the National Library of Medicine's MRI and CT images of the representative male. The wrist width was found to be 4.4 cm, the thickness was estimated at 1.5 cm, and carpal depth was set at 4 cm. A second source agreed with the measurements as seen in the X-ray of a male hand and wrist (Figure 24).

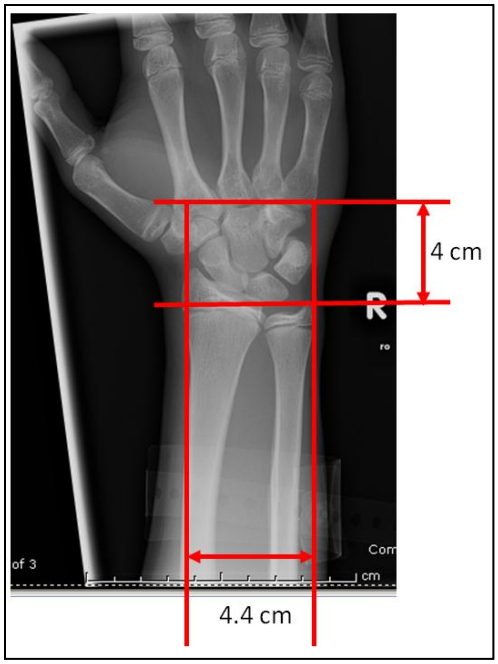

Figure 24: Male wrist X-ray [69]

Three holes were made in the bone mass: one 6.5 mm diameter hole for the central peg and two 4.5 mm holes 15 mm from the center on the sides for the screws. The central hole and one of the screw holes were 20 mm deep and the other screw hole was made 25 mm deep according to standard technique for the Universal 2 implant. As the exact thread geometry, pitch and other properties of the screws used in these implants were not known, the holes were left unthreaded. A model of the bone with these parameters was created using SolidWorks [70] model of the bone as shown below in Figure 25.

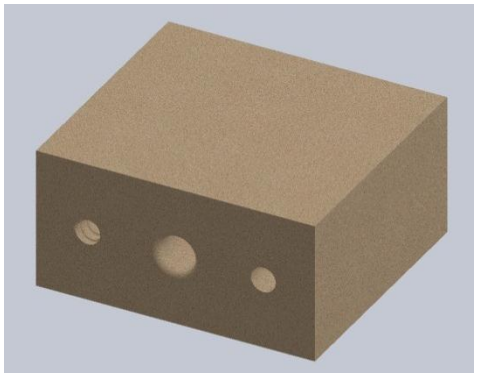

Figure 25: Carpal bone mass

2.2.4 Building a Carpal Assembly

The carpal assembly for a sample ellipsoidal wrist implant was modeled. Though no sample implants were available for measurement, the shape of the carpal plate and depth of the central pin and screws were approximated from radiographs and pictures of the Universal2 Total Wrist System. The screws and pins were designed to fit the holes. The carpal plate was made out of Ti-6Al-4V and the screws were assumed to be 316L stainless steel (some implants use titanium alloy screws). Figure 26 shows the final assembly. The dimensions are 4.4 cm x 1.5 cm x 4 cm.

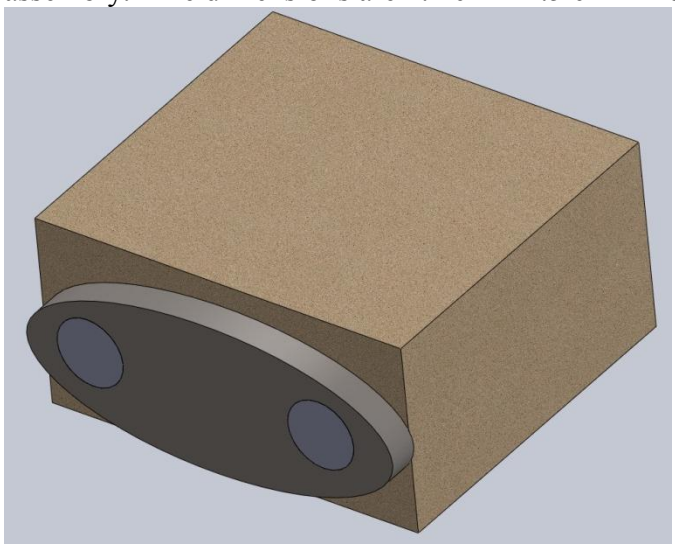

Figure 26: Carpal plate inserted into bone mass

2.3 ANALYSIS OF THE MODELS

2.3.1 Hand Calculations

To begin with, the extreme external load to be applied is the 16.2 Nm, and 8.1 Nm is the routinely experienced load as stated earlier in section 2.2.1. A moment can also be represented as a force couple using Equation (5) where M is the moment, F is the magnitude of the force couple, and s is the distance between the application of the forces.

$$M = Fs \tag{5}$$

In this case, the external moment acting on the carpal plate can be represented by a force couple at the two screw holes. The holes are each 15 mm from the center, so s is 30 mm. For the 16.2 Nm moment, the calculated forces are 540 N each based on Equation (5) (see Figure 27). Similarly, the calculated forces for the 8.1 Nm moment are 270 N each. Ideally, not all the torque would be handled by the screws, as most carpal plates are designed to resist wrist torques using friction between the carpal plate and bone; however, as soon as the screws loosen even slightly, the screw-bone interface becomes loaded as shown through Figure 27.

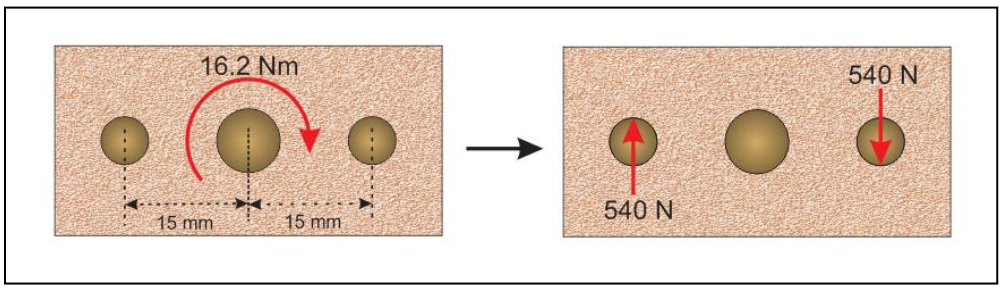

Figure 27: External moment to force couple

Hand calculations for the stresses assume the holes are not threaded and the forces are applied uniformly through the length of the holes. For the extreme loads, the stress

should not exceed 7 MPa, the conservative estimate for the compressive strength of cancellous bone (see Table 3). Using the basic equation for stress (Equation (6)) where σ is stress, F is the 540 N force, and A_N is the normal area, the minimal normal area can be calculated, which is the sum of the planar projections of half of the holes. The minimal area is 415 mm^2. Dividing this value by the diameter of the holes results in the length of the screw/hole required to handle the stress: 17.14 mm. This is less than the length of the smallest screw, so it should support this extreme loading based on the very conservative assumptions.

$$\sigma = \frac{F}{A_N} \tag{6}$$

For the fatigue case, the stress should not exceed the endurance limit for cancellous bone, which has been conservatively estimated to be 1.3 MPa (Table 3). Using the previous approach with a force of 270 N, the minimal normal area is calculated to be 208 mm^2, and the length of the screw/hole required to handle the stress in this case is 46.2 mm. This is over two times the length of the shorter screw, and thus fatigue failure/loosening can be expected in this case even with the conservative assumptions.

2.3.2 SolidWorks Simulations

A series of FEA simulations was conducted in SolidWorks to verify the hand calculations and further test the hypothesis. Von Misses stress were calculated and compared to the compressive strength (7 MPa) and endurance limit for the cancellous bone (1.3 MPa).

Simple Bone

This set of simulations applied forces on the bone mass itself and essentially validates the hand calculations. As shown in Figure 27, a simple vertical distributed load

was applied through the two holes on half of the face of each hole along the length of the holes.

Simple Bone - Extreme Case

For the extreme case, the 540 N force couples were applied as a distributed load in the holes and the results can be seen in Figure 28. In the shorter hole on the right, there are a few locations which exceed the 7 MPa compressive strength, which means there is a possibility for the bone to fail. However, most areas fall under the stress limit. This finding conflicts slightly with the hand calculations, since according to FEA some areas of the bone mass are likely to fail under this loading.

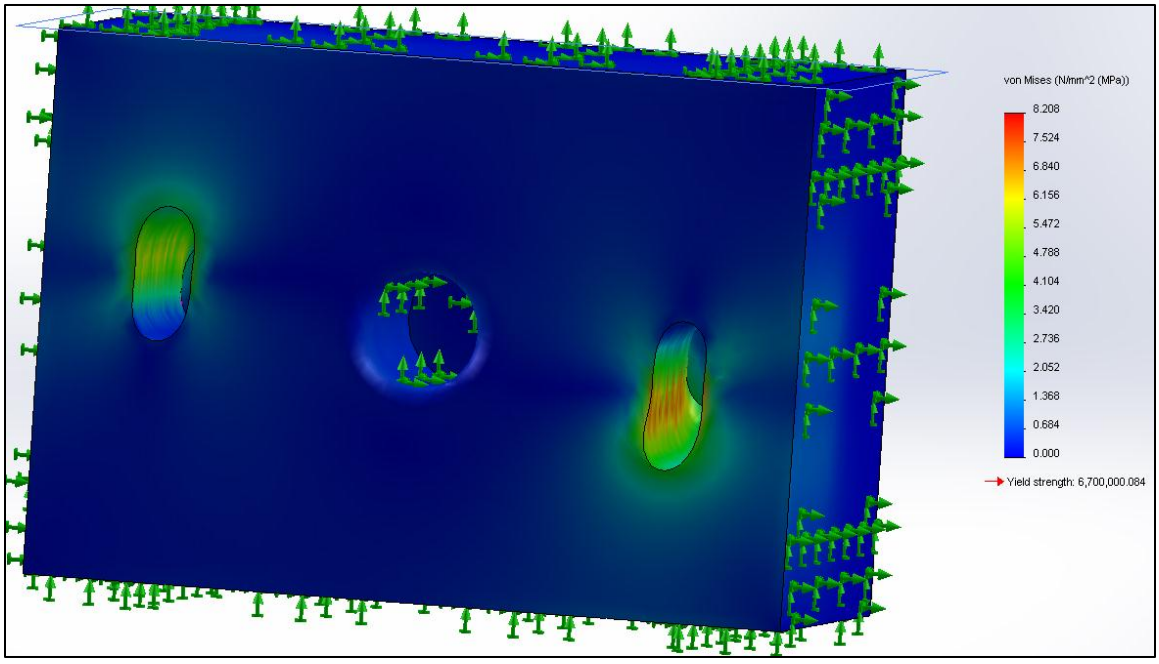

Figure 28: Simple bone, extreme case FEA results

Simple Bone - Fatigue Case

For the fatigue case, the 270 N force couples were applied as a distributed load in the holes and the results can be seen in Figure 29. In both holes it is easy to see many

locations that exceeds the 1.5 MPa endurance limit, as indicated by any area with a green, yellow and red color. Thus, the bone-screw interface is likely to fail in fatigue, which agrees with the hand calculations.

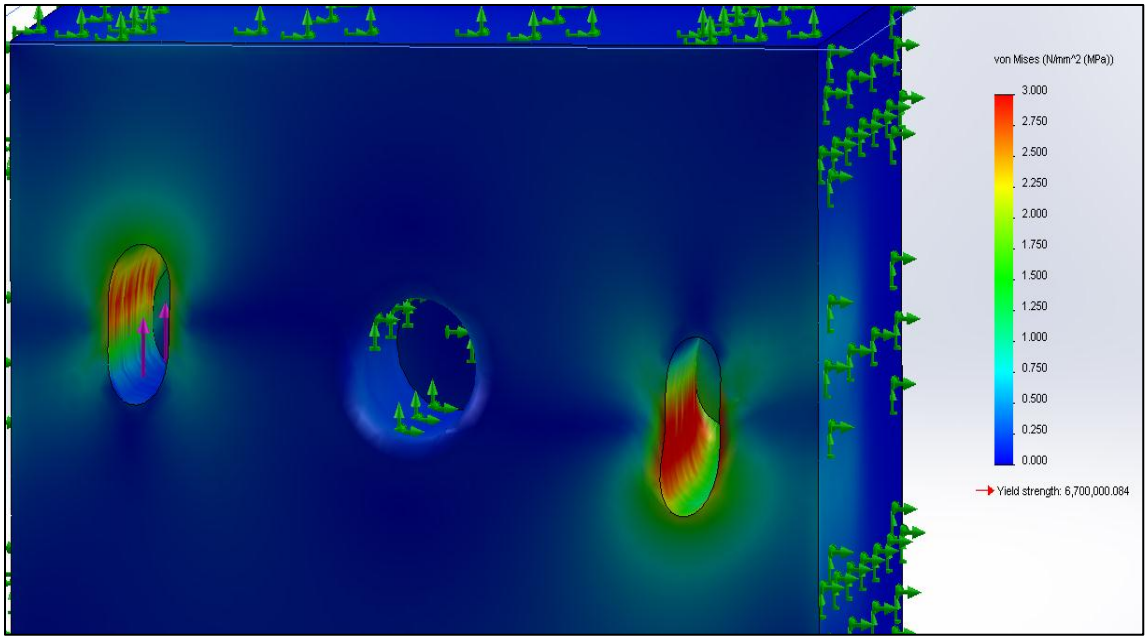

Figure 29: Simple bone, fatigue case FEA results

Screw-Bone Assembly

Figure 30 displays the next level of complexity in the simulations. The screws were inserted into the holes and represented as pin contacts as threads were not modeled. A miniscule gap was left between the bone and screws to represent the slight loosening overtime and friction effects were not modeled.

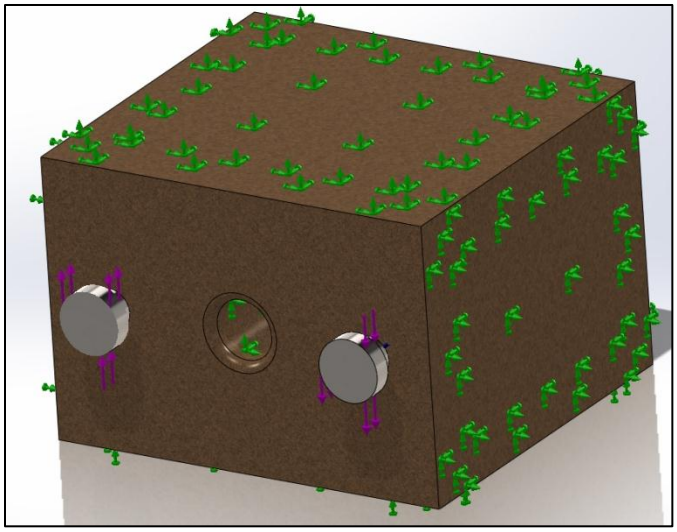

Figure 30: Screw-bone assembly

Screw-Bone Assembly - Extreme Case

Like before, 540 N vertical forces were applied, but this time on the screw heads as seen in Figure 30, and the FEA results are displayed in Figure 31. The screws are hidden to reveal the stresses in the holes. As expected the results differ from the previous cases in that the load in the holes is not a simple distributed load. The areas near the faces of both holes easily exceed the compressive strength value, unlike in the previous calculations. Also, the stresses in the hole decrease along the lengths of both holes. The bone is likely to fail very near the face in this case.

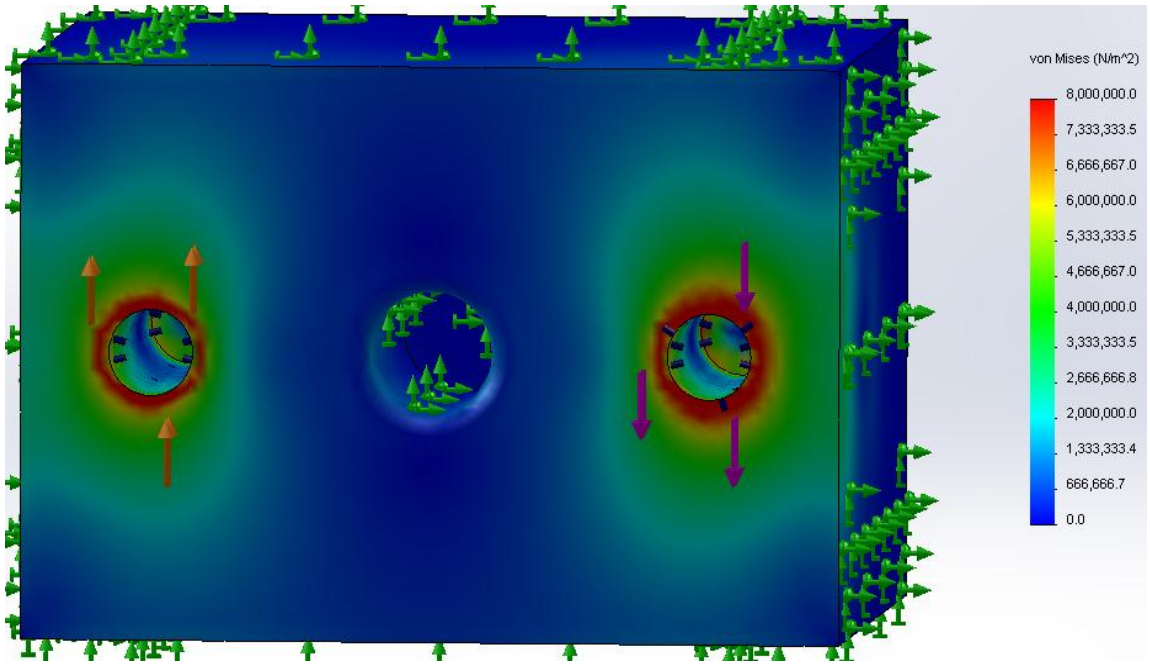

Figure 31: Screw-bone assembly, extreme case FEA results

Screw-Bone Assembly - Fatigue Case

A 270 N vertical force was applied to each screw head as seen before in Figure 30, and the FEA results are displayed in Figure 32. The bone is likely to fail in the hole near the face in this case as well as around the hole. These results are actually quite different from the simple bone case as most of the stress is seen at the face of the bone.

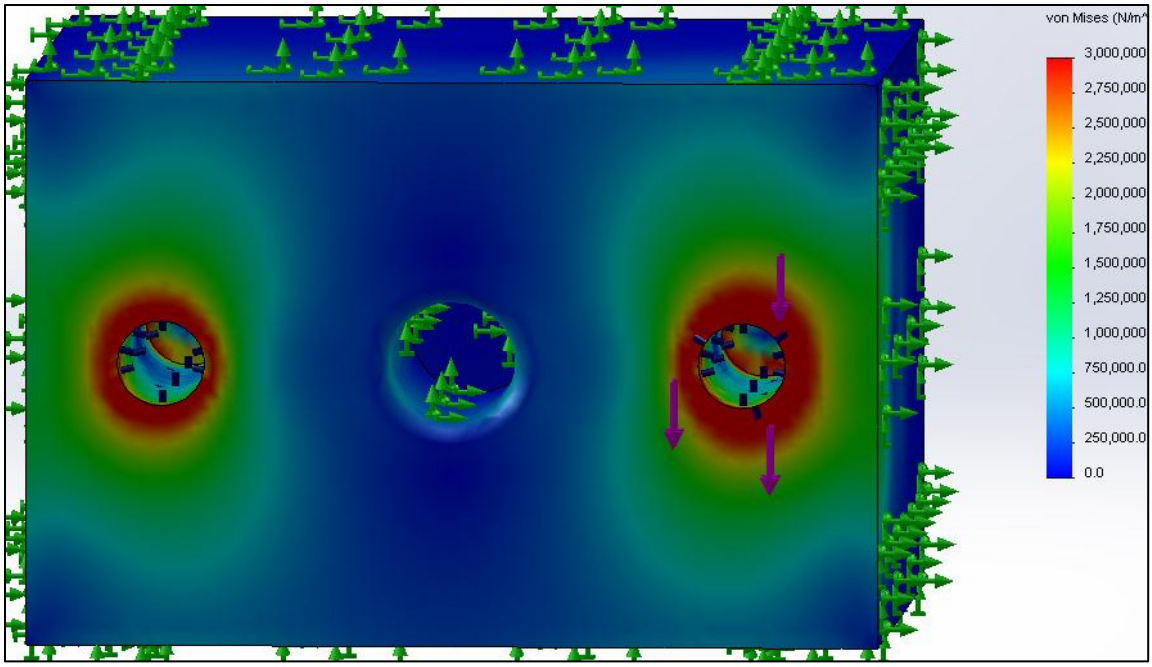

Figure 32: Screw-bone assembly, fatigue case FEA results

Full Carpal Assembly

The last case analyzed was the full carpal assembly that was shown in Figure 26 and is shown in its final form below in Figure 33. This is a unique simulation as torques were applied to the carpal plate, which were transferred through the screws into the bone as forces/stresses. As before, a miniscule gap was left between the plate and bone.

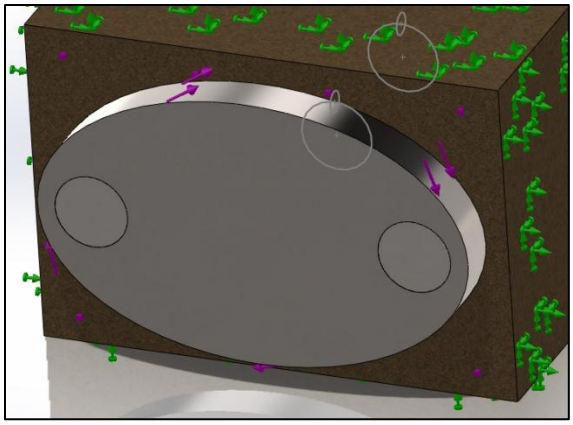

Figure 33: Full carpal assembly

Full Carpal Assembly - Extreme Case

For the extreme case, a 16.2 Nm torque was applied axially on the plate. Figure 34 displays the FEA results. As expected, the results look very similar to the screw-bone assembly simulation; stresses exceeding the compressive strength are seen at around the screw holes near the bone face and the bone will most likely fail near this location. The breadth of the area of highest stress is slightly reduced. Beyond the face the stresses are noticeably lower.

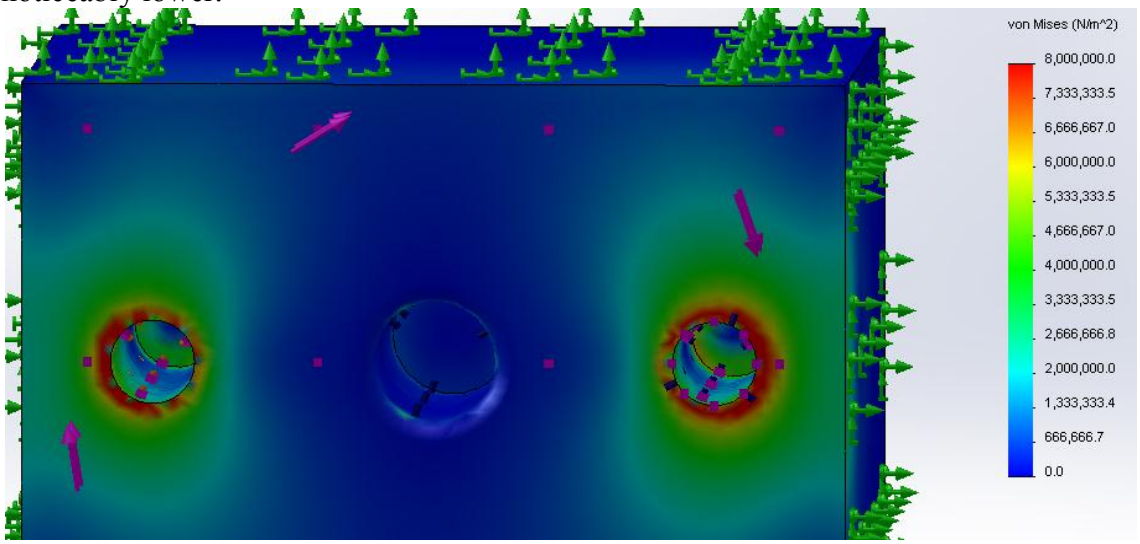

Figure 34: Full carpal assembly, extreme case FEA results

For sake of curiosity, the gap between the plate and bone was removed introducing some friction between the bone and plate to reduce or eliminate the loads on the screws. The FEA results are shown in Figure 35. The results surprisingly show an elliptical ring of stress levels greater than the compressive strength across the face. The ring is located at the edge of the plate. These results indicate that the bone will fail along the edge of the plate first, progressively failing towards the center of the implant. Eventually, a small gap would form between the plate and bone, which would result in the loading of the screw-bone interface. Note that this does not assume preloaded screws which would press the plate into the bone, though insight can be gained from this simple frictional case.

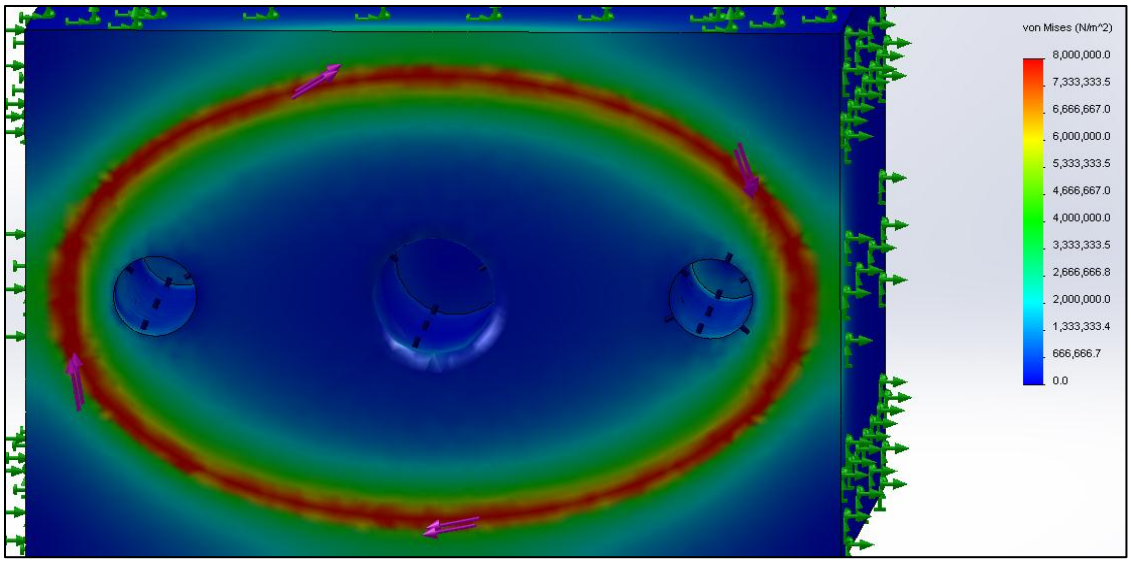

Figure 35: Full carpal assembly with plate friction, extreme case FEA results

Full Carpal Assembly - Fatigue Case

For the fatigue case, a 8.1 Nm torque was applied axially on the plate. Figure 36 displays the FEA results. Once again, the results look very similar to the screw-bone

assembly simulation. Stresses exceeding the endurance limit are seen at around the screw holes near the bone face, and the bone will most likely fail in fatigue near this location. Excessive stresses exist throughout much of bone.

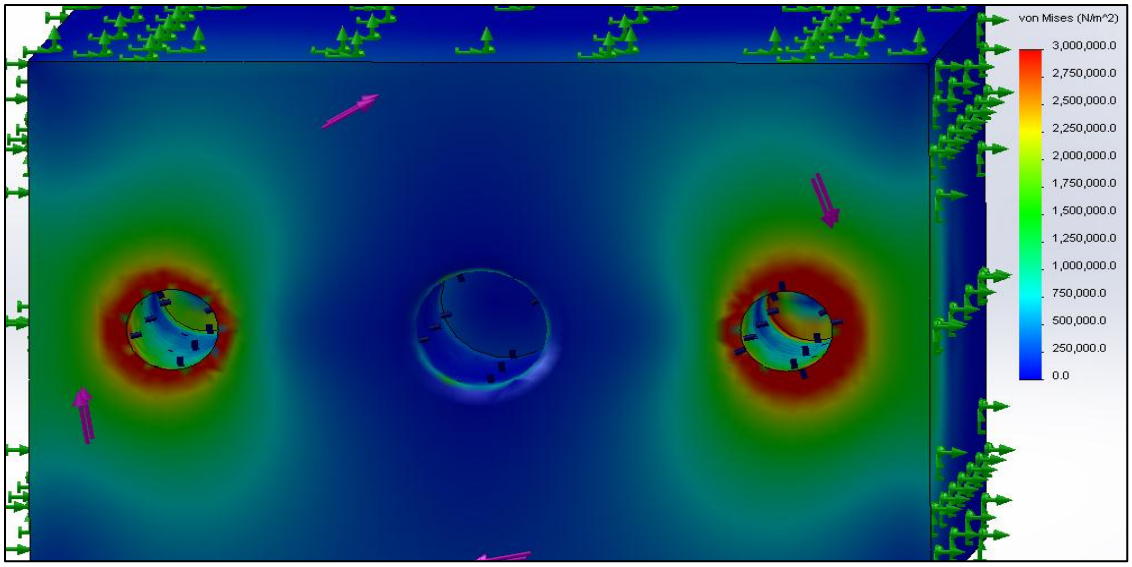

Figure 36: Full carpal assembly, fatigue case FEA results

Summary

From these SolidWorks FEA simulations, it is almost certain that the area around the holes near the bone face will fail in both fatigue and extreme load cases based on the assumptions. Similar simulations were conducted in ANSYS [130], and the results were in agreement. This verifies that an ellipsoidal implant will see substantial additional stresses compared to those seen in a ball and socket type wrist implant.

2.3.3 OpenSim Simulations

The open-source musculoskeletal modeling software OpenSim was used to create musculoskeletal models and conduct simulations to compare the required muscle forces and joint reactions for ellipsoidal type and ball and socket type wrist implants. The range

of motion differences between an original wrist model and the new models with the implants were also compared to predict the effects these implants will have on the motion of the wrist.

Methodology and Model Creation

An original model built by Gonzales et al. was modified [71] (Figure 37). This model consisted of all the bones in the arm with 10 total degrees of freedom and 23 Hill-type muscle actuators. The Hill-type muscle actuator is a commonly used muscle model that simplifies the muscle into a three-element model composed of a contractile element and two non-linear spring elements, one in parallel and one in series. The model approximated the wrist with a complex combination of revolute joints.

Figure 37: Original Gonzales et al. wrist model [71]

For the new models, all of the muscle actuators except the five prime wrist movers were removed: ECU (extensor carpi ulnaris), ECRL (extensor carpi radialis

longus), ECRB (extensor carpi radialis brevis), FCU (flexor carpi ulnaris), and FCR (flexor carpi radialis). Most of these muscles can be found in Figure 3. All joints other than the wrist were locked. The original wrist joint was replaced by the new wrist joints with centers of rotation at the head of the capitate; the ball and socket joint allowed rotation in all three axes (flexion-extension, radial-ulnar deviation, and axial rotation), and the ellipsoidal joint restricted axial rotation. The carpal bone relations were removed as they did not play a role in the movement for the new models. The masses of the bones were assigned as they were ignored in the original model, which had made simulation impossible. Using data from a comprehensive study, the mass of the ulna, radius, and hand were approximated; the center of mass of the hand was placed below the proximal end of the 3rd metacarpal [72]. Figure 38 shows the new model.

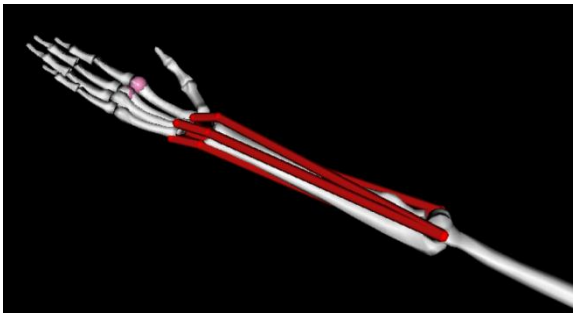

Figure 38: New wrist model

A motion analysis was conducted to compare the new models with a single center of rotation to the original model. Markers were placed at the ends of the 2nd and 3rd metacarpals in the ellipsoidal and original model as these points are commonly used in experiments to track wrist motion [73]. The positions of the points were tracked for both models through a FEM arc of 140° and a RUD arc of 55°.

The muscle forces required to produce simple movements for ball and socket and ellipsoidal models were then compared. These movements were extension and flexion (both 0° to 60°), radial deviation (0° to 25°), and ulnar deviation (0° to 35°), and all were carried out within one second. A motion file was created to track a standard arc for each type of motion. Computed muscle control was used to determine the muscle activations to accomplish the desired movements. As the desired movements only involved changes in one degree of freedom at a time, the tracking file emphasized tracking that degree of freedom foremost and gave some weight to the other degrees of motion to reduce changes in those variables.

Lastly, joint reaction forces and torques were compared for the two new models.

Results and Discussion

Motion Evaluation

The plots in Figure 39 compare the motion of the 3rd metacarpal marker in the two models. For all motions, the original and new models compare very well at the equilibrium position and deviate greater moving away from the equilibrium position. Despite sizable differences at extreme positions, simple ellipsoidal and ball and socket joints approximate the wrist joint very well for non-extreme degrees of wrist FEM and RUD. Decreased total range of motion could be explained from this analysis: the natural human wrist does not resemble a ball and socket or ellipsoidal joint at extreme ranges of motion.

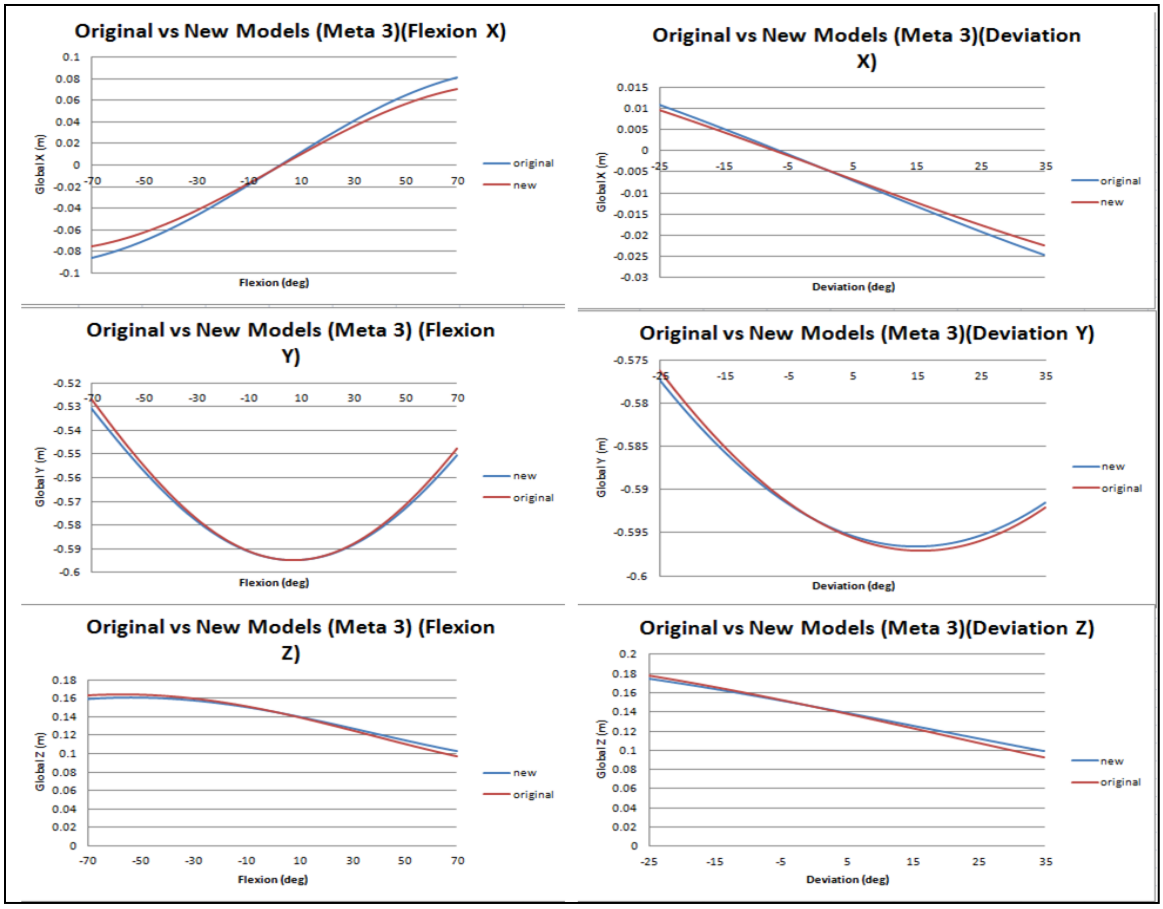

Figure 39: Comparing global position of 3rd metacarpal marker through FEM and RUD in orignal and new models

Muscle Force Differences

Figure 40 compares the total muscle forces for each movement. The greater forces up to about 0.3 seconds are from the muscles stabilizing the non-anatomical wrist. From 0.3 seconds onward, the forces are more representative of those required to carry out the desired movements. For flexion and extension, the ball joint requires slightly more total muscle force to carry out the extreme movements. However, for radial deviation, the ball joint consistently requires less total muscle force, and for ulnar deviation it requires much less force for the ball joint model to complete the motion.

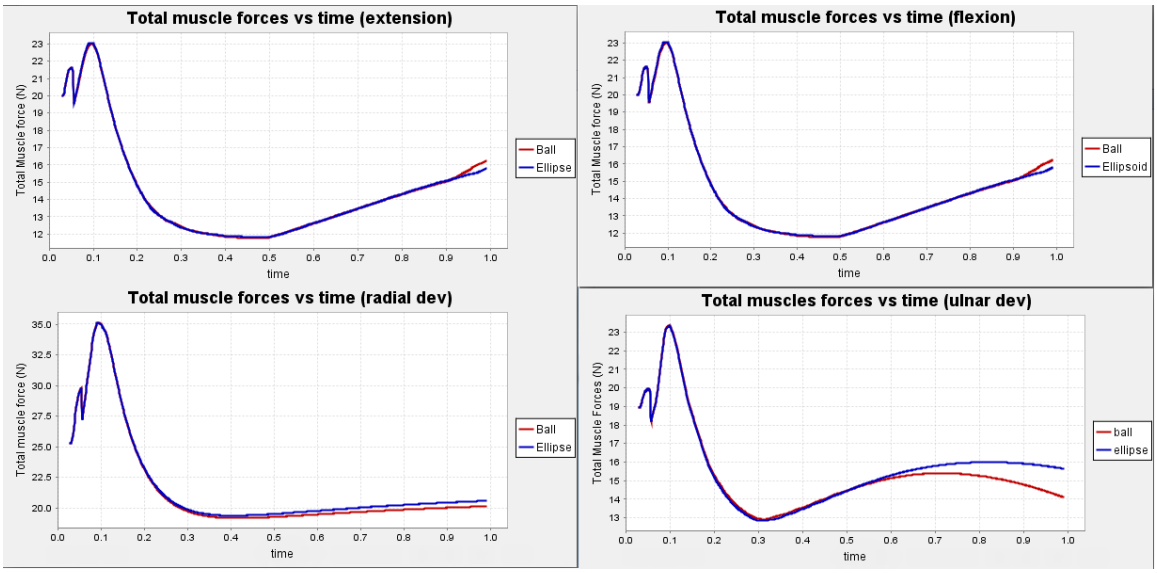

Figure 40: Total muscle force comparison

For flexion and extension, the ball and socket model may require more muscle force to stabilize the wrist at extreme positions, while the ellipsoidal joint passively handles axial rotation. On the other hand, for radial and especially ulnar deviation, the slight amount of rotation offered by the ball and socket design allows the motions to be completed with greater ease, due to changes in muscle moment arms and lines of action. This agrees with Crisco et al. as natural ulnar deviation occurs with a small degree of axial rotation, which reduces the muscle force required to accomplish the motion [56].

Joint Reaction Differences

Consistently, the joint reaction forces were slightly lower in magnitude for the ball and socket joint than for the ellipsoidal joint at the higher wrist angles as seen in Figure 41. This was due to the wrist undergoing a small degree of rotation at extreme ranges of motion and the moment arm of certain muscles changing.

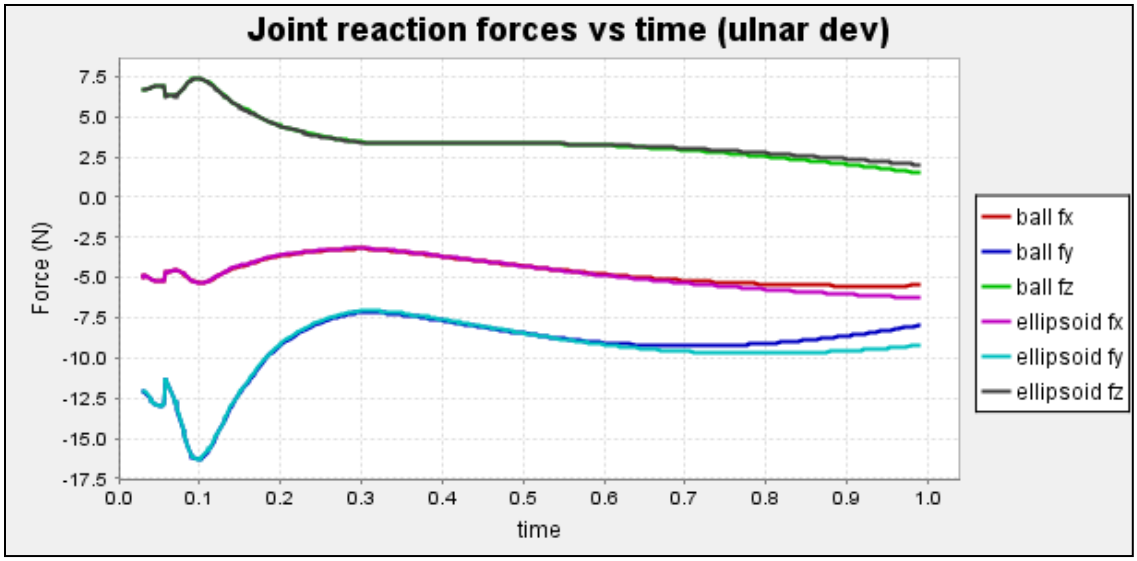

Figure 41: Joint reaction force comparison for ulnar deviation

The most significant difference is in the joint torques. As the ball joint does not constrict rotation in any direction, there were no joint reaction torques. The ellipsoidal joint saw torques over 0.035 Nm for every motion, with ulnar deviation exhibiting the greatest reaction torques (greater than 0.06 Nm) as seen in Figure 42. Conservatively assuming that a screw required to attach the implant is located 1.5 cm from the center of rotation, the wrist would routinely see forces greater than 2 N at the screw-bone interface. This is very significant because this translates into additional stress at the implant-bone interface. Cyclical stress at this interface causes loosening of the implant, which ultimately results in failure.

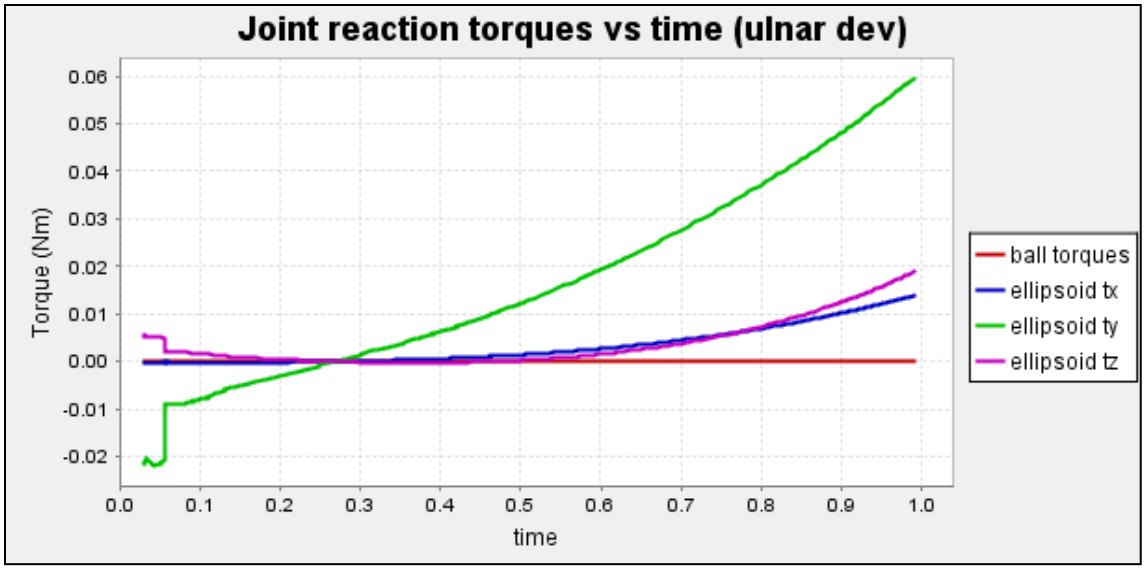

Figure 42: Joint reaction torque comparison for ulnar deviation

Limitations and Future Work

There were several limitations to this study. To begin with, due to the lack of motion capture instrumentation, the new models were compared to the motion of the original model which the authors admit is not fully anatomical. This said, the comparison was still useful as it helped explain why range of motion for these types of implants is less than that of the normal wrist. It would be helpful to compare this model to motion capture data from healthy, normal wrists.

Second, the model was built with only the five muscles required for wrist motion. This was justified by the fact that many experimental studies have used these five main muscles/tendons to perform wrist motion [74]. In vivo, people may use other tendons, such as finger flexors, to carry out the movements, but the majority of forces for these movements come from five main muscles.

The muscle properties and bone masses, moments of inertia and center of masses were estimated in this study. The muscle properties were imported from the original

model, and the mass properties were estimated using the study mentioned earlier [10]. In the future, it would be helpful to create models based on cadavers for greater accuracy.

Lastly, the simulations were unloaded in that there were no external loads applied. Applying external forces and torques in the future would provide insight on how these loads are handled by the wrist based on the type of implant. This could help elucidate why and how these implants fail.

Summary and Conclusion

The ellipsoidal joint based wrist prosthesis offers good stability by preventing axial rotation; however, it exhibits greater muscle forces for radial and ulnar deviation, often exhibits greater joint reaction forces, and has to endure notable joint reaction torques even for simple, unloaded movements. These factors may help to explain some of causes of the early failures of ellipsoidal joint wrist prostheses while providing evidence for better performance by for ball and socket joint wrist prostheses.

2.4 HYPOTHESIS AFFIRMED

As seen in the finite element simulations, it appears likely that the area around the holes near the bone face will fail in routine and extreme situations for ellipsoidal implants. From the OpenSim simulation study comparing the ellipsoidal and ball joints, it was also shown that the ellipsoidal joint exhibited greater joint reaction forces and torques. Thus, the hypothesis is affirmed: implants that restrict axial motion will loosen and fail over time due to the stresses due to the prosthesis preventing wrist rotation and transferring stresses to the bone-prosthesis interface. The next chapter describes the design of a new wrist implant system which improves on the current gold standard and uses a ball and socket type contact surface.

CHAPTER 3

DESIGN

3.1 DESIGN CRITERIA

To begin the design of the new prosthesis, a set of specifications must be identified. As this is not the first wrist prosthesis made, various options exist for design criteria for this type of prosthesis. Based on reviews of relevant literature and of previous prostheses, design criteria were chosen and are discussed in this chapter. . These criteria involve material selection, desired range of motion, maximum dimensions for the implant, kinematics, and strength of the components. The final subsection summarizes the design criteria in a concise table for easy reference.

3.1.1 Material Selection

The material for the four major components had to be determined: screws or pins, carpal and radial stems, and the articulation surface. There are many new experimental materials being tested and these will be discussed, but for the current design only materials that meet ASTM Standard F1357 are recommended for easier government approval for human testing [75].

Screw Material

The fixation technique may be the area with the greatest need for new materials. Currently, most implants use titanium or titanium alloy screws with older or cheaper designs using stainless steel screws. Often, an osseointegrative coating is applied to the screw, which encourages bone ingrowth to better anchor the screws; titanium is naturally osseoinductive, but the more bone ingrowth, the stronger the fixation. Several studies have shown that osseointegration of screws is essential for prevention of loosening and bone resorption [17, 28, 32, 76-77].

Though screw material has evolved greatly from the steel screws that were originally used, there is still much room for improvement. Screw breakage has not been much of a problem, but screw loosening is the main problem still faced today. Stress shielding is partly responsible for this. Stress shielding occurs when a material harder than bone, such as titanium or steel, is inserted into bone. The harder material absorbs most of the stresses and causes the bone to disintegrate or resorb as the body perceives that less bone strength is required in that area [78]. This bone disintegration and resorption causes bone loosening and weakening of the bone implant interface.

The solution to stress shielding is using screws with hardness similar to that of bone. The problem is currently there are no screw materials that match the strength of the titanium alloy screws used now with the hardness level of bone. Currently, research is being done to produce polymer screws that fit these conditions, but a solution has yet to be identified.

For the implant designed in this research, Ti-6Al-4V alloy is chosen for the screw material in accordance to the ASTM standard. An osseointegrative coating such as Bonit or calcium phosphate will be applied to promote bone ingrowth and reduce the chance of loosening [45].

Carpal Plate and Radial Stem Material

In the past, 316 L stainless steel, cobalt chromium, titanium, and titanium alloys have been commonly used for stem materials. 316 L stainless steel, also known as surgical steel, is very biocompatible and corrosion resistant; however, lighter, softer and stronger materials are available now. Stainless steel is still used when low cost and manufacturability are the most important requirements. Cobalt chromium has excellent mechanical properties and also forms an oxide layer for corrosion resistance. Of all the

materials considered here, it has the greatest wear resistance, so it is commonly used for bearing surfaces. Titanium is very light and biocompatible, but has poor mechanical strength. Titanium alloys such as Ti6Al4V and Nitinol overcome this strength issue. One of the key advantages of titanium and its alloys is that they have relatively low stiffness for metals and thus limit stress shielding in bone. One disadvantage of this group of materials is that they have poor tribological properties, so they are generally not used for bearing surfaces [79].

For this design, the carpal and radial stem will be made of a similar material as the screws since they both contact bone and require stable fixation. The Ti-6Al-4V alloy with the osseointegrative coating will be used for these components for the same reasons as the screws. A composite or polymer material with a hardness similar to bone and a strength similar to the titanium alloy would be preferred, but as of yet such a material is not approved for use and may not exist.

Articulation Surface Material

Most of the advances in articulation surface materials have come from innovations in the hip and knee prosthesis fields. The current gold standard for articulation surface design is a metal-polyethylene interaction where one material articulates against the other. This material combination gained popularity from the Charnley low friction arthroplasty total hip replacement, which had a metal ball that articulates against an ultrahigh molecular weight polyethylene (UHMWPE) cup [80]. Its low friction, self-polishing nature, and seemingly long life lead to increased popularity of this articulation surface type. The gold standard in wrist arthroplasty, the Universal2 Total Wrist System, has this type of articulation, along with almost every wrist implant produced currently. There have been advances in the plastic to improve wear resistance

by using highly cross-linked UHMWPE which has shown reduced wear. Also, the most common metal used is now cobalt-chromium alloy for its wear resistance and excellent tribological properties. Despite these improvements and the benefits of this combination of materials, the issue of polyethylene wear is very significant. It is known that polyethylene wear particles cause periprosthetic osteolysis, in which the bone around the implant begins to disintegrate in reaction to the wear particles [81, 82]. This is often the main limit in the life expectancy of hip and knee implants, especially in young patients. The same problem will be seen in wrist implants as they age.

There are several new articulation surface combinations that attempt to address these problems, including ceramic-on-polymer, ceramic-on-ceramic, ceramic-on-metal, and metal-on-metal. These have been studied for total hip replacements.

Ceramics have several pros and cons for articulation surface use. They are highly inert, so wear particles are much less likely to cause osteolysis. Because they can be manufactured with excellent surface finish and are very hard, ceramics have excellent tribological properties and wear resistance in the body. Ceramic-on-polymer jointsshows similar wear to the metal-on-polymer articulation *in vitro* operating in mixed lubrication, but 50% less wear has been seen *in vivo* in many cases. Ceramic-on-ceramic articulation can operate in the fluid-film lubrication regime in many circumstances (minimum wear); one drawback is if the two surfaces touch, there is a considerable increase in friction and wear. Lastly, ceramic-on-metal joints show interesting potential in that the ceramic heads act as fine polishing stones on the metal cups and steadily improve the surface finish and lubrication. Findings have been promising, though wear does not match that of the ceramic-on-ceramic combination. [80]

Despite these advantages, the drawbacks must be considered. In the past, fracture was very common with ceramics due to the brittleness and low toughness of most

ceramics. This has been largely solved with material advances in grain alignment, using zirconia over alumina for greater fracture toughness, precise manufacturing, and controlled surface finish, but it remains a concern with most metals used in the field showing much great fracture resistance [81, 83]. Ceramics also cannot be implanted directly into bone due to their extreme hardness resulting in stress shielding, so they usually have to be attached to a metal stem. Lastly, because of the high cost they may be prohibitively expensive in many cases.

Metal-on-metal articulation was originally a failure with the first steel on steel implants. Bad tribological properties, surface finishes, manufacturing and material choice were responsible for this failure, but these issues have been addressed [81, 83]. With advances in manufacturing, joint clearances have been greatly reduced and surface finishes have been improved. New metals, especially cobalt-chromium alloys, exhibit excellent tribological properties, with self-healing ability. The main drawback with metal-on-metal articulation is that the wear particles may be poisonous or cause osteolysis. Thus, minimized wear is a key requirement. Current metal-on-metal hip implants exhibit very little wear, with the Metasul coupling producing 100-fold less wear debris than metal-on-polyethylene coupling; however, heightened traces of cobalt and chromium are found in the blood of patients [82, 81]. Coatings to increase wear resistance are a feasible solution; currently, titanium nitride and chromium nitride coatings have seen success in cobalt-chromium alloy articulation [80, 45]. One interesting feature seen in the highly successful Metasul hip replacement was a polyethylene liner between the metal cup and metal head and stems to dampen impacts; this may reduce the stress at the implant-bone interface [81].

For the articulation surfaces for this wrist implant, cobalt chrome molybdenum alloy will be used with chromium nitride wear coatings similar to the MOTEC wrist joint

prosthesis [45]. This is because all these materials meet ASTM F1357 and the MOTEC prosthesis has demonstrated good results from this articulation surface. In the future, zirconia on this metal and zirconia-on-zirconia articulation surfaces would be interesting to investigate for this prosthesis.

Material Selection Summary

For the screws, Ti-6Al-4V alloy will be used with an osseointegrative coating such as Bonit or calcium phosphate. For both stems, the same material as the screws will be used to promote osseointegration. Lastly, for the articulation surface, cobalt chrome molybdenum alloy with chromium nitride wear coating will be used.

Some of the key properties of the metals are summarized in Table 4. Stainless steel for biomedical applications is also included for a baseline comparison of the properties.

Table 4: Metal properties [84- 87]

	Metal		
	Ti-6Al-4V	Cobalt-Chromium	Stainless steel (18-8)
Elastic Modulus (Pa)	1.05E+11	2.34E+11	1.93E+11
Poisson's ratio	0.31	0.31	0.31
Density (kg/m^3)	4428.78	8500	8000
Tensile strength (Pa)	8.27E+08	9.44E+08	6.17E+08
Yield Strength (Pa)	1.05E+09	6.11E+08	2.75E+08
Fatigue strength (Pa)	2.40E+08	2.07E+08	2.70E+08

3.1.2 Desired Range of Motion

As the main advantage of wrist arthroplasty over fusion is wrist movement, the necessary range of motion is an important design specification. There is considerable conflict in the literature for the required range of motion in the wrist to accomplish most

daily tasks. Most papers on wrist implants cite the Palmer minimum range of motion of 30° extension, 5° flexion, 10° radial deviation, and 15° of ulnar deviation to accomplish daily tasks [23, 25, 34-35, 42]. Conversely, studies by Shepherd et al. concluded that daily activities could be achieved with just 6° extension, 5° flexion, 6° radial deviation, and 6° of ulnar deviation [41]. Similarly, another study determined essential wrist motion to be 5° flexion, 6° extension, 7° radial deviation, 6° ulnar deviation, and, notably, 7° radiocarpal rotation, which means some axial rotation is desired [1]. Lastly, a comprehensive study on the required range of motion for daily living determined that all common activities could be accomplished with 60° extension, 54° flexion, 17° radial deviation, and 40° of ulnar deviation, and most of the activities can be accomplished with 40° extension, 40° flexion, 12° radial deviation, and 28° of ulnar deviation [41, 88]. After reviewing each source and how each source arrived at the desired range of motion, the last range criteria was found to be the best compromise. So the final range of motion specification for this implant will be 40° flexion, 40° extension, 12° radial deviation, and 28° ulnar deviation. Depending on orientation of the ball and socket joint in the wrist a greater range for radial deviation up to 28° can be accepted for symmetry in RUD.

Table 5 provides a comparison of the average ranges of motion *in vivo* of other implants for comparison. As can be seen, none of these implants matched the resolved required range of motion for daily living, but some designs did come close, such as the Trispherical, Biaxial, and Universal [41]. The RUD range seems to be the hardest to meet, especially ulnar deviation. With this in mind, the goals set can be expected to be difficult to reach *in vivo*.

Table 5: Ranges of motion of various wrist implants and the normal wrist [41]

	Flexion (°)	Extension (°)	Radial deviation (°)	Ulnar deviation (°)
Normal wrist	76	75	22	36
Swanson	39	6	-2	21
Meuli	30	40	10	10
Volz	32	17	2	23
Universal	41	36	7	13
Biaxial	29	36	10	20
Trispherical	50 Total (Flex + Ext)		10	10

3.1.3 Maximum Dimensions of Package

To preserve as much bone as possible and prevent soft tissue damage, the total implant package should be as small as possible. The distal rim of the radius must be preserved at all costs as damaging this area harms the essential wrist tendons attached there [23]. The goal is to limit the size of the prosthesis such that the bone resection required is no more than that required for the Universal2 TWA, which preserves most of the capitate and removes a plane of bone as shown in Figure 43.

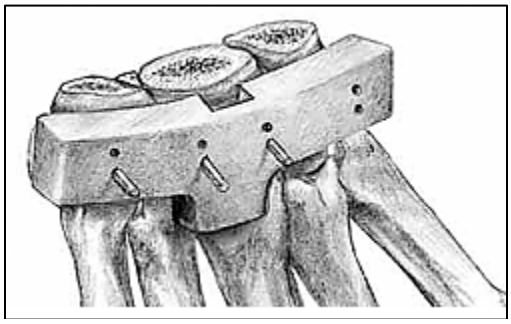

Figure 43: Universal2 TWA carpal bone resection [89]

In this case, using a normal male wrist, hand, and forearm based on the representative X-ray from the previous section shown below in Figure 44 the maximum

dimensions of the implant are established. The maximum envelope of the TWA package is 2.5 cm long along the axis of the wrist, 4.4 cm wide, and 1.5 cm deep.

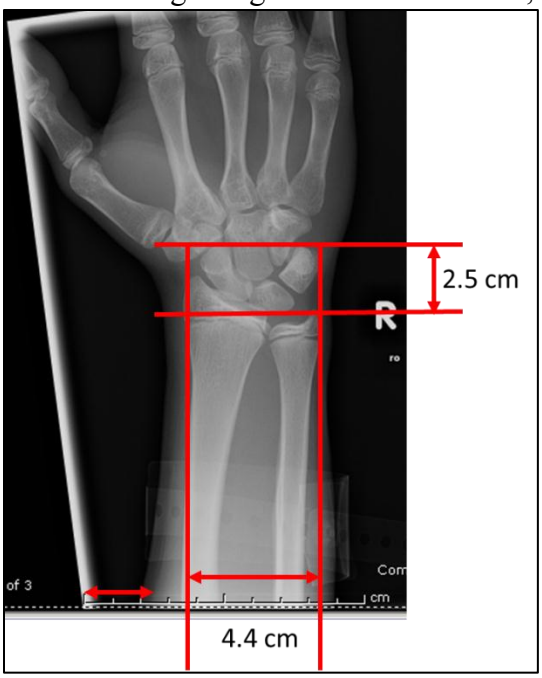

Figure 44: Maximum dimensions of TWA package [69]

3.1.4 Kinematics

The natural wrist has very complex kinematics with many bones articulating against each other causing unusual contact dynamics. As of yet, a full picture of wrist kinematics has not been developed due to the complexity of 8+ bones articulating against each other in various movements [90-91]. In reality, the natural wrist exhibits complex motion with rotation around a helical axis, whose position and orientation changes during movement and loading [92]. In order to design a suitable joint prosthesis, a simple yet sufficiently accurate approximation of the wrist must be made. There are several suggestions for the best approximation of the wrist. Currently, the most widely accepted model consists of two revolute joints obliquely oriented with some separation between the axes which is represented by a skew-oblique universal joint [54, 56, 92-94]; this is

illustrated in Figure 45. This is a fairly accurate approximation for the wrist; however, this type of joint has several drawbacks in this application. As discussed earlier, the fixed joint type prostheses have had much greater failure rates at the bone-implant interface due to the excessive constraint forces introduced by the joint. Also, the skew separation between the two axes varies greatly between subjects, so the implants would have to be specifically modified for each patient or many variants would have to be mass produced.

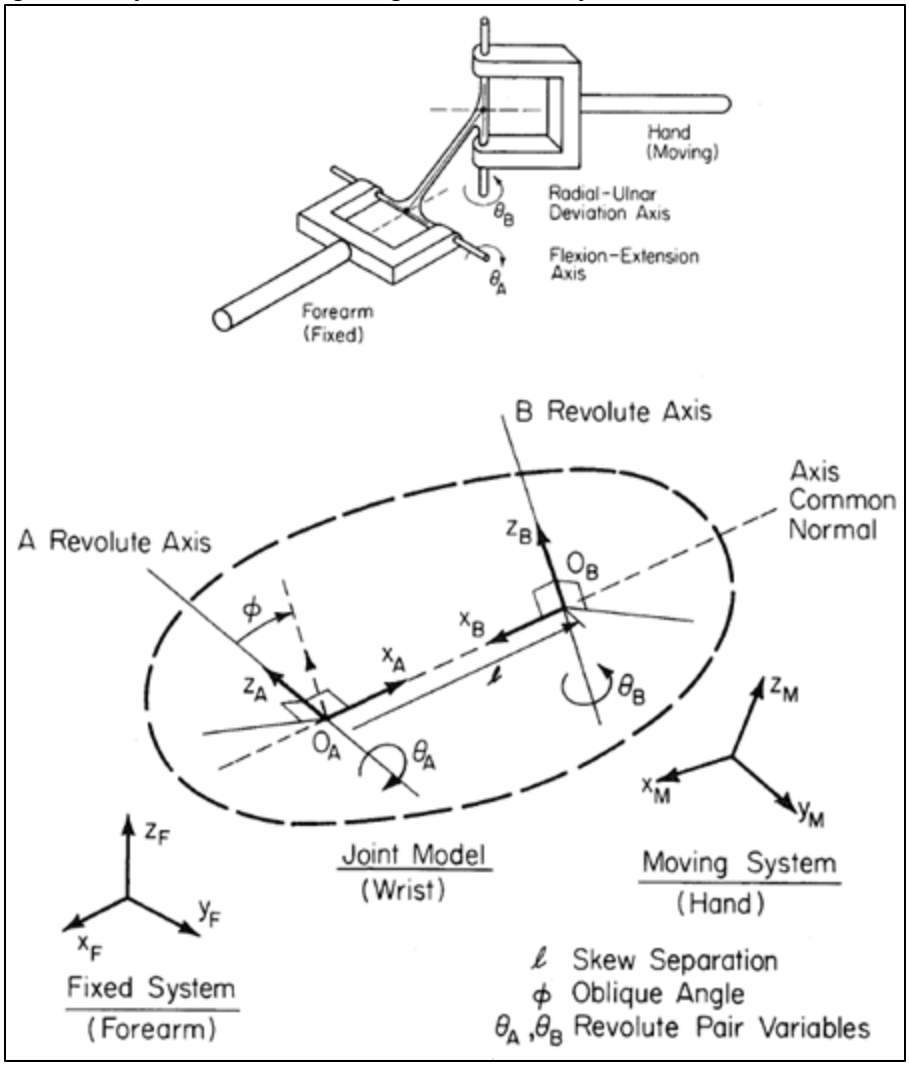

Figure 45: Skew-oblique universal joint wrist approximation [93]

The historically accepted approximation for the wrist is a universal joint with the center of rotation located near the head of the capitate bone [73, 95]. As shown in Figure 46, the center of rotation in RUD is located about ¼ of the capitate length distal to the proximal head of the capitate and the center of rotation in FEM is located on the proximal head of the capitate. These distances are often approximated as a single center of rotation in the proximal head of the capitate. As demonstrated in vivo, current implants with a ball and socket or ellipsoidal joint and a center of rotation located as stated have shown much better performance than early implants [27]. The main advantage of having a single center of rotation is that it allows the use of ball and socket and ellipsoidal joints which are only semi-constrained, compared to the universal joint which is fully constrained [27]. This allows the muscles and soft tissues to absorb some of the forces that would otherwise be transmitted to the bone-implant interface. The main drawback is a less natural range of motion, but most patients are very satisfied with the stability and range of motion of current implants; durability and pain relief are the immediate concerns [3, 21]. The new implant will be designed with a single center of rotation placed in the proximal head of the capitate approximately 1/8 of the length of the capitate distal to the proximal end.

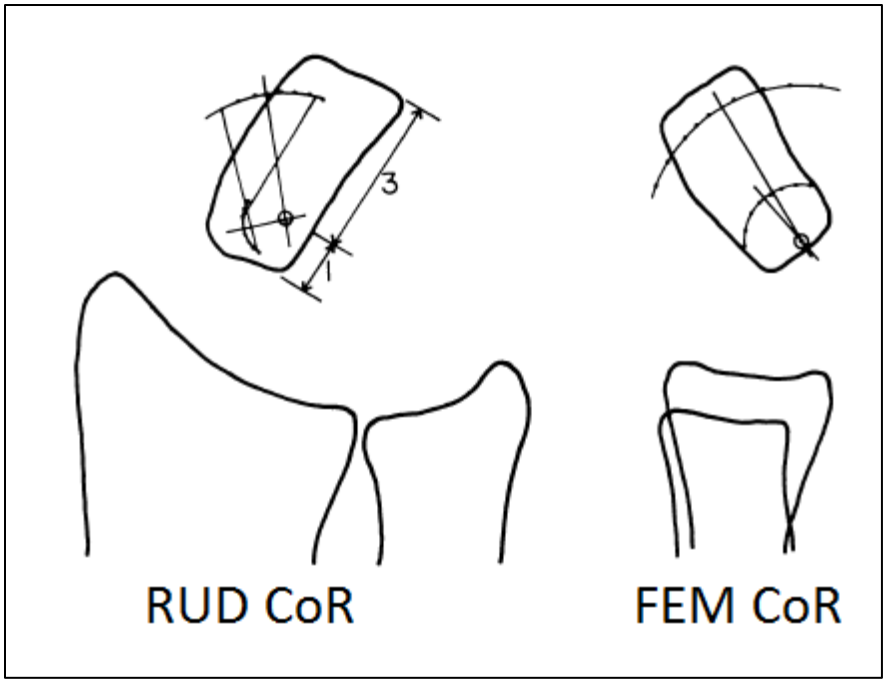

Figure 46: Centers of rotation for wrist [73]

3.1.5 Strength of Components

As discussed extensively in Chapter 2, the implant is being designed for the healthy, young, adult male. The implant will be designed to regularly accommodate forces of 1200 N with extreme loads of 3600 N (3 times the standard loading).

3.1.6 Attachment Method

There are several ways to attach the device to human bone. The most popular include bone cement, press fitting, and bone screws. For this device, bone screws are desired for implant attachment for several reasons.

Bone cement has been the traditional choice for surgeons for many years. Bone cement, which is polymethyl methacrylate (PMMA), is essentially a biomedical adhesive commonly used for surgical applications. It provides excellent initial fixation and allows faster surgery as using the cement is quick and simple compared to the alternatives.

However, its use is being reconsidered for wrist implants based on the high failure rate of wrist implants. Cemented implants are vastly more difficult or impossible to revise compared to other implants [27]. This is the main issue with respect to bone cement in this application. Other disadvantages include the curing process for PMMA is highly exothermic; PMMA cannot be seen in an X-ray; and it does not support new bone growth [96]. In the future, suitable bone cements may be available, but currently PMMA is not a viable option.

Press fitting is commonly used in place of cement fixation. Press fitting relies on friction to hold the implant in place; for example, a radial stem is commonly hammered into a slightly smaller hole to produce a press fit, or friction fit. The dimensions of the component and hole need to be precise and accurate for a proper fixation, but besides that requirement this is a relatively simple surgical technique. The main drawback is weak fixation due to the need for a large surface area and less effective bony ingrowth.

Screw fixation relies on holding the implant in place by compressing the implant against the bone through the use of screw threads; this holds the implant in place with friction against the bone. Screw fixation can potentially be more difficult than the other methods of fixation, depending on the type of screw and method of insertion. However, the benefits are definitely worth the greater difficulty in this case. Screw fixation allows much easier revision surgery as the damaged components can be removed by loosening the screws. Screws potentially offer much stronger fixation than press fits through the increased surface area of the threads and the design of the screw. Lastly, bone ingrowth between the threads greatly strengthens the fixation, which is not found in the other two fixation methods. Thus, screw fixation will be used for the new prosthesis design, with a central press-fitted peg (to attach the articulation piece).

3.1.7 Specifications Table

This chapter discussed the important design criteria for the new prosthesis design. The criteria are summarized in the table below. The details of the new design are discussed in the next chapter

Table 6: Specifications Table

Materials	
Screw	Ti-6Al-4V with osseointegrative coating
Carpal Plate	Ti-6Al-4V with osseointegrative coating
Radial Stem	Ti-6Al-4V with osseointegrative coating
Articulation surface	Cobalt chrome molybdenum alloy with chromium nitride coatings
Range of Motion	
Flexion	40°
Extension	40°
Radial deviation	12°
Ulnar deviation	28°
Maximum dimensions	
Width	4.4 cm
Length	2.5 cm
Depth	3 cm
Kinematics	
Joint type	Single center of rotation: Ball joint
Center of rotation location	In proximal head of the capitate 1/8 length of capitate distal to proximal end
Strength of Components	
Fatigue load	1200 N
Extreme load	3600 N
Fixation	
Fixation type	Bone Screws and Central Peg

CHAPTER 4

DESIGN OF THE IMPLANT

With the design specifications established, the next step is designing the implant. The design process focuses on the following subsystems for clarity: attachment screws, carpal plate, radial stem, ball and socket joint, and joint attachment mechanism. This chapter discusses the design of each of these subsystems in detail.

4.1 SCREW CHOICE

4.1.1 Commercial Solution

With a large variety of bone screws available, it is important to choose the right screw for the application. The Universal2 implant utilizes an excellent product from Synthes: the variable angle 4.5 mm locking cancellous bone screw [21]. This screw can be angled up to 30° to be anchored into a solid bone mass, has a thread design specific to cancellous bone, and has a locking feature integrated into the plate and screw head which prevents the screw from backing out and loosening. This is a proprietary design, so detailed specifications are not available currently, but the screw has shown great success in the Universal2 implant and a similar screw is used currently in the newer Remotion implant [23]. So, the Synthes variable angle 4.5 mm locking cancellous bone screw is desired for this design due to its previous success and continued use. Figure 47 displays a common application of this type of screw in a cervical plate.

Figure 47: Synthes locking screw application [97]

4.1.2 Screw design guidelines

If this screw cannot be purchased, a new screw must be designed and tested. Screw fixation in bone is not fully understood currently, so this field relies greatly on experimentation. The scope of this research does not permit fully designing and testing a reliable bone screw, but some general rules for bone screw design are discussed below.

Factors influencing screw failure

The tension present in the compression plate, the axial tension of the screws, and screw design are the three main parameters to consider in order to prevent screw failure. As the compression between the plate and the bone increases, friction will support more of the implant loads instead of the screw. Screws are designed to handle axial loads, not shear, so to address both these factors the screws should be used to produce as large a compression force as possible [98]. While in many cases of fastener design the fastener is most likely to fail, in this case, the bone is much more likely to fail, especially in fatigue [99]. So the focus is shifted to maximizing the holding capacity of the screw, which is the tension load the screws can withstand before the bone is sheared out.

Terminology

As many variables are involved in the selecting the geometry of a screw as seen in Figure 48, first some key terms are defined. Threads are the uniform ridges which on the inner or external surface of a cylinder which form a helix. External threads are the screws on bolts and screws, and internal threads are found in nuts and tapped holes. The profile of the thread consists of 3 parts: the crest at the top of the thread, the root at the bottom and the flanks which join the crests and roots. In Figure 49, the respective major and minimum diameters for internal and external threads are shown; for external threads, the thread crest is the major diameter, and the thread root is the minor diameter. It is vice versa for internal threads. The flank angle is the angle between a flank and a perpendicular. The thread height is the distance between the major and minor diameters. The thread pitch is the distance between adjacent threads. The pitch diameter is the diameter at which the width of the thread ridges and thread grooves are equal. The thread shear area is the effective cross sectional area through the ridges supporting the applied load in shear; for this case where the tapped bone hole is likely to fail, the thread shear area is taken at the major diameter of the screw. [100]

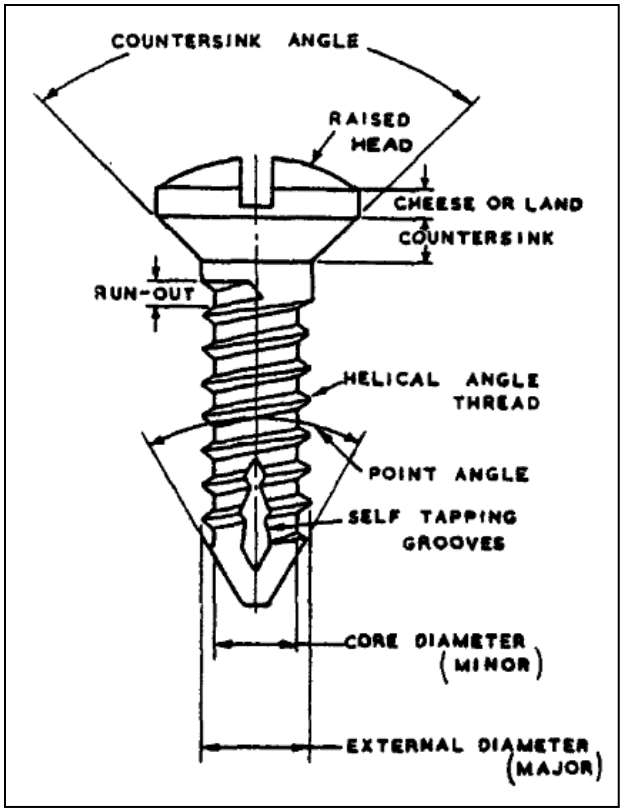

Figure 48: Common geometrical measures for screw [101]

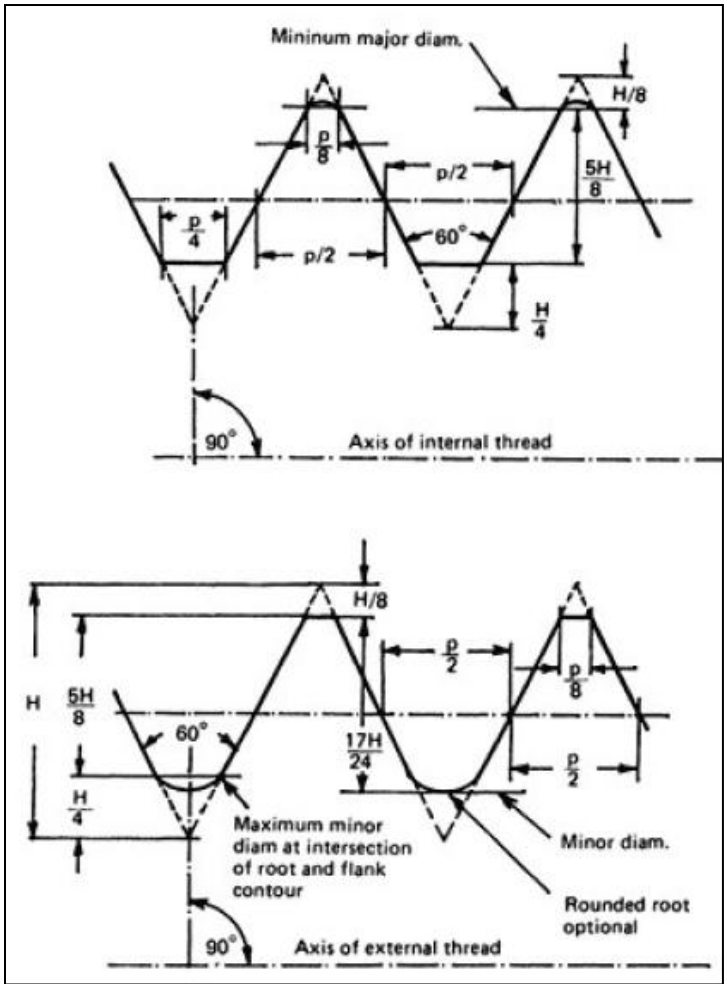

Figure 49: Internal vs. external thread and common measurements [100]

Maximizing Holding Capacity

As stated, holding capacity must be maximized to design the optimal bone screw. Holding capacity is hard to characterize and is often quantified by pullout force, which is the force required to pull a screw out of bone. Once again, this is a very experimental field, but some relationships can be drawn from previous work.

To begin with, Equations (7) and (8) describe the internal thread strength for common nuts [102]. F is the pullout force, S_u is the shear strength of the tapped material, A_{ts} is the thread shear area, n is the pitch, L_e is the length of thread

engagement, $D_{s\min}$ is the minimum major diameter of the external threads, and $E_{n\max}$ is the maximum pitch diameter of the internal threads. Figure 50 allows better visualization of some of the variables.

$$F = S_u * A_{ts} \tag{7}$$

$$Ats = \pi n L_e D_{s\min}\left[\frac{1}{2n} + 0.57735\left(D_{s\min} - E_{n\max}\right)\right] \tag{8}$$

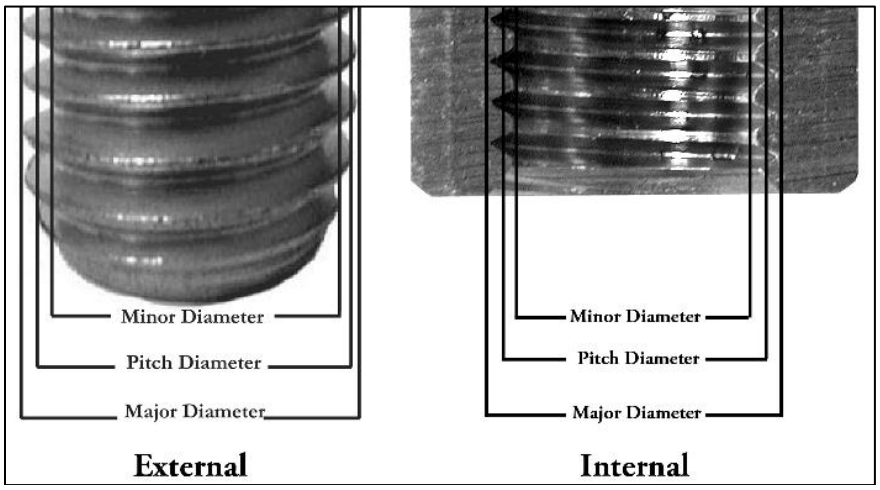

Figure 50: Various measures of internal and external thread [102]

From the first equation, the pullout force can be increased by increasing the shear strength of the tapped material or increasing the thread shear area. As the shear strength of the bone is an inherent property of the patient, it cannot be altered. Thus, to increase the pullout force of a screw, the thread shear area must be increased.

From the second equation (with several other sources agreeing), the thread shear area is directly proportional to L_e and $D_{s\min}$, so increasing the length of thread engagement and minimum major diameter of the external threads will increase the shear area. This means engaging more threads in the screw and maximizing the major diameter of the screw threads. To maximize A_{ts}, $E_{n\max}$, the maximum pitch diameter of the internal

threads, must be minimized. This essentially means that the threads should be as deep as possible in the bone. Lastly, the effect of the pitch depends on the other variables that define A_{ts}. From these two equations, the pull out force of a screw can be maximized by using deep threads, the maximum possible major diameter for the screw and maximum thread engagement in the length of the screw. Optimal pitch can then be determined experimentally.

There are many experiments conducted in animal bone, cadaver bone, and bone-like foam that agree with these findings as well as offer some conflicting results on pilot hole size, tapping, etc [103-107]. While a few factors can be optimized from the equations above, these studies reinforce the fact that the design of bone screws will require much trial and error.

Other important factors

One of the greatest surgical challenges is regulating the preload or installation torque for screws. Overtightening or undertightening screws can result in screw failure or early loosening problems [108]. Bone conditions and many screw design parameters affect the installation torque, so it is difficult to regulate. Though this area requires much more experimental research, one thing that must be addressed is reducing the required installation torque. Minimum installation torque allows the surgeon to efficiently use screw torque to increase plate compression or fixation rather than just overcoming friction or reactions due to the geometry of the screws. In essence, the greater the ratio of induced screw tension to installation torques the better [107]. Equation (9) is a general estimate for the torque required for a certain preload. In this equation, M_t is the installation torque, F_i^r is the preload desired, α is the helix angle of the thread, β is the half angle of the thread profile, μ is the coefficient of friction, R_o is the effective radius of the frictional area inside the bone, and r is the mean radius of the screw thread [100].

$$M_t = F_i^r \left(\frac{\cos\beta \tan\alpha + \mu}{\cos\beta - \mu \tan\alpha} + \frac{\mu R_o}{r} \right) \tag{9}$$

Another source compares the ratio of induced screw tension to installation torques for several installation methods, as shown in Figure 51 [107]. Case 1 is a tapped hole lubricated with oil, case 2 is a tapped hole lubricated with water, case 3 is a tapped hole with no lubricant, and case 4 is an untapped pilot hole with no lubricant.

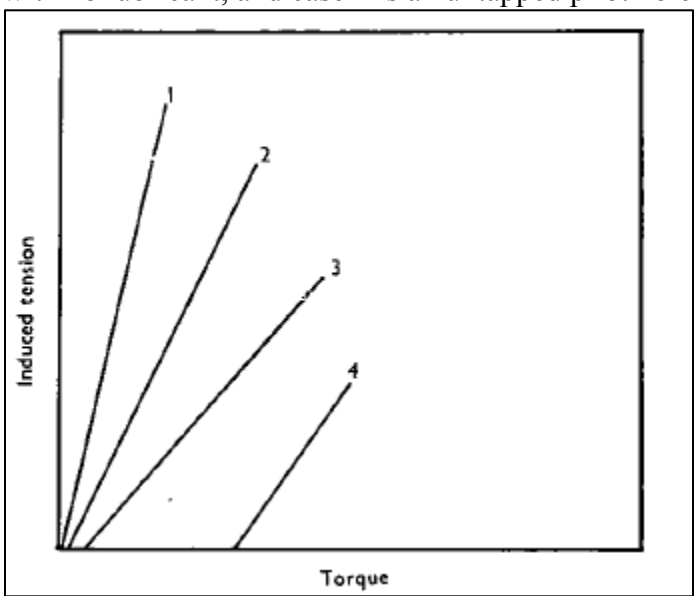

Figure 51: Induced tension vs. insertion torque for 4 cases [107]

From the formula and figure, the simplest and surest way to reduce the installation torque is lubricating a tapped hole properly with oil or saline solution before installing the bone screws. The geometry of the screw would have to be experimentally determined to maximize the ratio of induced screw tension to installation torques.

4.1.3 First steps to screw design

Various limitations prevent the full design of a suitable bone screw; still, some initial design choices can be made. Key parameters for screw design include material, length, nominal diameter, thread design, and head design. The material has been chosen

already to be Ti-6Al-4V with an osseointegrative coating as discussed earlier. The lengths of the screw vary from 15-35 mm, but as discussed in Chapter 2 the screw lengths can be conservatively estimated to be 20 mm and 25 mm: larger screws could generally be used in young male wrists, while most current implants are designed for elderly women. The Universal 2 can be used as a baseline, so the nominal diameters for screws will be 4.5 mm for the side screws for the plate and 6.5 mm for the central screw/peg. Thread design would require much experimentation and possible reverse engineering. A star head would be used for good torque transmission despite the small screw head [100, 109].

4.1.4 Fastener for Prototype

For cost, ease of machining of other parts, and lack of detailed specifications for the Synthes screw, a similar available common screw is used in place of the Synthes bone screw for the prototype (not to be implanted in humans). A comparison of various cancellous bone screws against common machine screws, shows that deep threads and greater pitch characterized the bone screws. A sample veterinary 4.5mm cancellous bone screw was ordered for a rough estimate of the Synthes screw. Using this screw, the closest match was found at a local hardware store to be a 10x1 oval head sheet metal screw, which is reasonable as these screws are often used in sheet metal and soft materials and thus have relatively deep threads. Using a scanner, the key dimensions of the two screws were roughly compared in Figure 52.

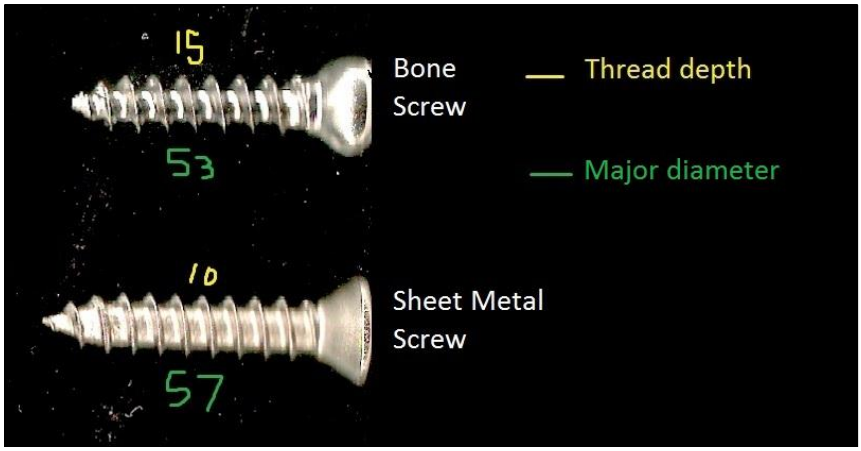

Figure 52: Bone screw and sheet metal screw compared

The thread depth (distance from thread crest to root) and major diameter (diameter at the thread crests) were measured in pixels for both screws. Though the major diameter and length are comparable, the thread depth/height is about 50% smaller for the sheet metal screw. Although this would likely not be a viable screw for the final implant, this screw will be used for the prototype for a rough substitute with the limitations in mind.

Some key dimensions for the sheet metal screw are the head diameter, nominal diameter, head angle, head height, countersunk height and length (referenced from Figure 53). Some of these dimensions were also estimated for the desired bone screw for the final design. These dimensions are summarized in Figure 53.

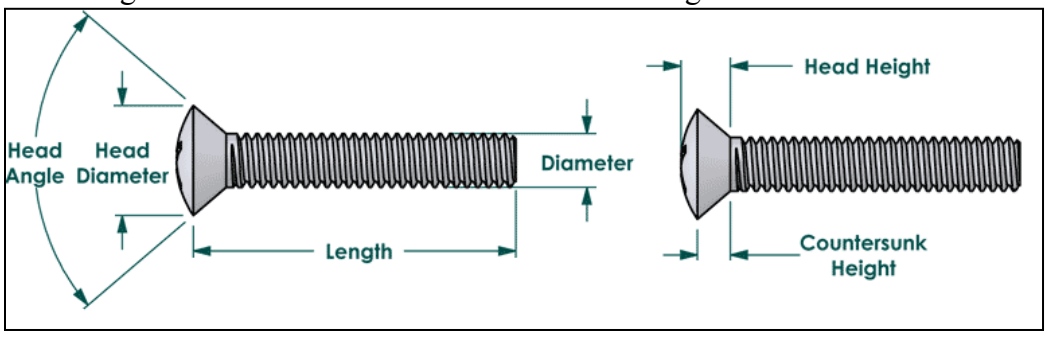

Figure 53: Dimensions for sheet metal screw [110]

Table 7: Key dimensions for screws [110, 111]

	#10-24 x 1" oval head	4.5 mm cancellous bone screw
Diameter	0.190 in. (#10)	4.5 mm
Thread count	24	-
Length	1 in.	20-30 mm
Head angle	82°	
Head height	0.176 in.	
Countersunk height	0.116 in.	
Head diameter (max)	0.362 in.	8 mm

4.2 CARPAL PLATE DESIGN

The Universal2 carpal plate shown in Figure 54 is a good baseline. Still, the new design will be very different in several ways. This part must be designed to withstand the loads defined earlier. Also, there is a new joint design, and the dimensions must be determined. The design of the carpal plate consists of shape design, specification of clearance, attachment of the articulation components, and thickness.

Figure 54: Universal2 Carpal Plate [112]

4.2.1 Shape

The basic shape will be an ellipsoid flat plate. To determine the final dimensions, the surgical technique for the Re-motion implant was studied to help determine more

accurate dimensions. From Figure 55, the installation location was determined and the approximate width-to-height ratio for the ellipse is found to be 2.5:1.

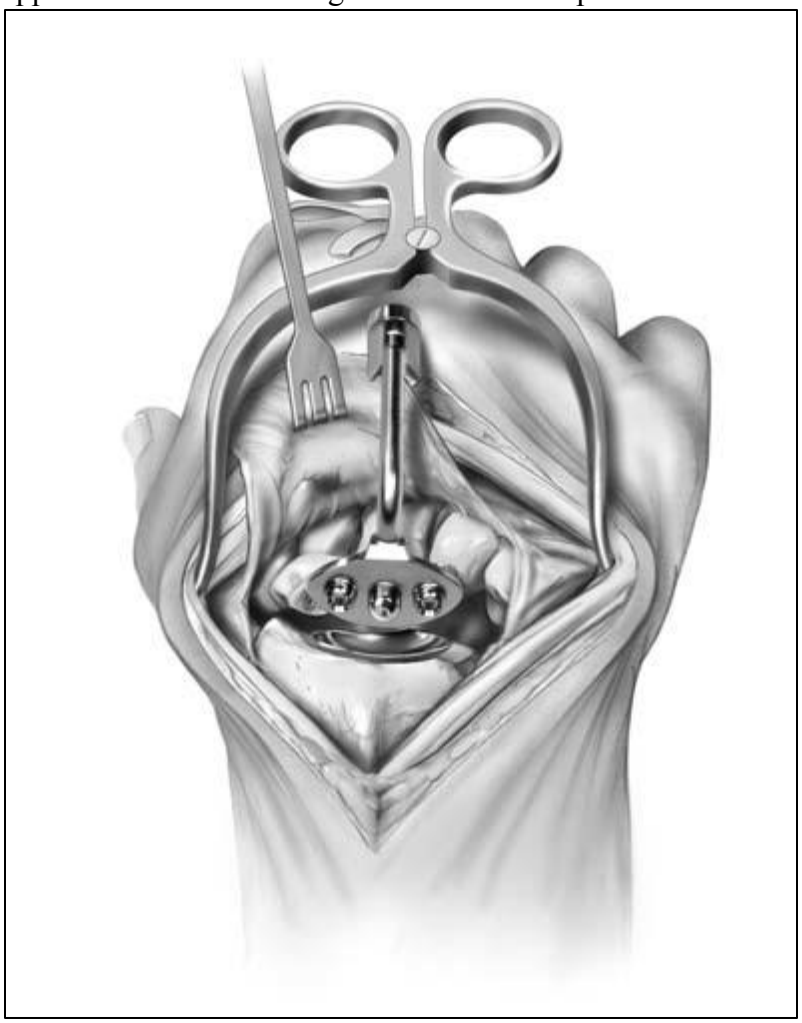

Figure 55: Accurate placement of Re-motion carpal plate [113]

The width of the plate is determined from an x-ray of a successful implant of the Universal2 device in Figure 56. As this x-ray did not include the scale that was needed to measure the width, the scale from an x-ray of a similar hand (Figure 44) was used and the scale was super imposed as seen bellow the x-ray.

Figure 56: Determining width of carpal plate [40, 69]

From the x-ray, the width of the plate should be 3.8 cm. Using the 2.5:1 width to height ratio, the height of the ellipse should be 1.52 cm. The shape of the ellipse is shown below. This will be the shape of the carpal plate prototype.

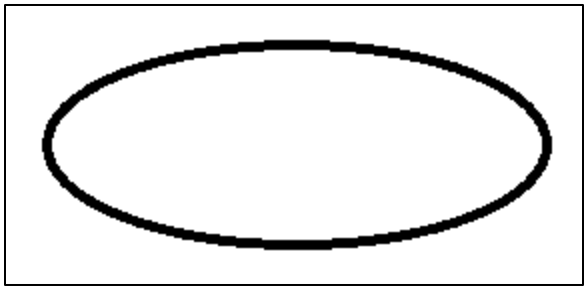

Figure 57: Shape of carpal plate

4.2.2 Fastener locations

For the fixation, one central peg and two screws will be used. Initially, the central peg was chosen to be a screw, but to reduce the required thickness and allow more room for the latching mechanism for the articulation piece the screw was replaced by the peg. The central peg will be 20mm long, have a 6.5 mm diameter, and have areas for bone ingrowth. Both dimensions are conservative and may be increased after cadaver studies. As noted earlier, the two 4.5 mm bone screws will be replaced with the 10x1 oval head sheet metal screws for the prototype. The two screws will be placed 10 mm from the center as shown in Figure 58. One of the major strengths of the ball and socket design is there will normally be no axial torque on the plate (as axial rotation is not restricted), so the screws will not have to handle this torque. Thus, if needed, they can be placed much closer to the center than in implants that do not allow axial rotation.

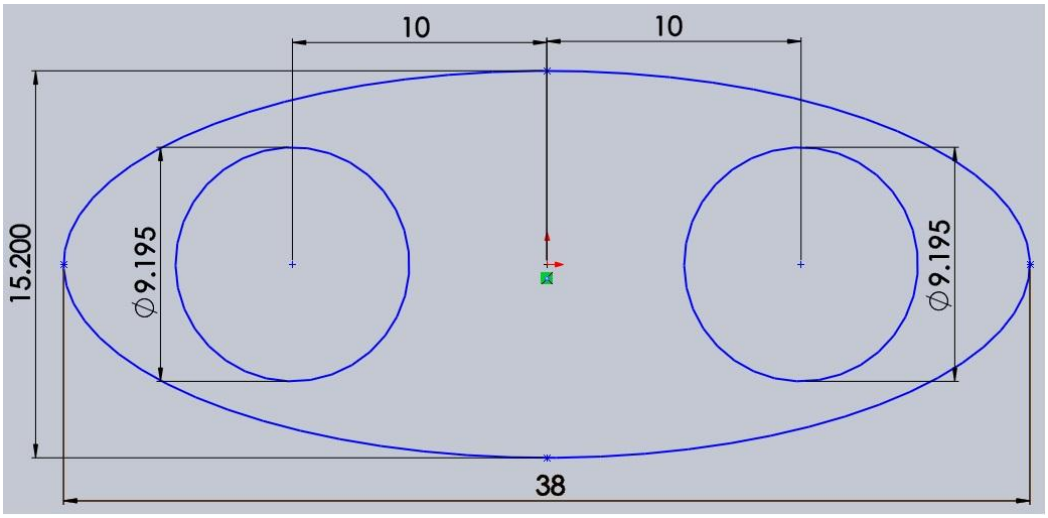

Figure 58: Hole locations in carpal plate

4.2.3 Articulation surface attachment design and thickness of plate

Concept Selection

To determine the method for inserting the articulation piece into the plate, several concepts were generated and the best one for the application was selected. The key desires were minimum required thickness of the plate, durable fixation, ease of installation for the surgeon, and easy removal if necessary. For the requirements and constraints established, four concepts were chosen to be further considered: threaded fastening, press fit, adhesive, and locking pin.

The threaded fastening concept consists of essentially threading the end of the articulation surface piece, creating a threaded hole in the center of the plate, and screwing the piece into the plate. The hole can actually go through the peg allowing a thinner carpal plate. Threaded fasteners provide excellent compression/fixation with greater surface area used for fixation compared to other friction fit methods. This can be combined with a thread lock or adhesive if loosening becomes an issue. Also, the

articulation piece can be easily removed and installed with a custom screwdriver or wrench.

The press fit concept requires more surface area than the threaded fastening concept for a suitable, durable fixation and may result in a thicker carpal plate. It would definitely be more difficult to remove as it would require pulling or heating to dislodge the component; however, installation is fast and simple with a few knocks from a hammer.

The adhesive concept would use bone cement (PMMA) to adhere the articulation component to the carpal plate through a central hole in the plate. It would most likely require a similar amount of surface area as the press fit or slightly less, so a similar thickness for carpal plate. Adhesives like PMMA result in very difficult revision surgeries, so removal would require bio-inert solvents or a great deal of force. Installation is as simple as the press fit, but slightly more complicated to account for the curing of the adhesive

Lastly, the locking pin would work similar to the pin seen in Figure 59: the locking pin would pass through the thin plane of the carpal plate to lock the articulation piece into the plate. This would require more clearance than the other concepts due to the horizontal pin and the need for a thick pin to sustain the high shear loads. The pin will provide a durable fixation if combined with the application of an adhesive. Without the adhesive, the pin is likely to back out and impinge on surrounding areas. Installation would be difficult as the pin would be inserted in an inconvenient plane for the surgeon, and removal would be very difficult, especially if adhesive is also used.

Figure 59: Locking Pin [114]

Based on the rationale presented above, the Pugh chart in Table 8 was developed to determine the best attachment method for this application. The threaded fastening method was chosen as the reference concept for the Pugh method. A higher number for a category means better performance in that category, and the concept with the greatest sum is determined to be the best design for the application. The threaded fastener concept is determined to be the best design and was developed further.

Table 8: Articulation surface attachment method comparison

	Threaded fastening	Press fit	Adhesive	Locking pin
Minimum plate thickness	0	-1	-1	-2
Durable fixation	0	-1	-1	-1
Ease of removal	0	-1	-2	-2
Ease of installation	0	1	0	-1
SUM	**0**	**-2**	**-4**	**-6**

Concept Development

Essentially, the purpose of this part of the design is to attach the articulation piece to the plate in a feasible, durable manner through threaded fastening. The key parameters that need to be established are the major diameter of the thread, the thread type, the thread length, and desired tensile load.

The major diameter of the thread is constrained by the space available on the plate after determining the location of the other two holes in Figure 58. There is about 10 mm between the edges of the holes, so the major diameter must be less than 10 mm or 0.394 in. From Figure 60, taken from notes on mechanical design [116], a minimum hole spacing edge to edge of "2T" is recommended, where T is thickness of the plate. For the prototype, the plate must be a minimum of 0.176 in. thick, which is the head height for the sheet metal screws, rounded up to 0.18 in. thick. So ideally, there should be 0.36 in. or 9.144 mm between the edges of the new hole for the articulation piece and the holes for the screws, which is impossible for the constraints given. However, this minimum hole spacing constraint can be relaxed as this is mainly for less stiff materials like aluminum and low carbon steel. Also, the hole for the articulation piece will not be a through hole. Still, from this information, the minimum necessary major diameter for the hole should be used to retain rigidity and strength in the plate.

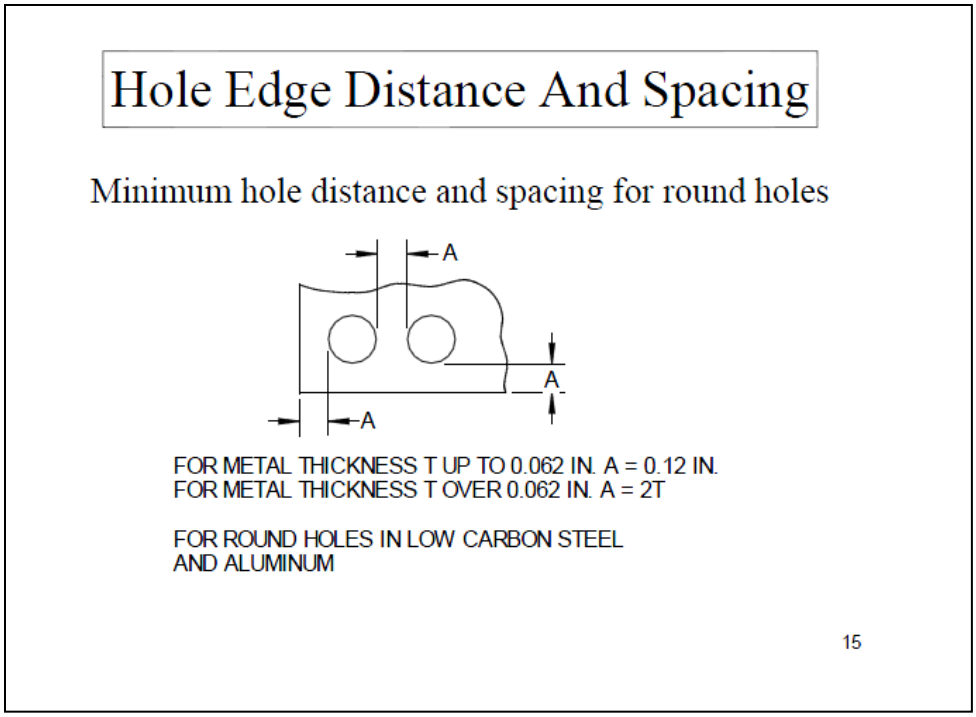

Figure 60: Holes spacing recommendations [116]

For the thread type, a universal thread will be used as metals are fairly predictable, well tested materials. The decision for whether to use coarse threads or fine threads was based on the demands of the application. Coarse threads have larger pitch and a smaller minor diameter than fine threads [115]. Generally, coarse threads have greater stripping strength, better fatigue resistance, easier assembly and disassembly, and have larger thread allowances compared to fine threads. Fine threads are generally stronger in tension due to their smaller pitch allowing more contact points, and they have higher torsional and transverse shear strengths [102]. Though fine threads would provide higher holding capacity for a given thread length, the tendency for them to strip and cross thread would introduce much more risk in a revision surgery. So, a Unified National Coarse (UNC) thread type will be utilized.

Next, the minimum major diameter has to be determined, and this will be based on the prestress tensile load. The purpose of the prestress load in this case is to attach the articulation piece to the carpal plate, resist any tensile loads and prevent loosening over time. The implant will mainly see compressive forces as muscles pull, and the tensile forces are so negligible that they are usually not even considered. Regardless, a minimum tensile load of 400 lb. will be established. This is about 2 times the force the wrist sees in compression during light everyday activities [1, 3, 49]. Using this value, the minimum required tensile stress area can be calculated using Equation (10), where A_s is the tensile stress area, P is the desired tensile load, and S_t is the tensile strength of the weakest material in the joint.

$$A_s = \frac{P}{S_t} \tag{10}$$

The desired minimum tensile load is 400 lb. and the tensile strength of the weaker of the two materials in the joint is 8.27 MPa for the titanium alloy [86]. Using these values results in a minimum tensile stress area of 0.00333 in.^{2}. This information can be used to determine the minimum major diameter for the joint using Table 9, which ends up being #2 or 0.086 in.

Table 9: United National thread tensile stress area chart [102]

Unified National Thread Tensile Stress Area (As)

Nominal Size		Coarse Thread		8 Thread Series		Fine Thread	
		Thread Pitch (tpi)	Tensile Stress Area (sq in.)	Thread Pitch (tpi)	Tensile Stress Area (sq in.)	Thread Pitch (tpi)	Tensile Stress Area (sq in)
0	0.060					80	0.00180
1	0.073	64	0.00262			72	0.00278
2	0.086	56	0.00370			64	0.00394
3	0.099	48	0.00487			56	0.00523
4	0.112	40	0.00604			48	0.00661
5	0.125	40	0.00796			44	0.00831
6	0.138	32	0.00909			40	0.01015
8	0.164	32	0.0140			36	0.0147
10	0.190	24	0.0175			32	0.0200
12	0.216	24	0.0242			28	0.0258
1/4	0.250	20	0.0318			28	0.0364
5/16	0.313	18	0.0525			24	0.0581
3/8	0.375	16	0.0775			24	0.0878
7/16	0.438	14	0.106			20	0.119
1/2	0.500	13	0.142			20	0.160
9/16	0.563	12	0.182			18	0.203
5/8	0.625	11	0.226			18	0.256
3/4	0.750	10	0.335			16	0.373
7/8	0.875	9	0.462			14	0.510
1	1.000	8	0.606	8	0.606	12 UNF	0.663
1	1.000					14 UNS	0.680
1 1/8	1.125	7	0.763	8	0.791	12	0.856
1 1/4	1.250	7	0.969	8	1.000	12	1.073
1 3/8	1.375	6	1.155	8	1.234	12	1.315
1 1/2	1.500	6	1.406	8	1.492	12	1.581

With a range for the diameter established, a compromise must be reached for the thread length. The plate should not be thicker than required for the screws, which is 0.18 in. Also, drilling into the central peg should be avoided if possible and hole spacing should be maximized. With these objectives in mind, a nominal hole size and thread length must be chosen.

The minimum thread engagement length (thread length in this case) is calculated using Equation (11), where L_c is the minimum thread engagement length, A_t is the tensile stress area, D is the major diameter, and p is the reciprocal of the pitch.

$$L_c = \frac{2A_t}{0.5\pi\left(D - 0.64952\,p\right)} \tag{11}$$

This formula and the information from Table 9 are used to create Table 10, which displays the calculations for the various viable hole diameter choices.

Table 10: Minimum thread length calculations

Major diameter (in.)	Pitch (tpi)	At (in.^2)	Lc (in.)
0.086	56	0.0037	0.063318
0.099	48	0.00487	0.072549
0.112	40	0.00604	0.080307
0.125	40	0.00796	0.093185
0.138	32	0.00909	0.098331
0.164	32	0.014	0.124043
0.19	24	0.0175	0.136751
0.216	24	0.0242	0.163083
0.25	20	0.0318	0.186136
0.313	18	0.0525	0.241392
0.375	16	0.0775	0.29508

From Table 10, any hole diameter less than 0.216 in. (#12) can be used without increasing the thickness of the plate or drilling into the central peg. To maximize hole spacing, the smallest diameter necessary is desired, which is 0.086 in. (#2). However, the smaller hole would create more manufacturing difficulty as materials are likely to deform at that scale when forming and tooling is likely to break. Also, smaller holes are more likely to strip and cause disassembly and assembly issues. So a 0.125 in. (#5-40) hole is specified for the final design as a compromise for now until mass production becomes an issue. For the prototype, the common 0.164 in. (#8-32) hole will be used for manufacturing ease. A close tolerance hole will be used for the final design and a standard tolerance hole for the prototype [116]. The plate will be the minimum 0.18 in. thick, which could be reduced to less than 0.10 in. if the head heights of the two screws were smaller.

The possibility of galvanic corrosion was considered; however, both metals function well together according to the galvanic series and do not require additional protection [117].

Lastly, the installation torque is determined with Equation (12), where τ is torque, K is the nut factor (assumed to be 0.15 for a lubricated hole), d is the nominal diameter, and F is the bolt tension [102].

$$\tau = KdF \tag{12}$$

For the 0.125 in. hole, an installation torque of 7.5 ft-lb. was calculated. An installation torque of 9.84 ft-lb will be used for the 0.164 in. hole. As the joint will be loaded primarily in compression and a close tolerance hole will be used for the final design, the joint is not likely to loosen, and thread adhesive will not be applied unless loosening becomes an issue in testing.

4.2.4 Stress Calculations

With the design variables chosen, the carpal plate design was modeled in SolidWorks, as shown in Figure 61. A 0.5 mm fillet was employed to remove sharp corners and stress concentrations, and ribs and a dome were added to the central peg.

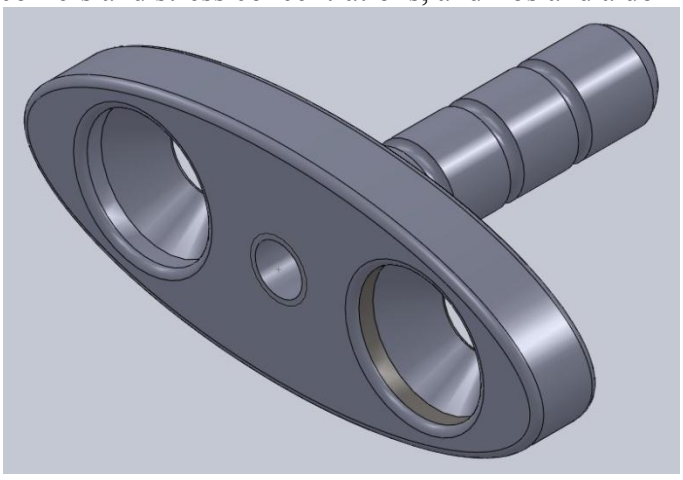

Figure 61: Carpal plate prototype

With this part modeled, stress calculations were performed to ensure that it is feasible for implant. First of all, the stresses on the bone through the bone-plate interface must be checked. Two FEA simulations were carried out with different loads on the proximal face of the plate: one with the extreme load of 3600 N and one with the fatigue load of 1200 N. One key difference between this simulation and the previous torque simulations must be clarified. In this case, the bone is being loaded in pure compression and the plate is placed in an area that contains a significant amount of cortical bone as well as cancellous. Thus, the stresses the bone can endure are much greater: 50 MPa for the extreme case and 30 MPa for the fatigue case. For a factor of safety of 2.5, the bone will be assumed to have a compressive strength of 20 MPa and fatigue strength of 10 MPa [65].

For the simulations, the back face of the plate was held fixed and the load was applied on the front face of the plate. The focus is on stress on the back face of the plate (the side with the central peg) which represents the stress on the bone.

Figure 62 displays the results of the simulation of the extreme case. The red areas on the edges are areas where the stresses in the bone are slightly above the 20 MPa compressive strength limit. Since the screw holes for the prototype are larger than those for the final design with the bone screws (the hole for the sheet metal screw in this prototype is 0.190 in. or 4.826 mm diameter; the hole for the bone screw would be 4.5 mm), the stresses will fall under the limit. The rest of the areas of concern experience stress levels of about 10 MPa or less.

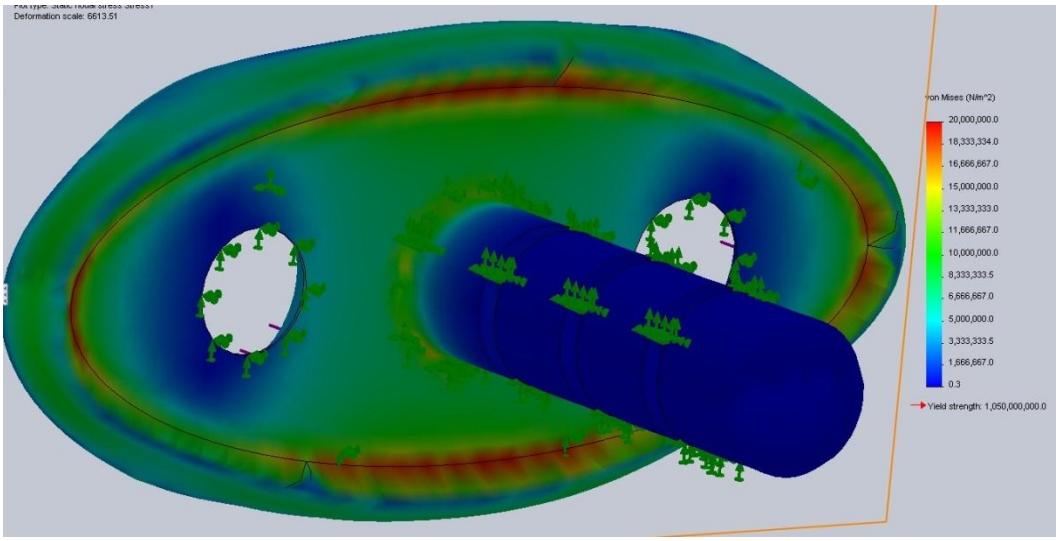

Figure 62: Carpal plate bone stress extreme simulation

Figure 63 displays the results of the simulation of the fatigue case. The stress limit is set at 10 MPa. The results show that no areas are stressed close to the limit. The areas of interest experience stress levels of 6 MPa or less.

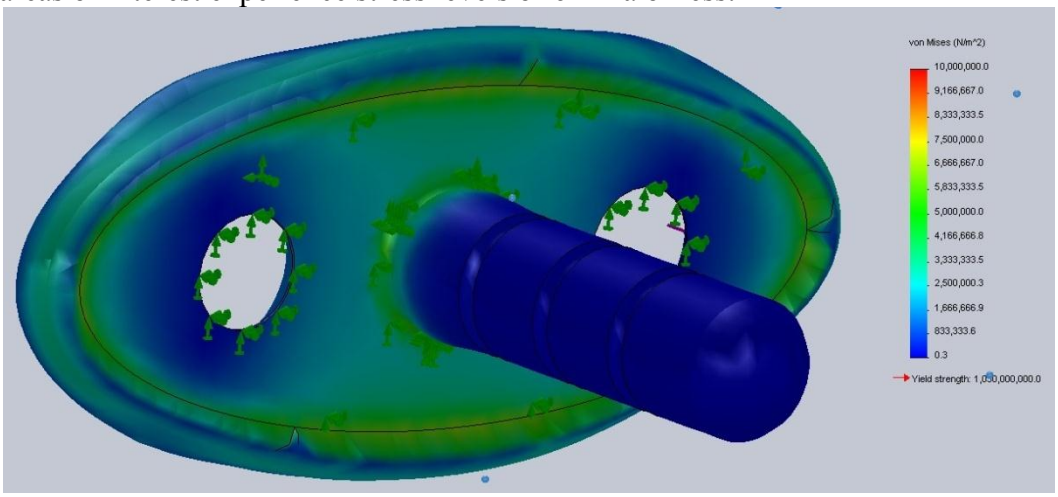

Figure 63: Carpal plate bone stress fatigue simulation

These simulations demonstrate that no major changes are needed to accommodate bone stress. Next, the diameter of the articulation piece should be determined. A simple

assembly was created, as seen in Figure 64, where the part in the central hole represents the shaft of the articulation piece.

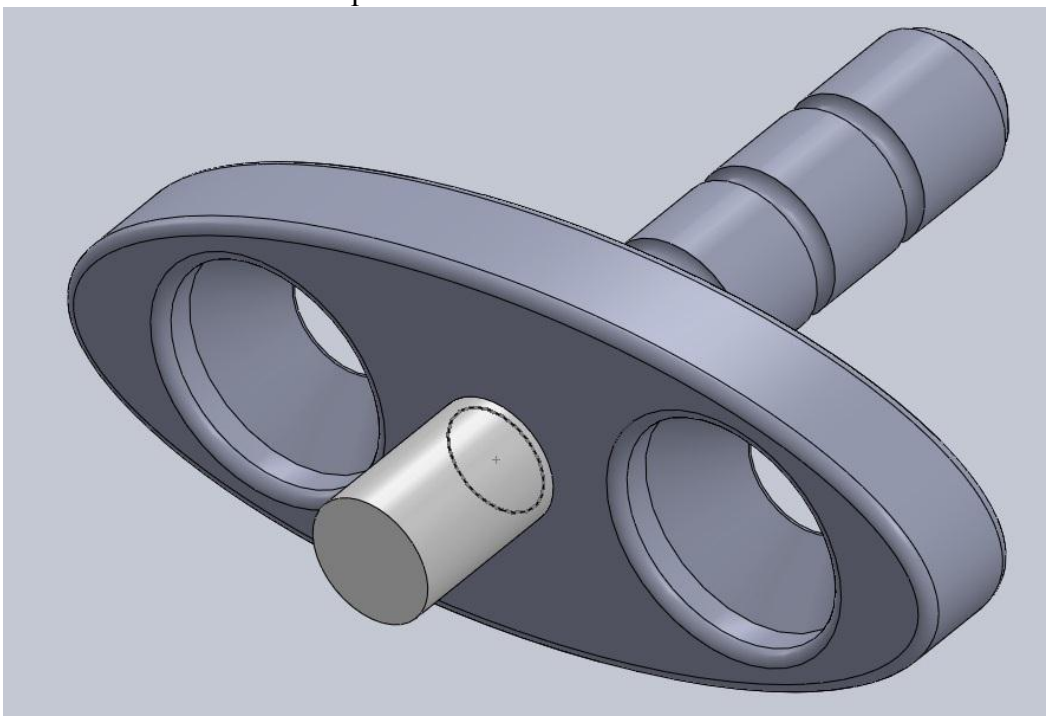

Figure 64: Carpal prototype assembly

The diameter of this shaft is stepped. The smaller diameter is the size of the #8 hole major diameter, 0.164 in. or 4.1656 mm, and outside the hole the shaft was chosen to be 5 mm in diameter. The 3600 N extreme load was applied to the shaft and the FEA simulation was conducted. The area of focus is the interface between the shaft and carpal plate face.

Figure 65 shows the results of the simulation. The area of focus experiences stress levels under 500 MPa which is well under the yield strength of the titanium alloy (1050 MPa) and under that of cobalt chromium (611 MPa). So the 5 mm diameter for the shaft of the articulation piece above the threaded section would pass is the minimum

diameter, but if feasible a larger diameter will be specified (for a larger factor of safety) when designing the articulation piece later.

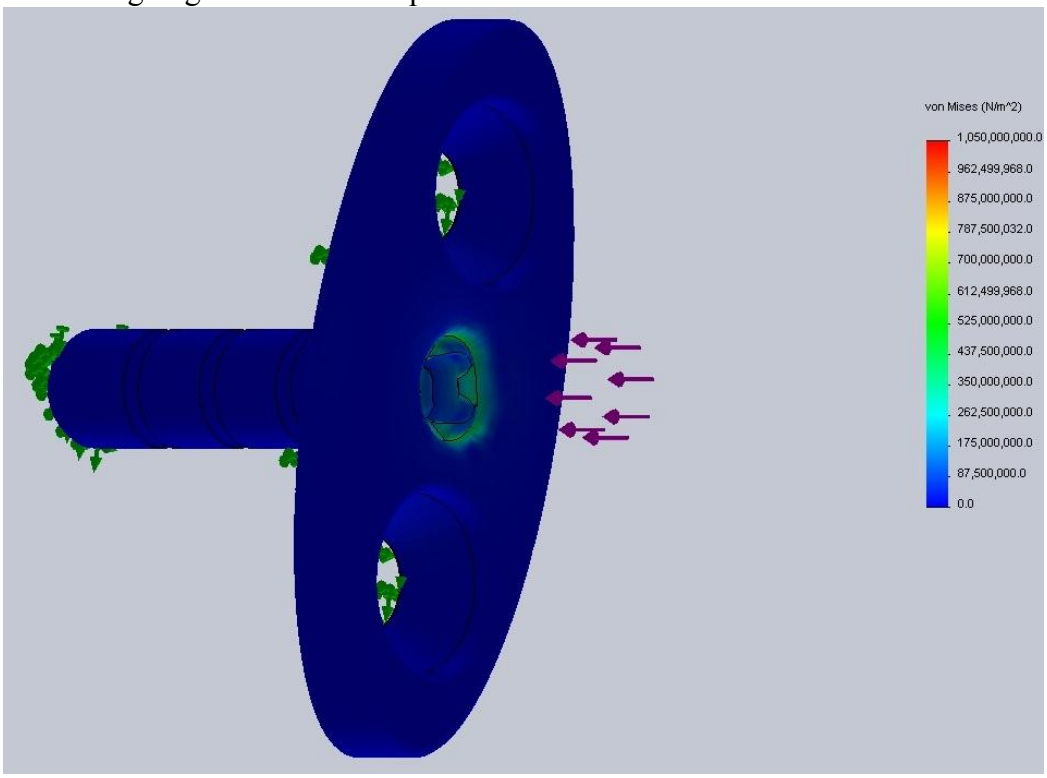

Figure 65: Verification of articulation piece shaft diameter

4.2.5 Summary of Carpal Plate Design

Table 11 supplements Table 6 and summarizes the key design variables of the carpal plate design.

Table 11: Carpal plate design summary

Carpal Plate Design Specifications	
Carpal plate material	Ti-6Al-4V with osseointegrative coating
Screw type	#10-24 x 1" oval head
Screw location	10 mm from center
width of plate ellipse	3.8 cm
height of plate ellipse	1.52 cm
thickness of plate	0.18 in.
Central peg diameter	6.5 mm
Central peg length	20 mm
Central peg rib diameter	1 mm
Central peg rib spacing	5 mm
Articulation piece connection	#8-32 central threaded fastening
Articulation piece installation torque	9.84 ft-lb
Fillet diameter	0.5 mm

4.3 RADIAL COMPONENT DESIGN

4.3.1 Key Radius Dimensions

To begin the radial stem design, the dimensions of the young male radius must be determined. No cadaver specimens were available, so an approach similar to that used to determine the dimensions of the wrist was used. The key dimensions to be determined are those for the distal end of the radius and the diameter of the shaft (Figure 66).

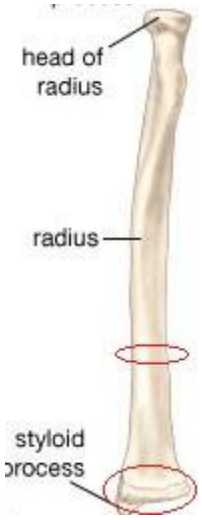

Figure 66: Areas of interest in radius [118]

To get the required dimensions, a literature review was conducted. Neu [119] measured the bone density in the radius and provided data on the distal cross section for young males. The cross sectional area was measured at the location shown in Figure 67. The cross sectional area here near the distal rim of the radius was seen to vary from 313-441 mm^2 [119]. Dowthwaite [120] finds the cross sectional area 1/3 the forearm length from the distal end to be 30-40% lower than that near the distal rim (minimum of 187 mm^2) [120]. So the insertion method will either have to accommodate a gradually reducing diameter, be sized for 187 mm^2 minimum diameter of the bone, or be installed near the distal rim of radius to utilize the greater diameter there.

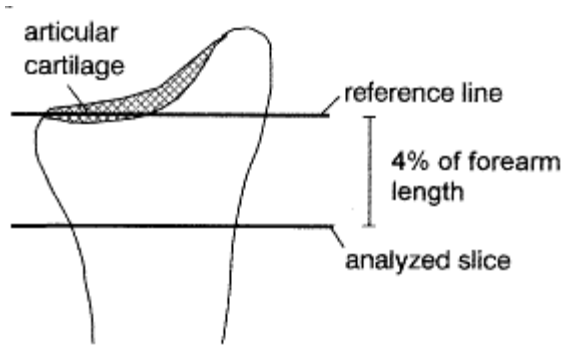

Figure 67: Cross sectional area measurement [119]

The cross section at the shaft is fairly uniform and assumed to be a circular cross section; however, near the distal rim the approximately quadrilateral cross section is not uniform [121]. So several x-rays were studied to determine the ratio of width to thickness of the radius. From the three x-rays of male wrist in Figure 68, the ratio of width to thickness is found to be about 1.15 to 1.

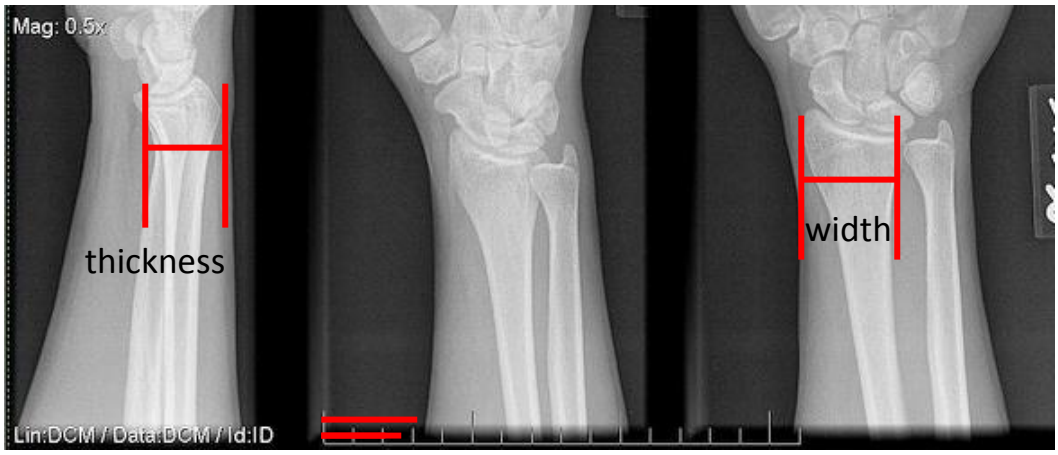

Figure 68: Male wrist cross sectional x-rays [122]

Using this information the minimum thickness of the radius at the shaft and near the distal rim were calculated. The thickness for the shaft can be calculated using Equation (13) (a rearrangement of the area of a circle formula) where d is the thickness and A is the cross sectional area. The value of d is 15.5 mm. The minimum thickness

near the distal rim can be calculated using Equation (14) (a rearrangement of the area of a rectangle formula) where t is the thickness, A is the cross sectional area, and w is the width. Using the ratio of width to thickness, t is calculated to be 16.5 mm.

$$d = \sqrt{\frac{4A}{\pi}} \tag{13}$$

$$t = \frac{A}{w} \tag{14}$$

Thus the maximum thickness of the radial stem is limited by these two dimensions which are summarized in Table 12.

Table 12: Key radius dimensions

Key Radius dimensions	
Minimum thickness near distal rim	16.5 mm
Minimum thickness at shaft	15.5 mm

4.3.2 Radius Bone Properties

Knowing the bone composition is important to estimate the strength of the radius, similar to estimating the strength of the carpal bones for the carpal plate design. Though all bone is a mix of cancellous and cortical material, the distal end of the radius is made mostly of cancellous bone with the shaft made up mostly of cortical bone. The radial component will mainly be inserted into the distal end of the radiusm, with a portion residing in the shaft of the radius, and will be loaded in compression. So, the compressive strength of a combination of cancellous bone and cortical bone was used once again for the stress calculations 30 MPa ultimate compressive strength and 10 MPa endurance compressive strength.

4.3.3 Stem Design

External Specifications

There are many accepted methods of radial component insertion as this component fails very rarely. Two main types considered are the press-fit (with optional cement) and screw fixation. Found in Chapter 1, Figure 16 and Figure 17 display the press-fit radial component of the Universal2 implant, and Figure 11 displays an example of the screw fixation option.

For the same reasons discussed earlier, screw fixation was chosen over press-fit for a more reliable fixation.

Similar to the Motec/Gibbs implant, shown again in Figure 69 and Figure 70 below, the implant is engaged from the distal end of the radius to part way into the shaft to reach the cortical bone. To minimize the stress concentrations, the tip is rounded with threads starting a few millimeters beyond the shaft. As the cross section of the radius significantly reduces from the end to the shaft, the diameter of the stem varies. Lastly, the threads are designed for cancellous bones, and, as before, they are proprietary designs that will need to be outsourced.

Figure 69: Radial component of Motec implant [45]

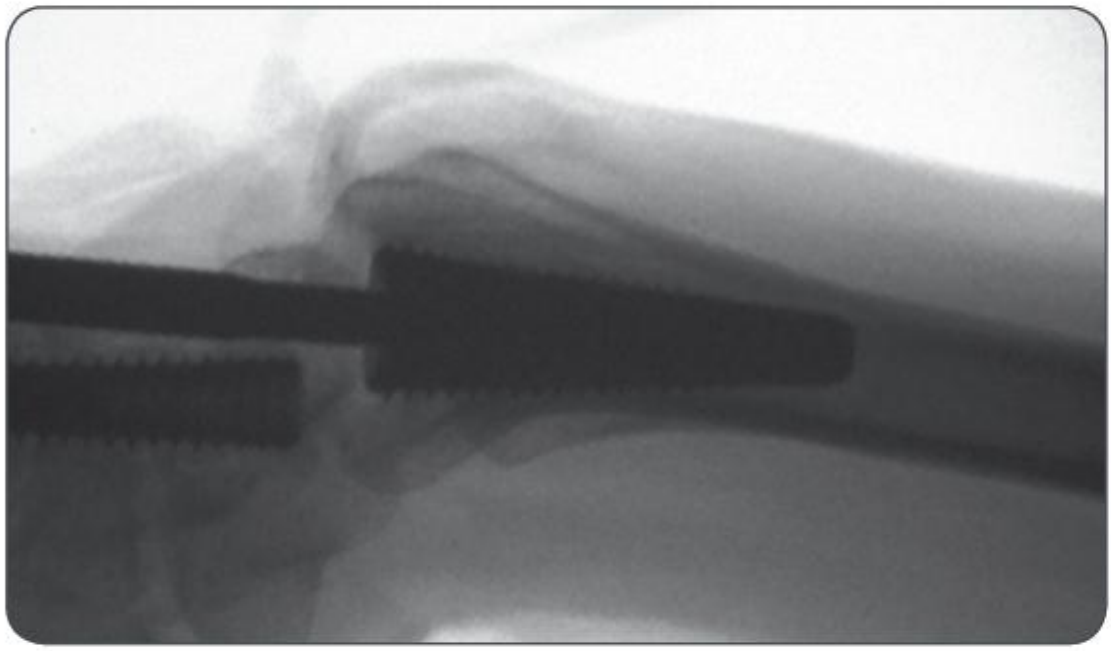

Figure 70: X-ray showing fixation of Motec radial component [45]

The total length into the radius of the stem is 1.5 times the length of the central peg in the carpal component (30 mm) for minimal bone resection balanced with sufficient fixation surface area. The minimum diameter of the stem at the end of the stem is 7 mm, about 45% of the minimum thickness of the shaft of the radius. The maximum diameter of the stem at the top of the stem is 8 mm, about 50% of the minimum thickness of the rim of the radius. The non-threaded portion will extend 10 mm up from the tip. As the bone screw thread design specifications are not available currently, a standard M8x1.25 thread is designated for the threaded portion[123]. The non-threaded section of the stem tapers from 8 mm to 7 mm.

The external features were constructed using SolidWorks and the result is shown in Figure 71.

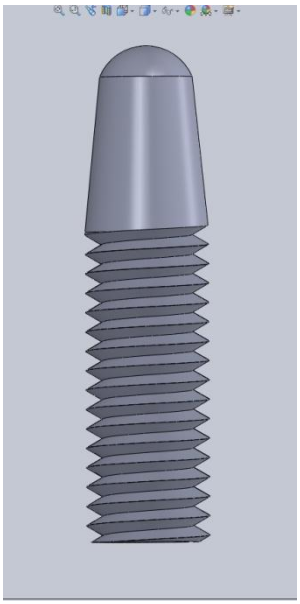

Figure 71: External design of radial stem

Internal Specifications

With the external features determines, there are two internal features left: the screw head and the articulation piece attachment. To torque the radial stem into the bone, a screw head must be machined into the top of the stem. At the same time, clearance is needed for attaching the articulation piece. Essentially, the section used to transmit the torque must be a smaller diameter than the section of the stem used to attach the articulation piece. The minor diameter of the M8x1.25 thread is 6.466 mm, which means any internal hole must be less than this.

For simplicity, it was assumed that the same thread type used for the carpal component articulation piece would be used here, the #8-32 thread. This thread has a maximum major diameter of 4.267 mm (0.168 in.) and is tapped using a 3.454 mm (0.136 in.) hole. This leaves slightly more than 3 mm for the torque transmitting section. For efficient torque transmittal and to reduce chance of stripping, a 3 mm socket head is chosen. This head allows close to 8 Nm of torque to be transmitted to fasten the implant

into the bone [124]. The articulation piece attachment section is a minimum of 0.124 in. or 3.15 mm deep (specified from Table 10). The torque transmitting section is 3 mm deep [125].

The internal features were added to the model and the result is shown in Figure 72.

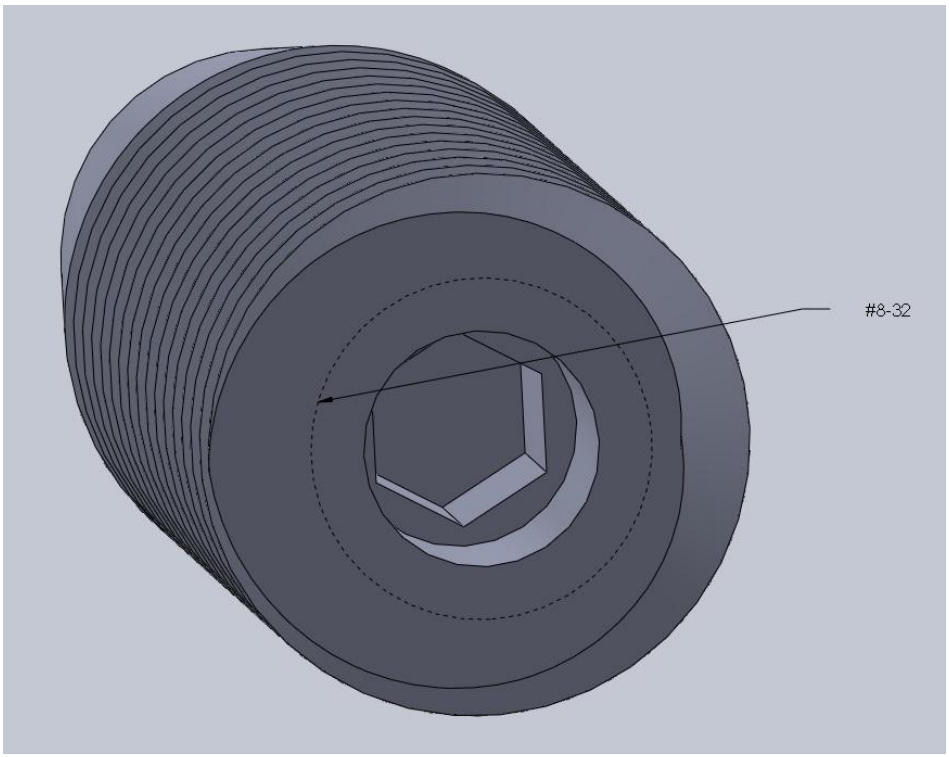

Figure 72: Internal design of radial stem

Stress Analysis

FEA was performed on the model to determine if the bone will experience excessive stresses. The threads were removed, the load was applied on the face, and the 10 mm long unthreaded portion was held fixed and assumed to be the main area where the bone supports the load. First the 3600 N extreme load was applied and the results are seen Figure 73.

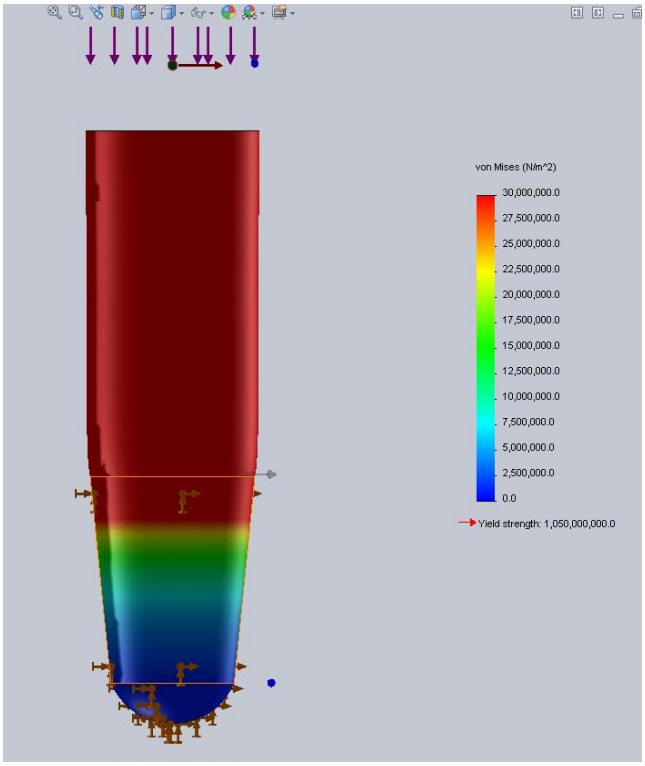

Figure 73: Radial component extreme test 1

The area of interest is the highlighted area, the tapered end, which is assumed to be bearing the compressive loading. As the color plot indicates, there is clearly stress exceeding the strength of the bone. Thus, the part must be redesigned to reduce the stresses seen on the bone. The new design features a wide head on the top of the stem to distribute the load over a greater area. After several iterations, the part was redesigned with a 15 mm diameter head (Figure 74), which is still under the minimum thickness at the rim of the radius .

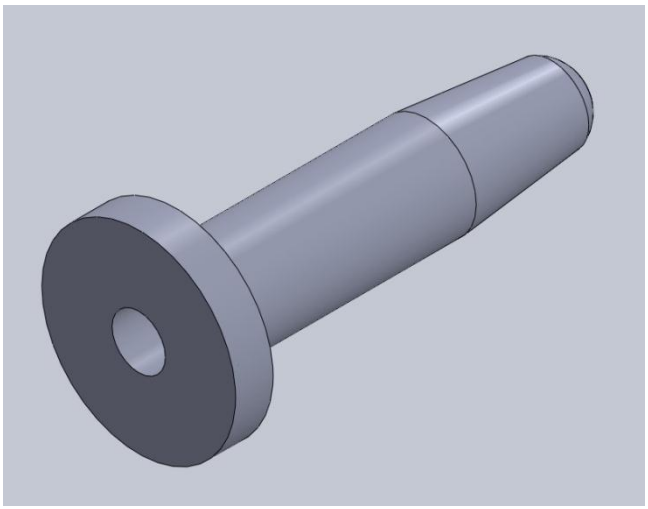

Figure 74: Radial stem redesigned

The results from the stress analysis with the extreme load are shown in Figure 75. The stress in the bone has been reduced to acceptable levels. Though there are small areas of excessive stress around the rim, but the screw threads will bear a significant portion of the load in practice and reduce the overall stress in the bone.

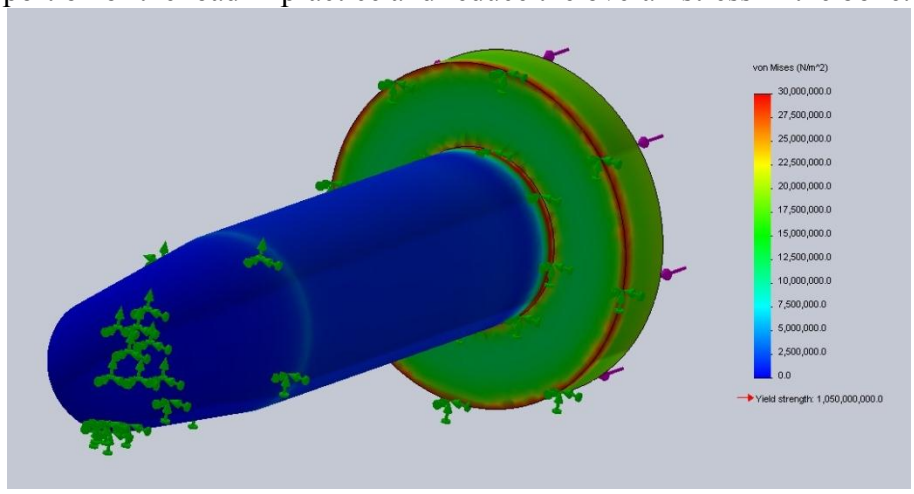

Figure 75: Radial component extreme test 2

Lastly, the component was analyzed for the fatigue case with the 1200 N load. As expected, the results in Figure 76 reflect those of the extreme case; the component will

not fail due to fatigue. These results show that the radial stem will perform its function without transmitting excessive stress to the radial bone.

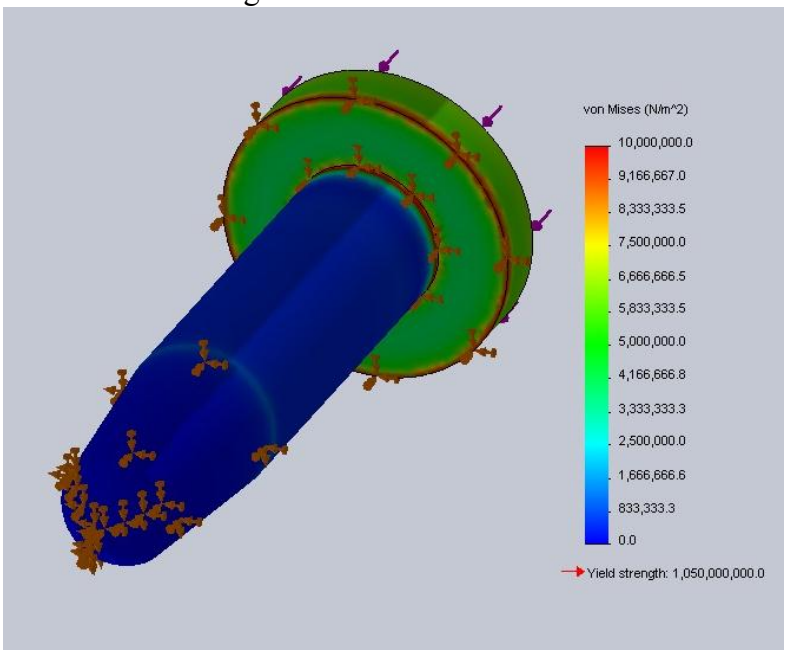

Figure 76: Radial component fatigue test

4.3.4 Summary of Radial Stem Design

Table 13 supplements Table 6 and summarizes the key design variables of the radial stem design.

Table 13: Summary of radial stem design

Radial Stem Design Specifications	
Length of stem	30 mm
length of head	3 mm
Diameter of head	15 mm
Unthreaded stem length	10 mm
Threaded stem length	20 mm
Taper for unthreaded section	7 mm to 8 mm
Thread type	M8x1.25
Torque transmittal section length	3 mm
Torque transmittal head size	2.5 mm
Articulation piece attachment length	3.15 mm

4.4 JOINT DESIGN

The final subsystem of the implant to be designed is the joint, the core component of the implant. From Table 6, the material, the necessary strength, dimensions, center of rotation and minimum range of motion have been specified. The kinematics have been set by locating the center of rotation of the ball and socket joint 1/8 of the length of the capitate length distal to the proximal end. The key dimension for this section is the available length, *l*, the distance between the end of the carpal plate and the radial stem. Using Equation (15), *l* is calculated to be 1.74 cm.

$$l = 2.5 - t_{carpal} - t_{radial} \tag{15}$$

One additional requirement to these is minimizing wear, which deals with tribology. So the joint is designed to accommodate the necessary strength, minimum range of motion, center of rotation location, available length, and optimal tribology.

4.4.1 Tribology

Tribology focuses on the interaction of bodies in contact. Essentially, it is the study of contact, friction, wear and lubrication [126]. With any joint, and especially with one being implanted in the body, wear, and consequently tribology, is of upmost concern.

Wear should be minimized, while observing constraints and accomplishing the joint's purpose. To begin, the natural synovial joints are discussed briefly to establish the high standard for a human joint replacement.

Natural synovial joints are outstanding self-contained bearings. They are excellent lubrication mechanisms that operate between boundary and fluid film regimes. The friction is very low with a coefficient of friction, μ, of 0.02. With synovial joints lasting over 70 years, they have a wear factor, k, of $10^{-9}\,\frac{\text{mm}^3}{\text{Nm}}$ [126].

In this case, a suitable replacement for the wrist joint has to be created for a metal-on-metal contact ball and socket joint. While this may not match the performance of the synovial joint, it can be a suitable replacement if it can outlast or match current implants. The aim is to design the joint to operate between the mixed and fluid film region, which is the mode of lubrication that minimizes friction of the joint as displayed by the Stribeck diagram in Figure 77.

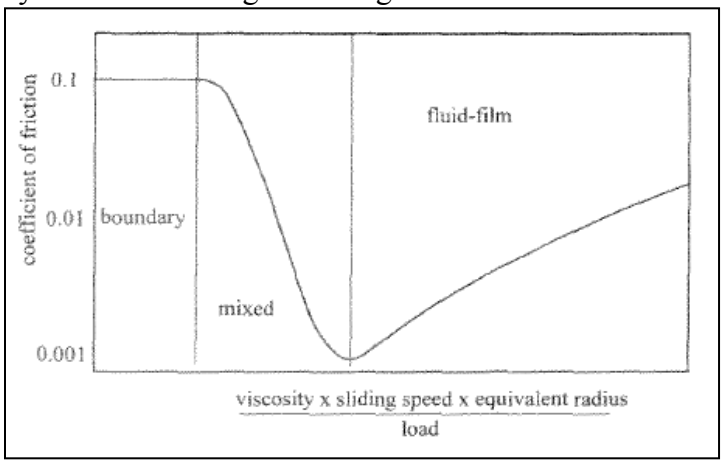

Figure 77: Stribeck diagram [80]

Determining the mode of lubrication is simplified through the use of the lambda ratio, λ, derived from elastohydrodynamic lubrication theory. Equation (16) is used to

compute the lambda ratio, where $h_{\min}$ is the minimum film thickness (nm), and R_{a1} and R_{a2} are the respective surface roughness averages of the two surfaces (nm). As shown in Figure 78, a higher lambda ratio results in longer life with a ratio over 3 generally resulting in the greatest possible life with fluid film lubrication [80].

$$\lambda = \frac{h_{\min}}{\left[\left(R_{a1}\right)^2 + \left(R_{a2}\right)^2\right]^{1/2}} \tag{16}$$

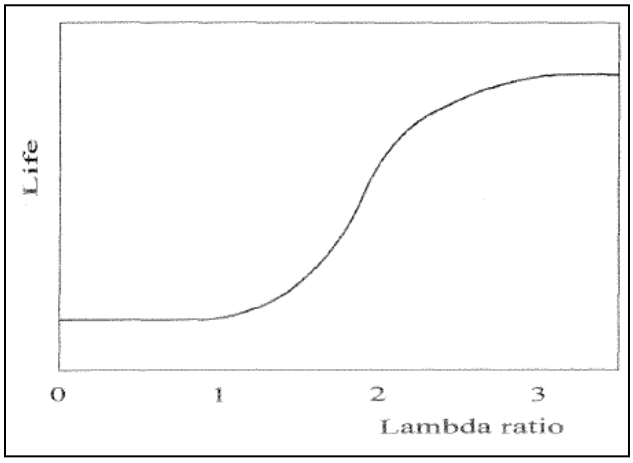

Figure 78: Relationship between lambda ratio and life/wear [80]

For this application a lambda ratio of 3 is desired for minimal wear. Assuming that both articulation surfaces will be manufactured with the latest technology, surface roughness averages of less than 10 nm are possible. The addition of the wear coating will increase the roughness slightly, but due to the self polishing nature of metal-on-metal implants the surface roughness will also be reduced over some use [127]. Thus, a surface roughness of 10 nm was used based on the data mentioned. With this information, a minimal film thickness of 42.4 nm or greater is desired.

Before moving further, an equivalent radius is defined in Equation (17); R is the equivalent radius, r is the radius of the ball in the joint, and c is the radial clearance. The radius of the ball is essentially what is being determined and is subject to constraints.

The radial clearance can now be as low as 20 um using current advanced manufacturing techniques and these advanced materials [80].

$$R \approx \frac{r}{c} r \tag{17}$$

With R defined, the minimum film thickness can be computed using Equation (18), where η is the viscosity of the fluid, u is the entraining velocity, w is the load, and E' is the effective elastic modulus. Once all these values are determined, a minimum radius for the joint can be determined [80].

$$H_{\min} = \frac{h_{\min}}{R} = 2.80 \left(\frac{\eta u}{E' R} \right)^{0.65} \left(\frac{w}{E' R^2} \right)^{-0.21} \tag{18}$$

To begin with, the viscosity, η, of the synovial fluid varies with age and by person. However, a correlation has been found for healthy synovial fluid and is described by Equation (19). A is the age of the individual, taken as 30 as an upper bound for the young athletic male, and the viscosity is calculated to be 9.3 P (poise=0.1 $\frac{kg}{m \cdot s}$) [128].

$$\eta = 12.6 - 0.11A \tag{19}$$

The entrainment velocity, u, in this case of hydrodynamic fluid film lubrication, is the average velocity of the two surfaces, where one is assumed to be held constant (the radial side of the implant). While it would be possible to calculate this velocity for a given radius, it would be more useful to specify an angular velocity u/R instead of just u. An upper bound on wrist angular velocity was found to be 3.05 rad./s (175 deg/s) [129].

The load, w, is the design load of 1200 N. The extreme load of 3600 N is also considered and designed for, for additional factor of safety, if it will meet the constrained dimensions.

Lastly, the effective elastic modulus, E', can be calculated using Equation (20), where v and E are the Poisson's ratio and elastic modulus of each material respectively

[80]. In this case, the material of both articulating surfaces is cobalt-chromium with the properties given in Table 4. The effective elastic modulus is calculated to be 468 GPa, two times the original elastic modulus.

$$E' = \frac{2}{\frac{1-\nu_a^2}{E_a} + \frac{1-\nu_b^2}{E_b}} \tag{20}$$

Using these values, R is calculated with Equations (17) and (18). The minimum radius of the contacting surfaces for fluid film lubrication is 6.75 mm for the 1200 N load and 7.32 mm for the 3600 N load. As an aside, for an implant designed for elderly patients, the minimum radius could have to be large as 1.4 cm accounting for the decrease in viscosity of the synovial fluid with age and increased surface roughness. Table 14 summarizes all the calculations in this section.

Table 14: Summary of tribology calculations

hmin	42.4 nm
c	20 um
η	9.3 P
u/R	3.05 rad./s
w	1200 or 3600
E'	4.68E+11
R	**6.75 or 7.32 mm**

4.4.2 Design of the Joint

With a lower bound on the minimum radius determined by the tribology calculations, the iterative design process can be begun for the joint. With just 1.74 cm of length to fit the joint into and with the 1.049-1.114 cm minimal radius for the ball joint, the length will be the constraining dimension. The most difficult range of motion requirement is the 40° of flexion and extension, so the joint will have to achieve this

range of motion in every direction (as it is a ball and socket joint). And of course, it must withstand the 1200 N fatigue load and 3600 N extreme loads.

As the center of rotation must be placed 1/8 the length of the capitate bone distal to the proximal end of the capitate, the joint components must be arranged to allow this while accommodating the desired range of motion. Using the x-ray from Figure 44 as the reference, the center of rotation for this case would be located 9.4 mm from the cut made for the carpal component. The 1-dimensional representation in Figure 79 elucidates the design envelope, the desired center of rotation, and the available space after accounting for the other components. Dimension X, which is the distance between the center of rotation and end of the carpal plate (4.83 mm), is the limiting dimension.

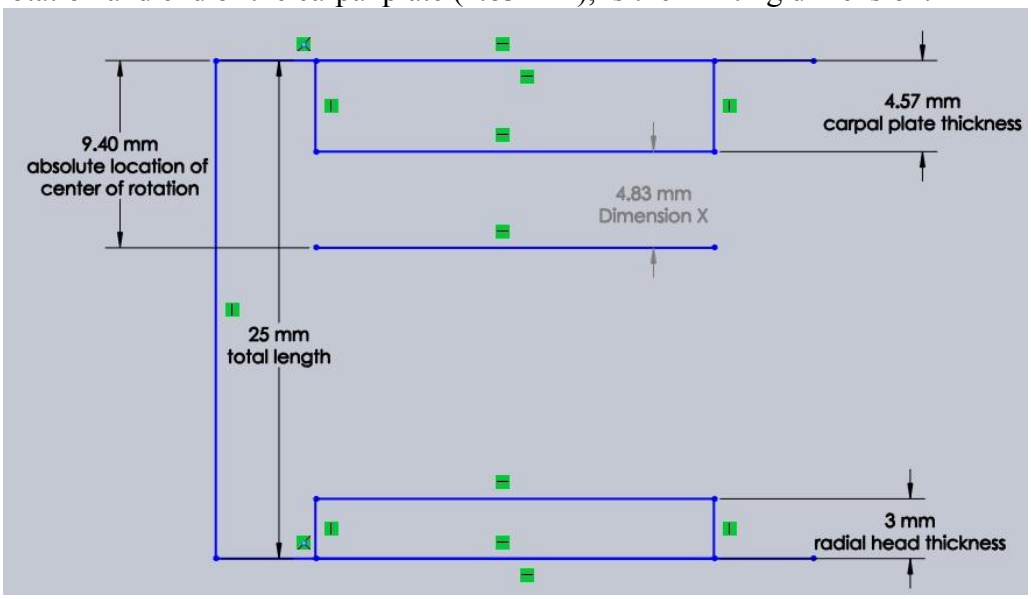

Figure 79: Center of rotation relative location

With that distance being so small, the ball portion of the joint will be attached to the carpal plate as this allows the center of rotation to be placed near to the carpal plate (the center of rotation of the ball and socket joint is at the center of the ball. Consequently the socket will be attached to the radial stem.

To check if the joint will be able to achieve the 40° of motion in every direction a simple trigonometry calculation is carried out. There must be enough room between the center of rotation and the carpal plate to allow the socket to achieve the desired range of motion without impingement on the carpal plate. This means that the relation in Equation (21) must be met. In this case, it means the radius must be less than 7.5 mm. While the radii determined from the lubrication calculations both fall under this, the smaller radius is used for a greater factor of safety for impingement (an additional 5°). The decision is made because the damage caused by impingement onto the plate is much greater than operating in slightly worse lubrication regime during the occasional extreme loadings.

$$R\sin(40°) \leq \text{Dimension X} \tag{21}$$

On a very important side note, "Dimension X", and consequently the range of motion, can potentially be much greater with a thinner carpal plate. The limiting factor for the carpal plate thickness in this design was the head size of the two common screws. Custom bone screws in the final product could be designed to accommodate a thinner plate and up to 90° of motion in each direction depending on the head size of the bone screws. Still, 40° of motion is more than enough for daily activity and is on the conservative side.

The ball component consists of a half sphere, a shaft, and a connection piece. The half sphere has a radius of 6.75 mm, the minimum radius for fluid film lubrication for the fatigue load. The shaft diameter is chosen to ensure the socket impinges on the shaft rather than the carpal plate. The diameter is determined to be about 4.75 mm. A small section of the shaft is designed to accept a 4 mm wrench to accommodate installation into the carpal plate. Lastly, the connection is the #8-32 thread; the major diameter is 0.1640 in., which is the dimension specified for the end of the ball articulation piece as this is the

maximum diameter that alleviate interference issues. A 2 mm radius fillet was added between the half sphere and shaft to reduce stress concentrations. The completed design is shown in Figure 80.

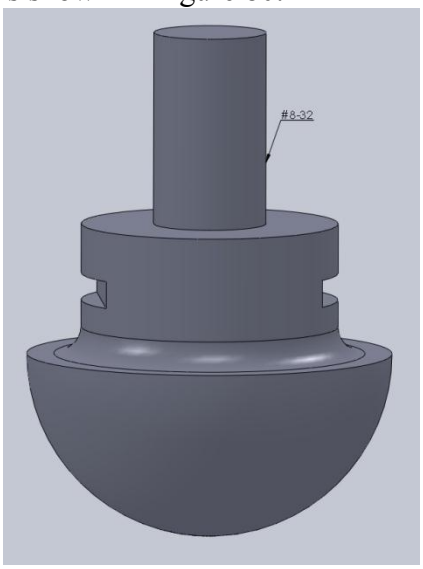

Figure 80: Carpal articulation piece first iteration

The socket component consists of a mating cup for the half sphere, a shaft, and a connection piece. The cup is 6.75 mm in radius interiorly to match the ball and 8.75 mm on the exterior radius. To prevent impingement on the carpal plate, a 45° chamfer is cut from the rim of the component, leaving a 0.5 mm thickness at the rim. The 8.12 mm shaft is placed at the other end of the cup 1 mm into the cup extending 4.85 mm. Lastly, the connection piece is the #8-32 screw thread 3.15 mm long to match the radial stem. The finished product is seen in Figure 81.

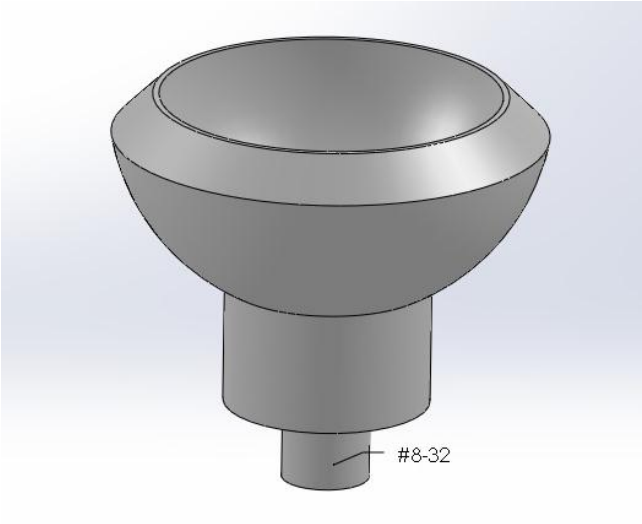

Figure 81: Socket articulation piece

4.4.3 Stress Analysis

With the joint designed, the design must be analyzed to ensure the stresses are not too great. Finite element analysis is used to determine whether the fatigue strength of the metals will be exceeded in the fatigue case and the yield strength in the extreme case (both found in Table 4). The key areas to be checked were the contact surfaces of the joint and the surfaces connecting the joint components to the radial and carpal plates. Unsurprisingly, the components easily meet the strength requirements. Figure 82 through Figure 85 display the results from the fatigue and extreme tests, and it can be seen that the areas of interest do not exceed the stress limits.

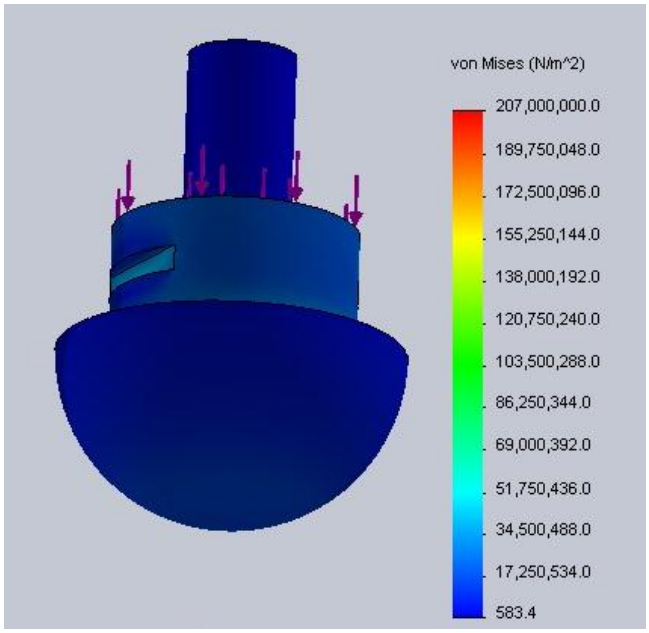

Figure 82: Joint fatigue test, joint surface

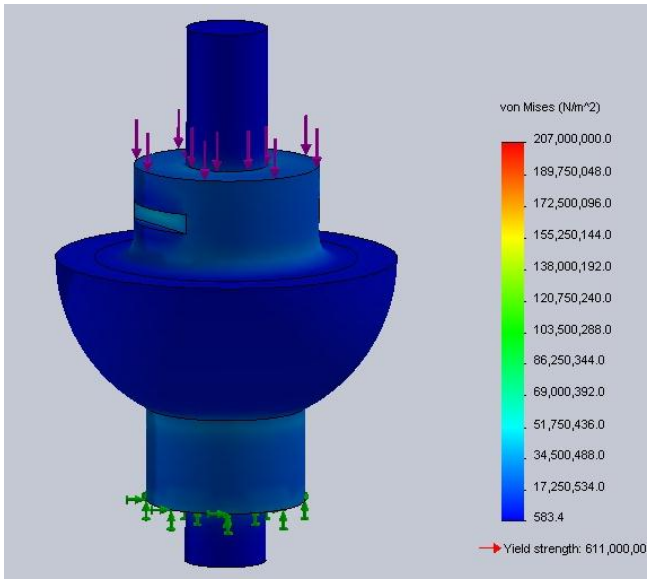

Figure 83: Joint fatigue test, mating surfaces

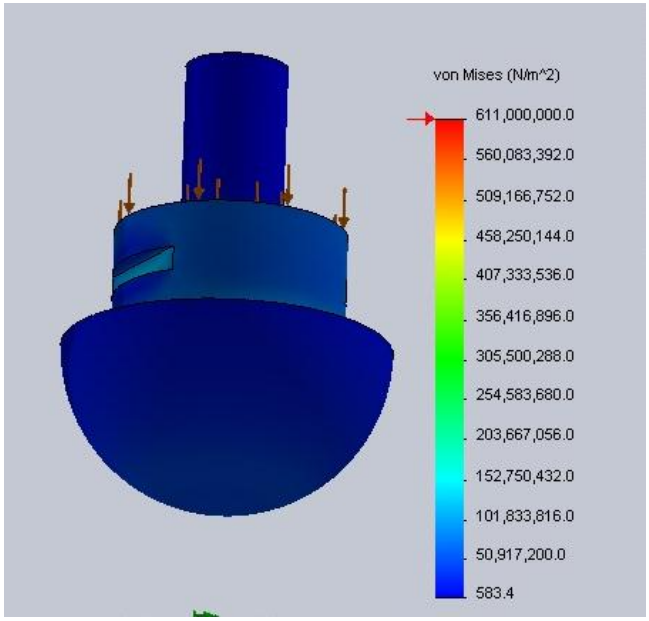

Figure 84: Joint extreme test, joint surface

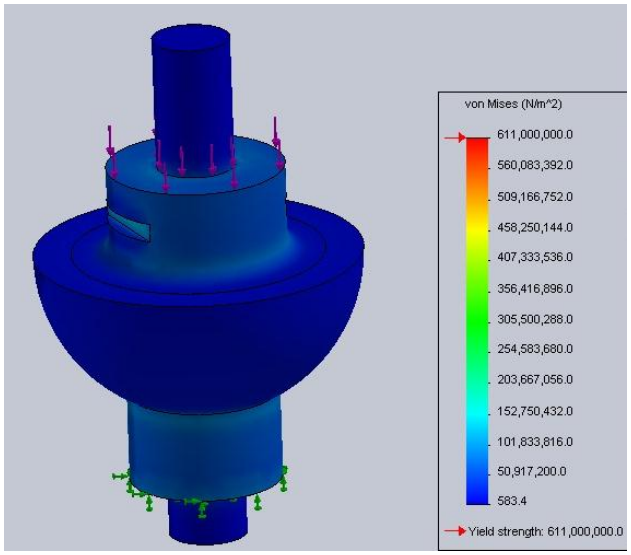

Figure 85: Joint extreme test, mating surfaces

4.5 FULL PROTOTYPE

Figure 86 below displays the final configuration of the prototype with all of the components assembled together. Figure 87 shows an exploded view of the prototype.

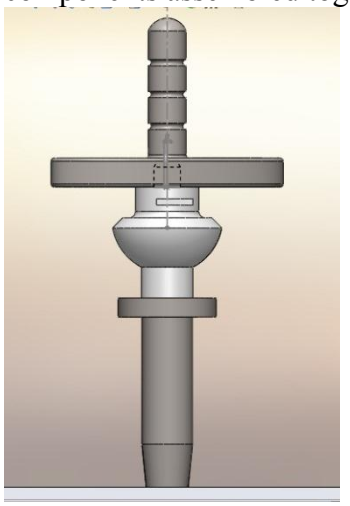

Figure 86: Full prototype

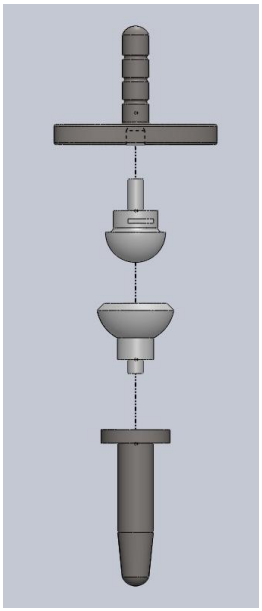

Figure 87: Prototype Exploded View

4.5.1 Range of Motion Check

As a final check, it was verified using SolidWorks Motion Analysis that the full assembly could accomplish the 40° of motion desired without interference. Figure 88 also shows that at that extent, the joint will contact the shaft of the ball component rather than impinging on the carpal plate.

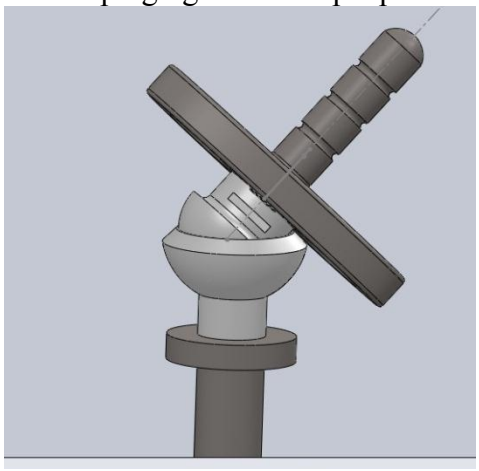

Figure 88: Range of motion and contact test

4.5.2 Surgery Procedure

As the implant is not ready for human implant yet and no cadavers were used in the study, a specific surgery procedure has not been developed. However, the surgery procedure will be very similar to that described by Menon for the Universal 2 implant [21] and the procedure for the Motec implant [45].

CHAPTER 5

CONCLUSION

5.1 SUMMARY

The human wrist is a vital joint in daily life, and it is subject to injuries and disease. As yet, a suitable wrist implant has not been implemented, especially for young males. Current wrist implants have improved greatly over the years with new materials, advances in surgical techniques, and wrist kinematics research. Many designs exist on the market currently. The current gold standard is the Universal2 Total Wrist System which is based on the ellipsoidal joint.

A hypothesis is proposed which states that the wrist implants based on any joint that restricts axial rotation would loosen and fail over time due to the extra stresses transmitted to the bone-implant interface from preventing wrist rotation. As experimentation was not possible, simulation was used to test the hypothesis.

The first step in simulation was building a model of the bone mass of the wrist. For this a thorough literature review was performed to determine the loading of the wrist and to complete the difficult task of estimating the strength of bone. Using these properties and dimensions from x-rays, the bone mass was determined. A series of simulations were conducted with the final result showing the stresses from restricting axial rotation would contribute substantially to implant failure. A joint that does not restrict axial rotation requires the wrist muscles to stabilize the wrist, which would not be an issue in the young male. Overall the results support the hypothesis.

With the hypothesis confirmed, a new implant was designed featuring a joint that allows axial rotation as well as improved fixation and joint wear, an acceptable range of

motion, and correct kinematics. Through background research, the desired specifications were determined and the design process was begun to create a prototype.

Compromises were made for the screws for implantation into bone for the prototype, and Synthes will be consulted for a final screw design if the final product is produced.. The carpal plate, radial component, and articulation pieces were successively designed for manufacture and assembly. Each component was analyzed through FEA to ensure the bone would not be overstressed and the component would not fail. To reduce wear as much as possible, a lubrication study was conducted to determine how to design the joint to operate in the fluid film lubrication regime. Lastly, the components were assembled to ensure proper operation and fit, and the design was completed.

5.2 CONTRIBUTION

This study made several contributions to the field of wrist implants. A literature review was conducted which will be useful to future researchers; previous implants were compared and background on various design aspects for developing a device was provided. It was also shown that implants which restrict axial rotation will be more prone to failure than those that don't. Finally, a new implant design was created comprehensively addressing the design criteria.

5.3 FUTURE WORK

With the prototype design completed, much work is left for full implementation of this wrist implant.

First, the design must be finalized with proper screws and dimensions. Then, the design should be manufactured with the desired materials after checking fit and function with a rapid prototype. An optional step, and possibly a project in itself, would be

developing a testing machine for the wrist implant to verify the simulation results or analyze the joint and joint reactions further.

After the final design is established, cadaver studies would be performed to determine proper surgical technique and obtain surgeon feedback about the design and ease of implantation. Following this, the suggested modifications would be made, and human trials would begin. Finally, if successful, the device could be released for sale and large-scale implementation.

This research may aid in the development of an effective wrist implant for the post-traumatic, young male's wrist in the near future.

Bibliography

1. Shepherd, D., and A. Johnstone. "A New Design Concept for Wrist Arthroplasty." Proceedings of the Institution of Mechanical Engineers, Part H: Journal of Engineering in Medicine 219.1 (2005): 43-52. Print.
2. "Wrist Joint Replacement (Wrist Arthroplasty)." Orthoinfo. N.p., n.d. Web. 24 Mar. 2013. <http://orthoinfo.aaos.org/topic.cfm?topic=A00019>.
3. Shepherd, D. "Design Considerations for a Wrist Implant." Medical Engineering & Physics 24.10 (2002): 641-50. Print.
4. Majors, BJ, and JS Wayne. "Development and Validation of a Computational Model for Investigation of Wrist Biomechanics." Ann Biomed Eng 39.11 (2011): 2807-815. Print.
5. Bajuri, Mohd N. "Biocomputational Comparative Study of Rheumatoid Arthritis of the Wrist Joint before and after Arthroplasty; Carpal Stability Analysis." Proc. of IEEE EMBS Conference on Biomedical Engineering and Sciences (IECBES),. N.p.: n.p., n.d. 270-75. Print.
6. Horii, E., M. Garciaelias, K. An, A. Bishop, W. Cooney, R. Linscheid, and E. Chao. "Effect on Force Transmission across the Carpus in Procedures Used to Treat Kienböck's Disease." The Journal of Hand Surgery 15.3 (1990): 393-400. Print.
7. Netter, Frank H., and Sharon Colacino. Atlas of Human Anatomy. 5th ed. Summit, NJ: CIBA-GEIGY, 1989. Print.
8. Gelberman, Richard H. The Wrist. Philadelphia: Lippincott Williams & Wilkins, 2002. Print.

9. "Wrist-joint." Wikipedia. Wikimedia Foundation, 03 Dec. 2013. Web. 24 Mar. 2013. <http://en.wikipedia.org/wiki/Wrist-joint>.
10. "Wrist AROM and Stretching." Therapy Library. N.p., n.d. Web. 24 Mar. 2013. <http://www.therapylibrary.com/index.php?option=com_content&view=article&id=105&Itemid=2208>.
11. Kamal, R., and A. P. Weiss. "Total Wrist Arthroplasty for the Patient with Non-rheumatoid Arthritis." J Hand Surg Am 6.36 (2011): 1071-072. Print.
12. Board, A.D.A.M. Editorial. "Osteoarthritis." U.S. National Library of Medicine, 18 Jan. 0001. Web. 24 Mar. 2013. <http://www.ncbi.nlm.nih.gov/pubmedhealth/PMH0001460/>.
13. Rizzo, M., and W. P. Cooney, 3rd. "Current Concepts and Treatment for the Rheumatoid Wrist." Hand Clin 27.1 (2011): 57-72. Print.
14. Cavaliere, C. M., A. J. Oppenheimer, and K. C. Chung. "Reconstructing the Rheumatoid Wrist: A Utility Analysis Comparing Total Wrist Fusion and Total Wrist Arthroplasty from the Perspectives of Rheumatologists and Hand Surgeons." Hand (N Y) 5.1 (2010): 9-18. Print.
15. Board, A.D.A.M. Editorial. "Rheumatoid Arthritis." U.S. National Library of Medicine, 18 Jan. 0001. Web. 24 Mar. 2013. <http://www.ncbi.nlm.nih.gov/pubmedhealth/PMH0001467/>.
16. Youm, Youngil, and Adrian E. Flatt. "Design of a Total Wrist Prosthesis." Annals of Biomedical Engineering 12.3 (1984): 247-62. Print.
17. Levadoux, M. "Total Wrist Arthroplasty with Destot Prostheses in Patients with Posttraumatic Arthritis." The Journal of Hand Surgery 28.3 (2003): 405-13. Print.
18. Cavaliere, Christi M., and Kevin C. Chung. "A Cost-Utility Analysis of Nonsurgical Management, Total Wrist Arthroplasty, and Total Wrist Arthrodesis

in Rheumatoid Arthritis." The Journal of Hand Surgery 35.3 (2010): 379-91.e2. Print.

19. Gummesson, Christina, Isam Atroshi, and Charlotte Ekdahl. "Abstract." National Center for Biotechnology Information. U.S. National Library of Medicine, 16 June 2003. Web. 24 Mar. 2013. <http://www.ncbi.nlm.nih.gov/pmc/articles/PMC165599/>.
20. McCullough, Matthew B., Brian D. Adams, and Nicole M. Grosland. "Post-Operative Analysis of Patients of the Universal 2 Total Wrist Implant System." Journal of Applied Biomechanics (2011): n. pag. Print.
21. Menon, J. "Universal Total Wrist Implant - Experience with a Carpal Component Fixed with Three Screws." J Arthroplasty 13.5 (1998): 515-23. Print.
22. Eustice, Carol. "What Is Arthrodesis?" About.com Arthritis & Joint Conditions. N.p., 1 Mar. 2013. Web. 24 Mar. 2013. <http://arthritis.about.com/od/surgicaltreatments/g/arthrodesis.htm>.
23. Gupta, A. "Total Wrist Arthroplasty Review." Am J Orthop (Belle Mead NJ) 37.8 (2008): 12-16. Print.
24. Ferreres, Angel, Alberto Lluch, and Montserrat Del Valle. "Universal Total Wrist Arthroplasty: Midterm Follow-Up Study." The Journal of Hand Surgery (2011): 967-73. Print.
25. Cavaliere, Christi, M.D., and Kevin Chung, M.D. "A Systematic Review of Total Wrist Arthroplasty Compared with Total Wrist Arthrodesis for Rheumatoid Arthritis."*Plastic & Reconstructive Surgery:* 112.3 (2008): 813-25. Print.
26. Grosland, N. M., R. D. Rogge, and B. D. Adams. "Influence of Articular Geometry on Prosthetic Wrist Stability." *Clinical Orthopaedics and Related Research* 421 (2004): 134-42. Print.

27. Taljanovic, M. S., M. D. Jones, T. B. Hunter, J. B. Benjamin, J. T. Ruth, A. W. Brown, and J. E. Sheppard. "Joint Arthroplasties and Prostheses." *Radiographics* 23.5 (2003): 1295-314. Print.
28. Reigstad, A., O. Reigstad, C. Grimsgaard, and M. Røkkum. "New Concept for Total Wrist Replacement." *Journal of Plastic Surgery and Hand Surgery* 45.3 (2011): 148-56. Print.
29. Johnson, S., A. Patel, R. Calfee, and A. Weiss. "Pisiform Impingement After Total Wrist Arthroplasty." *The Journal of Hand Surgery* 32.3 (2007): 334-36. Print.
30. Cavaliere, C. M., A. J. Oppenheimer, and K. C. Chung. "Reconstructing the Rheumatoid Wrist: A Utility Analysis Comparing Total Wrist Fusion and Total Wrist Arthroplasty from the Perspectives of Rheumatologists and Hand Surgeons." *Journal of Hand Surgery* 5.1 (2010): 9-18. Print.
31. Cooney, W. P., 3rd, R. D. Beckenbaugh, and R. L. Linscheid. "Total Wrist Arthroplasty. Problems with Implant Failures." *Clinical Orthopaedics and Related Research* 187 (1984): 121-28. Print.
32. Ward, C. M., T. Kuhl, and B. D. Adams. "Five to Ten-year Outcomes of the Universal Total Wrist Arthroplasty in Patients with Rheumatoid Arthritis." *The Journal of Bone & Joint Surgery* 93.10 (2011): 914-19. Print.
33. Rossello, Mario Igor, Margherita Costa, and Vincenzo Pizzorno. "Experience of Total Wrist Arthroplasty With Silastic Implants Plus Grommets." *Clinical Orthopaedics and Related Research* 342 (1997): 64-70. Print.
34. Herzberg, G. "Prospective Study of a New Total Wrist Arthroplasty: Short Term Results."*Chirurgie De La Main* 30.1 (2011): 20-25. Print.

35. "Total Wrist Arthroplasty in Patients with Rheumatoid Arthritis. Evaluation of Preliminary Results." *Revista Española De Cirugía Ortopédica Y Traumatología (English Edition)* 52.4 (2008): 199-205. Print.
36. Comstock, Curt P., Dean S. Louis, and James F. Eckenrode. "Silicone Wrist Implant: Long-term Follow-up Study." *The Journal of Hand Surgery* 13.2 (1988): 201-05. Print.
37. Krukhaug, Yngvar, Stein A. Lie, Leif I. Havelin, Ove Furnes, and Leiv M. Hove. "Results of 189 Wrist Replacements." *Acta Orthopaedica* 82.4 (2011): 405-09. Print.
38. Gunatillake, Pathiraja A., Gordon F. Meijs, Simon J. Mccarthy, and Raju Adhikari. "Poly(dimethylsiloxane)/poly(hexamethylene Oxide) Mixed Macrodiol Based Polyurethane Elastomers. I. Synthesis and Properties." *Journal of Applied Polymer Science* 76.14 (2000): 2026-040. Print.
39. Martin, D. J., L. A. Warren, P. A. Gunatillake, S. J. McCarthy, G. F. Meijs, and K. Schindhelm. "Polydimethylsiloxane/polyether-mixed Macrodiol-based Polyurethane Elastomers: Biostability." *Biomaterials* 21.10 (2000): 1021-029. Print.
40. Berger, Richard A., and Arnold-Peter C. Weiss. *Hand Surgery*. Philadelphia: Lippincott Williams & Wilkins, 2004. Print.
41. Tey, Ambrose. "The Development of Artificial Wrist Joint Replacements_FINAL." *Scribd*. N.p., n.d. Web. 18 Apr. 2013. <http://www.scribd.com/doc/12796643/The-Development-of-Artificial-Wrist-Joint-ReplacementsFINAL>.

42. Figgieiii, H., C. Ranawat, A. Inglis, L. Straub, and C. Mow. "Preliminary Results of Total Wrist Arthroplasty in Rheumatoid Arthritis Using the Trispherical Total Wrist Arthroplasty." *The Journal of Arthroplasty* 3.1 (1988): 9-15. Print.
43. Adams, B. "Total Wrist Arthroplasty." *Atlas of the Hand Clinics* 10.2 (2005): 263-70. Print.
44. O'Flynn, H. "Failure of the Hinge Mechanism of a Trispherical Total Wrist Arthroplasty: A Case Report and Review of the Literature." *The Journal of Hand Surgery* 24.1 (1999): 156-60. Print.
45. Swemac. *MOTEC Wrist Joint Prosthesis*. Linkoping, Sweden: Swemac, 2007. Print.
46. Winterswijk, P. "Promising Clinical Results of the Universal Total Wrist Prosthesis in Rheumatoid Arthritis." *The Open Orthopaedics Journal* 4.1 (2010): 67-70. Print.
47. Gíslason, Magnús K., Benedict Stansfield, and David H. Nash. "Finite element model creation and stability considerations of complex biological articulation: the human wrist joint." *Medical engineering & physics* 32.5 (2010): 523-531.
48. Lewis, G., and S. R. Vannappagari. "Finite element stress analysis of the wrist joint without and with an endoprosthesis." *Seminars in arthroplasty*. Vol. 6. No. 1. 1995.
49. Manal, Kurt, et al. "Force transmission through the juvenile idiopathic arthritic wrist: a novel approach using a sliding rigid body spring model." *Journal of biomechanics* 35.1 (2002): 125-133.
50. Zajac, Felix E. "Muscle and tendon: properties, models, scaling, and application to biomechanics and motor control." *Critical reviews in biomedical engineering* 17.4 (1989): 359.

51. Escorpizo, Reuben, and Anne Moore. "The effects of cycle time on the physical demands of a repetitive pick-and-place task." *Applied Ergonomics* 38.5 (2007): 609-615.
52. Genda, E., and E. Horii. "Theoretical stress analysis in wrist joint–neutral position and functional position." *Journal of Hand Surgery (British and European Volume)* 25.3 (2000): 292-295.
53. Hara, Toshiaki, et al. "Force distribution across wrist joint: application of pressure-sensitive conductive rubber." *The Journal of hand surgery* 17.2 (1992): 339-347.
54. Neu, C. P., J. J. Crisco, and S. W. Wolfe. "In vivo kinematic behavior of the radio-capitate joint during wrist flexion–extension and radio-ulnar deviation."*Journal of biomechanics* 34.11 (2001): 1429-1438.
55. Erhart, Stefanie, et al. "Measurement of intraarticular wrist joint biomechanics with a force controlled system." *Medical engineering & physics* 34.7 (2012): 900-905.
56. Crisco, Joseph J., et al. "The mechanical axes of the wrist are oriented obliquely to the anatomical axes." *The Journal of Bone & Joint Surgery* 93.2 (2011): 169-177.
57. Werner, Frederick W., et al. "Wrist tendon forces during different dynamic wrist motions." *The Journal of hand surgery* 35.4 (2010): 628.
58. Gislason, Magnus K., et al. "A three-dimensional finite element model of maximal grip loading in the human wrist." *Proceedings of the Institution of Mechanical Engineers, Part H: Journal of Engineering in Medicine* 223.7 (2009): 849-861.

59. Matsuoka, Juli, et al. "An analysis of symmetry of torque strength of the forearm under resisted forearm rotation in normal subjects." *The Journal of hand surgery* 31.5 (2006): 801-805.
60. O'Sullivan, Leonard W., and Timothy J. Gallwey. "Forearm Torque Strength and Endurance for Elbow and Forearm Angles." *Proceedings of the Human Factors and Ergonomics Society Annual Meeting*. Vol. 45. No. 14. SAGE Publications, 2001.
61. "Bone Structure & Composition." N.p., n.d. Web. 20 Apr. 2013. <www.eng.tau.ac.il/~gefen/BB-Lec1.PDF>.
62. "Bone Pathologies." N.p., n.d. Web. 20 Apr. 2013. <www.eng.tau.ac.il/~gefen/BB-Lec2.PDF>.
63. Rho, Jae Young, Richard B. Ashman, and Charles H. Turner. "Young's modulus of trabecular and cortical bone material: ultrasonic and microtensile measurements." *Journal of biomechanics* 26.2 (1993): 111-119.
64. Hastings, Abel Z. *An Investigation of the High Cycle Fatigue Behavior of Bovine Trabecular Bone*. Thesis. MIT, 2002. N.p.: n.p., n.d. Print.
65. Zioupos, Peter, M. Gresle, and K. Winwood. "Fatigue strength of human cortical bone: age, physical, and material heterogeneity effects." *Journal of biomedical materials research part A* 86.3 (2008): 627-636.
66. Taylor, M., J. Cotton, and P. Zioupos. "Finite element simulation of the fatigue behaviour of cancellous bone*." *Meccanica* 37.4-5 (2002): 419-429.
67. Bowman, Steven M., et al. "Compressive creep behavior of bovine trabecular bone." *Journal of biomechanics* 27.3 (1994): 301-310.
68. Caler, William E., and Dennis R. Carter. "Bone creep-fatigue damage accumulation." *Journal of Biomechanics* 22.6 (1989): 625-635.

69. "Effects 3 Bone 11." *Ahsmediacenter*. N.p., n.d. Web. 20 Apr. 2013. <http://ahsmediacenter.pbworks.com/w/page/2089727/Effects 3 Bone 11>.
70. Dassault Systèmes, Waltham, Massachusetts, USA
71. Gonzalez, R. V., Buchanan, T. S., Delp, S. L. How muscle architecture and moment arms affect wrist flexion-extension moments, Journal of Biomechanics Vol. 30, pp. 705-712. (1997)
72. Clauser, Charles E., John T. McConville, and John W. Young. Weight, volume, and center of mass of segments of the human body. ANTIOCH COLL YELLOW SPRINGS OH, 1969.
73. Youm, Youngil, et al. "Kinematics of the wrist. I. An experimental study of radial-ulnar deviation and flexion-extension." The Journal of bone and joint surgery. American volume 60.4 (1978): 423.
74. Youm, Y., and Y. S. Yoon. "Analytical development in investigation of wrist kinematics." Journal of biomechanics 12.8 (1979): 613-621.
75. ASTM Standard F1357, 2009, "Specification for Concrete Aggregates," ASTM International, West Conshohocken, PA, 2006, DOI: 10.1520/F1357-R09, www.astm.org.
76. Lundborg, G., and P. I. Brånemark. "Anchorage of wrist joint prostheses to bone using the osseointegration principle." *The Journal of Hand Surgery: British & European Volume* 22.1 (1997): 84-89.
77. Toby, E. B., et al. "A Comparison of Fixation Screws for the Scaphoid during Application of Cyclical Bending Loads*." *The Journal of Bone & Joint Surgery*79.8 (1997): 1190-7.
78. "Stress Shielding." *Stress Shielding*. N.p., n.d. Web. 21 Apr. 2013. <http://abr-denmark.com/home/abr-therapy/why-abr/stress-shielding/>.

79. Gibson, P. N., and Hermann Stamm. "The use of alloys in prosthetic devices."*Business Briefing: Medical Device Manufacturing and Technology* (2002): 48-51.
80. Dowson, D. "New joints for the Millennium: wear control in total replacement hip joints." *Proceedings of the Institution of Mechanical Engineers, Part H: Journal of Engineering in Medicine* 215.4 (2001): 335-358.
81. Santavirta, Seppo, et al. "Alternative materials to improve total hip replacement tribology." *Acta Orthopaedica Scandinavica* 74.4 (2003): 380.
82. Grübl, Alexander, et al. "Long-term follow-up of metal-on-metal total hip replacement." *Journal of orthopaedic research* 25.7 (2007): 841-848.
83. Jazrawi, Laith M., Frederick J. Kummer, and Paul E. DiCesare. "Alternative bearing surfaces for total joint arthroplasty." *Journal of the American Academy of Orthopaedic Surgeons* 6.4 (1998): 198-203.
84. Shi, Longquan, Derek O. Northwood, and Zhengwang Cao. "The properties of a wrought biomedical cobalt-chromium alloy." *Journal of materials science* 29.5 (1994): 1233-1238.
85. "Materials." *Materials*. N.p., n.d. Web. 21 Apr. 2013. <http://bme240.eng.uci.edu/students/10s/geslamia/simple_green_004.htm>.
86. Marrey, Ramesh V., Robert Burgermeister, Randy B. Grishaber, and R.o. Ritchie. "Fatigue and Life Prediction for Cobalt-chromium Stents: A Fracture Mechanics Analysis."*Biomaterials* 27.9 (2006): 1988-2000. Print.
87. "Fatigue Properties and Endurance Limits of Stainless Steels." *BRITISH STAINLESS STEEL ASSOCIATION*. BRITISH STAINLESS STEEL ASSOCIATION, n.d. Web. 21 Apr. 2013. <http://www.bssa.org.uk/topics.php?article=104>.

88. Ryu, Jaiyoung, et al. "Functional ranges of motion of the wrist joint." *The Journal of hand surgery* 16.3 (1991): 409-419.
89. "Universal 2™ Total Wrist Implant System - Preparation of Carpus." *Universal 2™ Total Wrist Implant System*. N.p., n.d. Web. 21 Apr. 2013. <http://www.ilstraining.com/upper extremity solutions/Uni2/Uni2_07.html>.
90. Kobayashi, Masayuki, et al. "Intercarpal kinematics during wrist motion." *Hand clinics* 13.1 (1997): 143.
91. Kobayashi, Masayuki, et al. "Normal kinematics of carpal bones: a three-dimensional analysis of carpal bone motion relative to the radius." *Journal of biomechanics* 30.8 (1997): 787-793.
92. Leonard, L., et al. "Engineering a new wrist joint replacement prosthesis—a multidisciplinary approach." *Proceedings of the Institution of Mechanical Engineers, Part B: Journal of Engineering Manufacture* 216.9 (2002): 1297-1302.
93. Sommer 3rd, H. J., and N. R. Miller. "A technique for kinematic modeling of anatomical joints." *Journal of biomechanical engineering* 102.4 (1980): 311.
94. Youm, Y. "Instantaneous center of rotation by least square method." *Journal of bioengineering* 2.1-2 (1978): 129.
95. McMURTRY, ROBERT Y., et al. "Kinematics of the wrist. II. Clinical applications." *The Journal of bone and joint surgery. American volume* 60.7 (1978): 955.
96. Ricker, Alyssa, Peishan Liu-Snyder, and Thomas J. Webster. "The influence of nano MgO and BaSO4 particle size additives on properties of PMMA bone cement." *International journal of nanomedicine* 3.1 (2008): 125.

97. Synthes. *Vectra. Anterior Cervical Plate System*. N.p.: Synthes, n.d. Web. 21 Apr. 2013. <http://www.synthes.com/MediaBin/International%20DATA/036.000.913.pdf>.

98. Zand, Martin S., Steven A. Goldstein, and Larry S. Matthews. "Fatigue failure of cortical bone screws." *Journal of biomechanics* 16.5 (1983): 305-311.

99. Evans, Mervyn, et al. "Design and testing of external fixator bone screws."*Journal of biomedical engineering* 12.6 (1990): 457-462.

100. Blake, Alexander. *Threaded Fasteners: Materials and Design*. CRC Press, 1986.

101. Ansell, R. H., and John T. Scales. "A study of some factors which affect the strength of screws and their insertion and holding power in bone." *Journal of biomechanics* 1.4 (1968): 279-302.

102. "Screw Thread Design." *Fastenal*. N.p., n.d. Web. 21 Apr. 2013. <http://www.fastenal.com/content/documents/FastenalTechnicalReferenceGuide.pdf>.

103. Hearn, T. C., J. Schatzker, and N. Wolfson. "Extraction strength of cannulated cancellous bone screws." *Journal of orthopaedic trauma* 7.2 (1993): 138-141.

104. DeCoster, Thomas A., et al. "Optimizing bone screw pullout force." *Journal of orthopaedic trauma* 4.2 (1990): 169-174.

105. Battula, Suneel, et al. "The effect of pilot hole size on the insertion torque and pullout strength of self-tapping cortical bone screws in osteoporotic bone." *The Journal of Trauma and Acute Care Surgery* 64.4 (2008): 990-995.

106. Leggon, Robert, et al. "The holding strength of cannulated screws compared with solid core screws in cortical and cancellous bone." *Journal of orthopaedic trauma* 7.5 (1993): 450-457.

107. Hughes, A. N., and B. A. Jordan. "The mechanical properties of surgical bone screws and some aspects of insertion practice." *Injury* 4.1 (1972): 25-38.

108. Cleek, Tammy M., Karen J. Reynolds, and Trevor C. Hearn. "Effect of screw torque level on cortical bone pullout strength." *Journal of orthopaedic trauma*21.2 (2007): 117-123.

109. Totten, George E., Lin Xie, and Kiyoshi Funatani, eds. *Modeling and simulation for material selection and mechanical design*. Vol. 166. CRC Press, 2003.

110. "Machine Screws, Phillips Oval Head, Stainless Steel 18-8, #10-24 X 1"" *Bolt Depot*. N.p., n.d. Web. 21 Apr. 2013. <http://www.boltdepot.com/Product-Details.aspx?product=1310>.

111. "Bone Screw." *Cannulated Screw Manufacturer & Wholesaler*. N.p., n.d. Web. 21 Apr. 2013. <http://www.indiamart.com/markmedisystems/screw-plate.html>.

112. "Universal Wrist System." *Implants International*. N.p., n.d. Web. 21 Apr. 2013. <http://www.implantsinternational.com/Universal Wrist System>.

113. "Remotion Surgical Technique." Small Bone Innovations, n.d. Web. 21 Apr. 2013. <www.totalsmallbone.com/uk/pdfs/MKT_1.pdf>.

114. *Release Pin and Key Ring Locking Pin*. N.d. Photograph. *Bnl*. Web. 21 Apr. 2013. <http://www.bnl.com.au/catalogue/Latches_magnets_locks/Latches-6x4/Release-Pin-and-Key-Ring-Locking-Pin.jpg>.

115. "Screw Thread." *Wikipedia*. Wikimedia Foundation, 19 Apr. 2013. Web. 21 Apr. 2013. <http://en.wikipedia.org/wiki/Screw_thread>.

116. Myers, Willbur. "Designing Sheet Metal Parts." 2 Feb. 2010. E-mail.

117. "Galvanic Series." *Galvanic Series*. N.p., n.d. Web. 21 Apr. 2013. <http://www.corrosion-doctors.org/Definitions/galvanic-series.htm>.

118. *Radius*. 2007. Photograph. *Britannica.com*. Web. 21 Apr. 2013. <http://media-1.web.britannica.com/eb-media/59/54759-004-C688D7B0.jpg>.

119. Neu, C. M., et al. "Bone densities and bone size at the distal radius in healthy children and adolescents: a study using peripheral quantitative computed tomography." *Bone* 28.2 (2001): 227-232.

120. Dowthwaite, Jodi N., et al. "Bone geometry, density, and strength indices of the distal radius reflect loading via childhood gymnastic activity." *Journal of clinical densitometry* 10.1 (2007): 65-75.

121. "Radius (bone)." *Wikipedia*. Wikimedia Foundation, 19 Apr. 2013. Web. 21 Apr. 2013. <http://en.wikipedia.org/wiki/Radius_(bone)>.

122. *Wrist X-ray*. N.d. Photograph. *Flickr.com*. Web. 21 Apr. 2013. <http://farm3.staticflickr.com/2435/3577220025_4c407ec2ed_z.jpg?zz=1>.

123. "Metric Screw Dimensions ISO Fasteners." *Metric Screw Dimensions ISO Fasteners*. N.p., n.d. Web. 21 Apr. 2013. <http://www.tribology-abc.com/calculators/metric-iso.htm>.

124. "Thread: Best Material for Allen Wrench." *Practical Machinist*. N.p., n.d. Web. 21 Apr. 2013. <http://www.practicalmachinist.com/vb/general/best-material-allen-wrench-225530/>.

125. "Socket Head Cap Screw Size Chart." *Csgnetwork*. N.p., n.d. Web. 21 Apr. 2013. <http://www.csgnetwork.com/screwsochdcaptable.html>.

126. Bryant. "Tribology." 17 Jan. 2006. E-mail.

127. Cockeram, B. V. "Development of wear-resistant coatings for cobalt–base alloys." *Surface and Coatings Technology* 120 (1999): 509-518.

128. pH, O. F. "ON THE VISCOSITY AND pH OF SYNOVIAL FLUID AND THE."*blood* 20.38 (1959): 58.

129. Jung, Myung-Chul, and M. Susan Hallbeck. "The effect of wrist position, angular velocity, and exertion direction on simultaneous maximal grip force and wrist torque under the isokinetic conditions." *International Journal of Industrial Ergonomics* 29.3 (2002): 133-143.

130. *ANSYS*. Canonsburg, PA, USA: ANSYS, Inc., n.d. Computer software.

131. "The Visible Human Project® Fact Sheet." *U.S National Library of Medicine*. U.S. National Library of Medicine, 11 July 2012. Web. 21 Apr. 2013. <http://www.nlm.nih.gov/pubs/factsheets/visible_human.html>.